

**Laboratory Studies Using Sodium-Bearing
Waste Simulant - ADL 26-94**

by

James Jason Stone

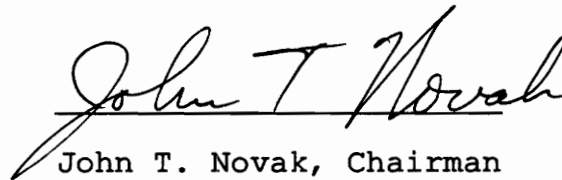
Thesis submitted to the Faculty of the
Virginia Polytechnic Institute and State University
in partial fulfillment of the requirements for the degree of

Master of Science


in

Environmental Engineering

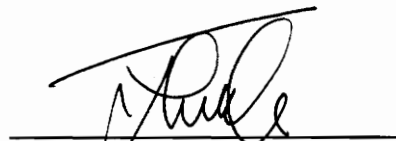
APPROVED:



John T. Novak, Chairman



William R. Knocke



John C. Little

February, 1995

Blacksburg, Virginia

c.2

LD
5/655
V855
1995
S7/658
c.2

Laboratory Studies Using Sodium-Bearing

Waste Simulant - ADL 26-94

by

James Jason Stone

John T. Novak, Chairman

Environmental Engineering

(ABSTRACT)

The purposes of this study were to develop a chemical precipitation procedure that would treat the sodium bearing waste (SBW) and to determine if polymer addition could condition the resulting sludge. Chemical precipitation parameters such as impeller mixing speed, rate of base addition, amount of added calcium to SBW, and solution precipitation pH were studied to determine the conditions for each parameter to achieve optimal solids removal rates and resistance to filtration. The organic polymers were gauged by their ability to properly condition the sludge by use of capillary suction time (CST) apparatus and wedge zone simulator (WZS).

Low impeller mixing speeds cause less excess floc deterioration and lower resistance to filtration. Slower base addition rates increase the overall titration time but improve sludge characteristics. Adding calcium to SBW decreases the specific resistance of the sludge. The best

dewatering rates occur when solution precipitation pH is between 8.5 and 9.5. This region provides the best cake solids and removal rates of the dissolved species. WZS and high speed centrifugation provide cakes solids above 20%. Medium to high molecular weight anionic polymers properly condition the SBW sludge.

ACKNOWLEDGMENTS

I would like to thank my main advisor, Dr. Novak, for all his help and guidance during the entire project. Without his superior laboratory and editing skills, this thesis may have never materialized. Dr. Knocke and Dr. Little also deserve thanks for pointing me in other directions and for serving on my committee.

Jenn-Hei Pao at The Westinghouse Nuclear Company merits special thanks for funding this project. I would also like to thank: Dennis Dove and Julie Petruska for their laboratory assistance with "big blue" and Marilyn Grender for both her Atomic Adsorption work and her patience with those "urgent deadlines".

Finally I would like to thank my family for their support during my college career. The good life is finally over.

TABLE OF CONTENTS

Introduction	1
Literature Review	3
Measurement of Sludge Dewatering Rates	3
Polymers	6
Factors Effecting Dewatering Rates	8
Mechanical Dewatering Equipment	12
Chemical Precipitation	13
Methods and Materials	22
Sodium Bearing Waste	22
Buchner Funnel Apparatus and Capillary Suction Time	24
Sludge Precipitation Procedures	26
Standard Mixing Procedure	28
pH Study	31
Mixing Speed Study	32
Base Addition Study	32
Reverse Addition Study	33
Spiked Reverse Addition Study	33
Mineql+ and Minteqa2 Chemical Equilibrium Modeling	34
Polymer Preparation	36
Mixing Apparatuses	36
Wedge Zone Simulator	37

Polymer Experimental Procedures	39
Centrifuge Procedure	41
Results and Discussion	43
Chemical Precipitation	43
pH Study	43
Mixing Speed Study	55
Base Addition Study	70
Reverse Addition Study	75
Spiked Reverse Addition Study	79
Mineql+ and Minteqa2 Chemical Equilibrium Modeling	84
Sludge Conditioning	89
Polymer Experiments	89
Wedge Zone Simulator Study	93
Summary and Conclusions	114
Bibliography	117
Appendix A - Wedge Zone Simulator Study Results	120
Appendix B - Mineql+ and Minteqa2 Results	125
Vita	138

List of Figures

Figure 1.	Standard belt filter press layout. From Reitz (18)	14
Figure 2.	Vermeulen's illustration of the effect of methods of alkali addition on the shape of the pH curve at 25°C. From Vermeulen (20)	17
Figure 3.	Buchner Funnel apparatus. From Reitz (18)	25
Figure 4.	Capillary Suction Time apparatus. From Bandak (12)	27
Figure 5.	Effect of solution pH on specific resistance for 430 rpm mixing speed at 10 min 2M NaOH addition time	45
Figure 6.	Effect of solution pH on specific resistance for 1870 rpm mixing speed at 10 min 2M NaOH addition time	47
Figure 7.	Effect of solution pH on cake solids concentration for 430 rpm mixing speed at 10 min 2M NaOH addition time	48
Figure 8.	Effect of solution pH on cake solids concentration for 1870 rpm mixing speed at 10 min 2M NaOH addition time	49
Figure 9.	Effect of solution pH on residual calcium concentration for 430 and 1870 rpm mixing speeds at 10 min 2M NaOH addition time	52
Figure 10.	Effect of solution pH on residual mercury concentration for 430 and 1870 rpm mixing speeds at 10 min 2M NaOH addition time	53
Figure 11.	Effect of solution pH on residual boron concentration for 430 and 1870 rpm mixing speeds at 10 min 2M NaOH addition time	54

Figure 12.	Effect of solution pH on residual molybdenum concentration for 430 and 1870 rpm mixing speeds at 10 min 2M NaOH addition time	56
Figure 13.	Effect of solution pH on residual nickel concentration for 430 rpm mixing speeds at 10 min 2M NaOH addition time	57
Figure 14.	Effect of solution pH on residual manganese concentration for 430 rpm mixing speeds at 10 min 2M NaOH addition time	58
Figure 15.	Effect of solution pH on residual cadmium concentration for 430 rpm mixing speeds at 10 min 2M NaOH addition time	59
Figure 16.	Effect of solution pH on residual lead concentration for 430 rpm mixing speeds at 10 min 2M NaOH addition time	60
Figure 17.	Effect of solution pH on residual iron concentration for 430 rpm mixing speeds at 10 min 2M NaOH addition time	61
Figure 18.	Effect of solution mixing speed on the specific resistance for 10 minute 2M NaOH addition	62
Figure 19.	Effect of solution mixing speed on CST for 10 minute 2M NaOH addition	63
Figure 20.	Effect of solution mixing speed on cake solids concentration for 10 minute 2M NaOH addition	66
Figure 21.	Effect of solution mixing speed on residual calcium for 10 minute 2M NaOH addition	67
Figure 22.	Effect of solution mixing speed on residual aluminum for 10 minute 2M NaOH addition ...	68
Figure 23.	Effect of 2M NaOH addition time on solution specific resistance for 430 rpm mixing speed	72

Figure 24.	Effect of 2M NaOH addition time on the solution CST for 430 rpm mixing speed	73
Figure 25.	Effect of 2M NaOH addition time on the residual calcium for 430 rpm mixing speed	74
Figure 26.	Effect of 2M NaOH addition time on cake solids concentration for 430 rpm mixing speed	76
Figure 27.	Effect of SBW simulant addition time (1, 8, and 17 min) on the specific resistance and residual calcium concentration during reverse addition study for 100 rpm mixing speed	78
Figure 28.	Effect of SBW simulant addition time (1, 8, and 17 min) on the specific resistance and residual aluminum during reverse addition study for 100 rpm mixing speed	80
Figure 29.	Effect of initial calcium concentration on the solution specific resistance and residual calcium concentration during the spiked reverse addition study for 100 rpm mixing speed and 10 min spiked SBW addition time	82
Figure 30.	Effect of initial calcium concentration on the solution specific resistance and residual aluminum concentration during the spiked reverse addition study for 100 rpm mixing speed and 10 min spiked SBW addition time	83
Figure 31.	pH versus percent distribution of calcium species according to Minteqa2	85
Figure 32.	Effect of solution pH on residual calcium for 1870 rpm mixing speed (observed), Mineql+, and Minteqa2	86
Figure 33.	Effect of mixing time on CST for 6.2, 8.7, and 12.5 mg/kg doses of A-M-30% polymer for 50 rpm mixing speed	91

Figure 34.	Effect of mixing time on CST for 6.2, 8.7, and 12.5 mg/kg doses of A-M-30% polymer for 75 rpm mixing speed	92
Figure 35.	Effect of mixing time on CST for 6.2, 8.7, and 12.5 mg/kg doses of A-M-30% polymer for 100 rpm mixing speed	94
Figure 36.	Filtrate solids and cake solids versus A-M-13% polymer dose determined by WZS for 100 rpm mixing speed and 2 min mixing time	97
Figure 37.	Effect of A-M-13% polymer dose on CST for 100 rpm mixing speed and 2 min mixing time	99
Figure 38.	Filtrate solids and cake solids versus A-M-30% polymer dose determined by WZS for 100 rpm mixing speed and 2 min mixing time	100
Figure 39.	Effect of A-M-30% polymer dose on CST for 100 rpm mixing speed and 2 min mixing time	101
Figure 40.	Filtrate solids and cake solids versus A-H-50% polymer dose determined by WZS for 100 rpm mixing speed and 2 min mixing time	103
Figure 41.	Effect of A-H-50% polymer dose on CST for 100 rpm mixing speed and 2 min mixing time	104
Figure 42.	Filtrate solids and cake solids versus C-M-30% polymer dose determined by WZS for 100 rpm mixing speed and 2 min mixing time	105
Figure 43.	Effect of C-M-30% polymer dose on CST for 100 rpm mixing speed and 2 min mixing time	106
Figure 44.	Filtrate solids and cake solids versus C-L-30% polymer dose determined by WZS for 100 rpm mixing speed and 2 min mixing time	107

Figure 45. Effect of C-L-30% polymer dose on CST for 100 rpm mixing speed and 2 min mixing time 108

Figure 46. Cake solids concentration obtained from WZS and high speed laboratory centrifuge for the optimal dose of each polymer and from unconditioned SBW sludge 110

Figure 47. Capture efficiency and cake solids concentration for the optimal dose of each polymer determined by WZS 112

Figure 48. Capture efficiency and optimal dose for each polymer determined by WZS 113

List of Tables

Table 1.	Sodium Bearing Waste chemical composition	23
Table 2.	Summary of chemical precipitation mixing procedure variables	29
Table 3.	Mineql+ and Minteqa2 initial input conditions	35
Table 4.	List of metals analyzed during the precipitation pH study	70
Table 5.	List of metals analyzed during the precipitation pH study	70
Table 6.	List of optimal dose, cake solids, and filtrate solids for each polymer as determined by WZS and CST	89

INTRODUCTION

At the Idaho National Engineering Laboratory (INEL), approximately 1.5 million gallons of high-level radioactive waste is stored. The Department of Energy is investigating different procedures to reduce the volume of this waste and to ultimately provide for its safe disposal. Due to the high sodium and aluminum content of the waste, chemical precipitation through hydroxyl ion addition was suggested as one potential option. Chemical precipitation involves adjusting the pH of solution to minimize the solubility of dissolved species, thereby forming a solid precipitate (sludge). The resulting chemical sludge can then be mechanically dewatered to minimize the sludge volume and improve handling of the waste.

Although the metal precipitate from the INEL waste is expected to be a complex mixture of metals, the high aluminum content suggests that it may be similar to alum sludge which is generated in surface water treatment plants. In this study, processes and procedures which are commonly used for handling and dewatering alum sludge were investigated. These include polymer conditioning and dewatering by belt press and centrifugation. Studies have also shown that the chemical and physical conditions under which the solids are precipitated, including mixing speeds and base addition rates, can influence the precipitation

process. These will influence both the residual metal content of the solution and the characteristics of the sludge.

The purpose of this study was to:

1. Characterize the sludge quality and dewatering properties as a function of precipitation variations, including rate of base addition and impeller mixing speed.
2. Study the dewatering characterization of the chemical sludge, including specific resistance to filtration, capillary suction time (CST) and cake solids concentration, as precipitation conditions are varied.
3. Select and optimize the use of conditioning chemicals to enhance dewatering of the sodium bearing waste (SBW) sludge.
4. Evaluate sludge dewatering using the bench scale wedge zone simulator and laboratory centrifuge.
5. Perform computer aided precipitation modeling using Mineql+ and Minteqa2 to predict metals removal during the chemical precipitation.

LITERATURE REVIEW

This chapter will present a review of the methods for characterizing sludges, factors affecting dewatering rates of sludges, the role of polymers in chemical sludge conditioning, and selection and performance of sludge dewatering equipment. These will be followed by a discussion on mixing and rates of base addition and their effects on metal precipitation.

Measurement of Sludge Dewatering Rates

The specific resistance to filtration (SRF) is the most commonly used test for measuring the dewatering rates of sludges. (1) The SRF test is a laboratory procedure that measures the rate at which a sludge will dewater under vacuum pressure. The test is based on an analysis of pressure drop for flow through a porous medium using the Darcy equation. The resulting sludge characterization parameter, specific resistance to filtration, is related to cake permeability. Vesilind (1) reviewed the literature regarding the origin and derivation of the specific resistance parameter. See this source for further information.

The rate of filtration is inversely proportional to the

specific resistance as follows (2):

$$\frac{dv}{dt} \propto \frac{1}{r^n} \quad [1]$$

where:

dv/dt = volume of filtrate passing through the sludge
per unit of time

r = specific resistance of sludge

n = fractional power less than one

Specific Resistance may be calculated from the following
equations:

$$r = \frac{2 A^2 P b}{u c} \quad [2]$$

where:

r = specific resistance [m/kg]

p = pressure differential [newtons/cm²]

A = filter area [cm²]

u = viscosity of filtrate [newtons-sec/cm²]

b = slope of plot of t/v versus v [sec/cm²]

t = time [sec]

v = volume [cm³]

$$c = \frac{1}{\frac{100 - c_i}{c_i} - \frac{100 - c_f}{c_f}} \quad [3]$$

where:

c_i = initial moisture content [%]

c_f = moisture content of filter cake [%]

The greater the specific resistance, the greater the time required for filtration.

Christiansen and Dick (3) have modified the specific resistance test so it can be used universally with different types of sludges. They modified the Buchner Funnel test so high pressures could be used, along with improving the accuracy and precision. Novak and Knocke (4) discussed the results of Christiansen and Dick (3) and suggested that there are still too many disadvantages to the test, primarily the time consuming nature of the test. They felt it was an applicable index for gauging sludge dewatering characteristics, and it should be used the same way BOD tests are used as an index for strength of waste water. Karr and Keinath (5) concluded that specific resistance is a poor test for estimating actual vacuum or filter performance of the sludge. They found the specific resistance test to be very sensitive to the concentration of fines located in the sludge. This occurrence is especially critical when these fines cause blinding of the sludge and the filter media (5). This blinding of the cake or filter medium increases the measured resistance.

Gale and Baskerville (6) developed a substitute to the specific resistance test, called the Capillary Suction Time (CST) test, which is a fast and easy alternative to the specific resistance test. This test is simple to run,

provides much information on sludge dewaterability, and has gained wide spread acceptance for sludge testing according to Novak and Knocke (4). For a complete description and detailed mathematical analysis of the CST apparatus, see Vesilind (1).

POLYMERS

The use of polymers to condition sludges has been common practice for many years. Many researchers have found polymers to work effectively; finding that they had the ability to treat a wide variety of sludges. Polymers are long chained molecules comprised of various types of monomers that provide the macromolecules with varying properties. Polymer chains may be linear or branched and may carry a negative charge (anionic) or a positive charge (cationic). Cationic polymers are often of lower molecular weight than anionics and are usually used as coagulants for water clarification or for conditioning organic sludges. Anionic and nonionic polymers are primarily used for chemical sludge conditioning (2).

Polymer Flocculation Theory

Two primary types of polymer flocculation mechanisms are thought to occur. They are interparticle bridging and charge neutralization.

Chemical bridging theory states that coagulation of particles can occur by either the bridging of two or more particles by one polymer molecule, or by joining of the polymer chains that had been adsorbed onto different particles (7). It was determined by Knocke et al (8) that interparticle bridging was the mechanism of polymer action in conditioning of metal hydroxide sludges. Knocke (9) noted that when metal hydroxide sludges possessed specific resistance values between 30×10^{11} and 50×10^{11} m/kg, the best conditioning occurred when high molecular weight polymers were used. The addition of polymer increased the particle size and decreased the specific resistance. Karr and Keinneth (5) stated that the use of medium and high molecular weight polymers cause bridging to be the sole mechanism of flocculation. Snodgrass et al (10) concluded that for particles less than 1 μ m in size, perikinetic flocculation (Brownian motion) should dominate over orthokinetic flocculation as the rate controlling transport mechanism. Perikinetic flocculation primarily is a function of the number of particles and the efficiency of the particle collisions. It is independent of fluid shear (10).

Charge neutralization is based upon electrostatic attractions from opposite charged particles. When an opposite charged particle is added to the solution, ions will be immediately adsorbed onto the particle through

electrostatic attraction, resulting in the neutralization of the negative charge on the particle, and a lowering of repulsive forces (11). The following particles are then free to coagulate and settle more effectively.

Factors Effecting Dewatering Rates

The process of producing a properly conditioned sludge relies heavily upon many interrelated conditions. Proper mixing, coupled with the use of a compatible polymer at its optimal dose, should produce suitable results.

The purpose of mixing during conditioning is to provide uniform distribution of the polymer throughout the sludge and to enhance particle-coagulant contacts (12). Improper mixing can influence the required polymer dose for optimal conditioning. Too vigorous or prolonged mixing can cause floc shearing and degradation. Too little mixing does not provide enough agitation to cause adequate polymer - sludge interactions.

Agitation or mixing is the main force required for particle aggregation. As agitation increases, particle aggregation likewise increases. However, there is a point when vigorous and/or extended aggregation proves to be detrimental to the flocs already formed (12). This occurs because as the size of the flocs grow, they become weaker and more fragile.

Argaman and Kaufman (13) modeled turbulent flocculation, hypothesizing that the particles that are suspended in turbulent fluid can experience random motion. This random motion was characterized by a diffusion coefficient which could be easily measured from hydrodynamic properties from the bulk fluid flow. They observed that two process are responsible for changes in particle concentrations during flocculation. The first process was aggregation of small flocs and the primary particles to form larger flocs. Second was the breakup of flocs into smaller fragments. Their results concluded that particle release is a function of the surface shear, floc size, and the size of the primary particles (13).

Novak and Haugen (14) concluded that mixing altered sludge dewatering rates for waste activated sludge and the extent of the effect was related to mixing intensity. They believed that turbulence would release weakly adsorbed colloids from the floc structure of activated sludge, causing a reduction in the sludge filtration rate and increasing the dose required. (14). They also concluded that sludges conditioned under intense mixing are more resistant to deterioration than sludges conditioned under less intense mixing (14). However, these intense mixing conditions do require a larger polymer dose.

Bandak (12) stated that high shearing forces resulting from high mixing speeds will disaggregate the larger flocs into fragments and therefore dewatering sludge filtering rates will decrease through decreased porosity. Excess mixing causes floc rupture or rupture of polymer surface bonding when a sludge is conditioned with polymer by intense or prolonged mixing (2).

Knocke *et al* (8) concluded floc size is the most important character in determining the specific resistance of a metal hydroxide sludge. An increase in the mean floc size caused a decrease in the sludge specific resistance. This parameter had a much greater effect on the sludge than either solution pH or metal content (8). Clark and Flora (15) concluded at higher mixing speeds, smaller floc fragments are created, which provide an increase in sludge specific resistance.

The use of an optimal dose is critical to achieve the best dewatering rates. According to Novak and O'Brien (2), the optimal dose is the amount of polymer needed to achieve a maximum decrease in specific resistance or CST. In their study, the optimal dose occurred when a minimum specific resistance or CST occurred. The specific resistance or CST decreased rapidly as polymer was added and immediately increased when the system was overdosed. When polymer did

not predict a well defined minimum resistance, the point at which the change in resistance became small with increasing polymer dose was defined as the optimal dose (2).

Many studies have been conducted on the polymer properties and their corresponding influence on the sludge conditioning process. Among the more important properties are molecular weight, charge type, and charge density. The molecular weight of polymers has been suggested as the main factor affecting efficiency of conditioning sludges (16). Bowen and Keinath (16) stated medium and high molecular weight polymers affect both the solids content of the sludge cake and the compressibility in dewatering tests. Novak and O'Brien (2) found as the molecular weight increased in both anionic and cationic polymers, the optimal dose decreased.

The type of polymer used also plays an important role in dewatering rates. O'Brien and Novak (17) concluded cationic polymers were most efficient at pH values of 7 or below, while nonionic and anionic polymers were found to function effectively over a pH range of 6.5 to 8.5. In general, as pH increased, the effectiveness of the polymer decreased.

Mechanical Dewatering Equipment

Centrifuge

Centrifuges play a significant role in dewatering of sludges. They make use of centrifugal force to separate solids from the liquid phase. (11) Three different types of centrifuges are manufactured: solids bowl, disk, and basket models. The solid disk centrifuge which consists of a cylindrical bowl with a rotating screw-type conveyor is the primary type used in sludge dewatering. The sludge enters the bowl while the bowl rotates. The particles then adhere to the wall of the bowl, and are removed through the tapered end by a conveyor system. The free water normally drains out of the opposite end. The basket centrifuge use a perforated bowl. In this bowl, solids are retained and water passes out through the sludge cake. Problems can occur when fines clog the release holes (11).

Belt Filter Press

The belt filter press consists of a pair of continuous belts positioned between rollers which dewater sludges by squeezing them between the belts (18). Three zones are incorporated into the design of a belt filter press. They are the gravity zone, wedge zone, and high pressure zone.

The gravity zone is where the flocculated sludge is introduced to the belt and where the free water drains under the influence of gravity. The wedge zone is where the two belts come together and the sludge is first subject to pressure. The gravity drained sludge travels to this zone and the sludge is subject to increasing pressure. The last zone is the high pressure zone. Here, the forces are exerted due to the high pressure created by the decreasing diameter of the rollers, the remaining movement of the belts, and the drive torque of the machine (18). Figure 1 shows the schematic of the belt filter press. Several variables influence the performance of the belt filter press, including pressure exerted, the number of rollers, belt speed, belt type, sludge type, and sludge conditioning (18). Several researchers have used laboratory scale filter presses to evaluate belt filter press performance. In most cases, bench-scale piston presses or wedge zone simulators have been used with much success (19).

Chemical Precipitation

The importance of mixing and base addition in association with chemical precipitation has been studied by many researchers. The main focus will be by the works of Knocke (9), Vermeulen (20), and Clark (21). Knocke's studies dealt with the characterization of metal hydroxide

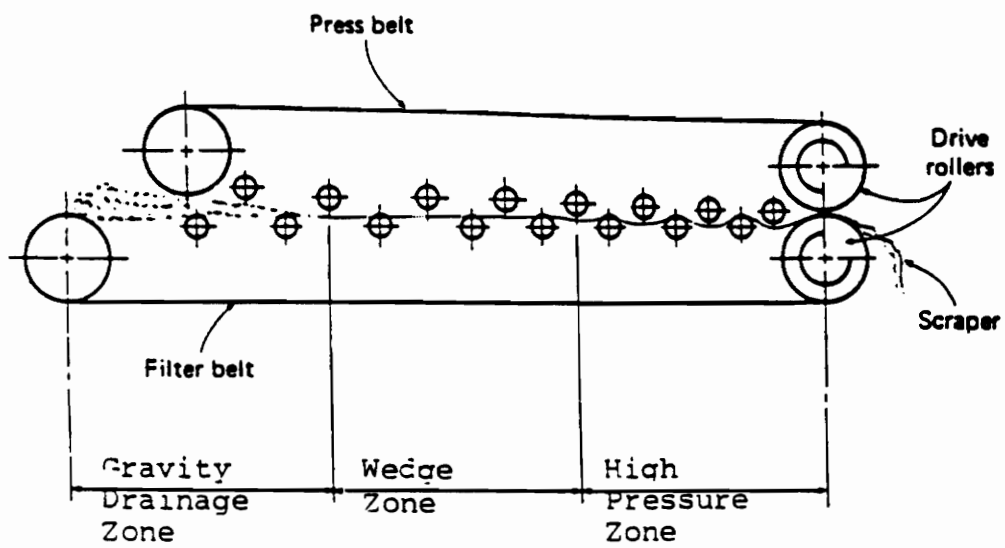


Figure 1. Standard belt filter press layout. From Reitz (18)

suspensions. Both Vermeulen and Clark studied aluminum precipitation. Due to the high concentration of aluminum in the SBW, most of the discussion will revolve around this metal. Discussion will involve role mixing speed and base addition play during the titration of aluminum solutions, along with the formation of many different aluminum species during the different stages of aluminum precipitation.

Knocke (9) studied the effect different types of metal hydroxide sludges had on the filtering rates. The study included various types of mixed metal sludges the effects each had on specific resistance, cake solids, and polymer conditioning. The study included chromium mixed metal sludge, iron and nickel sludge, copper and nickel sludge, and mixed chromium - cadmium - copper - and nickel containing sludge.

Most metal hydroxide sludges have low specific resistance values and high cake solids concentrations indicating favorable dewaterability characteristics. However, these sludges to possess the tendency to allow solids to breakthrough during filtration (9).

Coprecipitation accounts for the removal of a chemical species from a solution that normally would not be removed under the existing solution conditions. The process of coprecipitation was observed by Knocke (9) during his mixed

sludge study. The author observed that nickel, cadmium, and zinc all were coprecipitated with chromium. Even when trace amounts of chromium were added, the cations still coprecipitated. The mixed iron and nickel sludge, on the other hand, did not exhibit the feature of coprecipitation. Each of the cations were removed close to their actual theoretical insolubilization pH range. Knocke also concluded that not all trivalent cations participate in coprecipitation (9).

Vermeulen (20) proposed that during aluminum precipitation mixing, one must avoid localized hydroxyl ion concentrations that are much higher than the overall concentrations of hydroxyl ions. In order to eliminate localized OH^- variations, a baffled vessel was constructed for Vermeulen's (20) study that would allow proper agitation to the sludge and allow for the continuous observation of pH in the solutions to which base was added slowly. If proper mixing speeds were used, this mixing vessel would nullify the formation of local hydroxyl ion concentrations in the solution. The baffled mixing vessel used during the SBW study was constructed using Vermeulen's parameters.

The results of Vermeulen's (20) study indicated that rapid dropwise addition of alkali seems to eliminate the second platform of the titration curves generated (Figure 2,

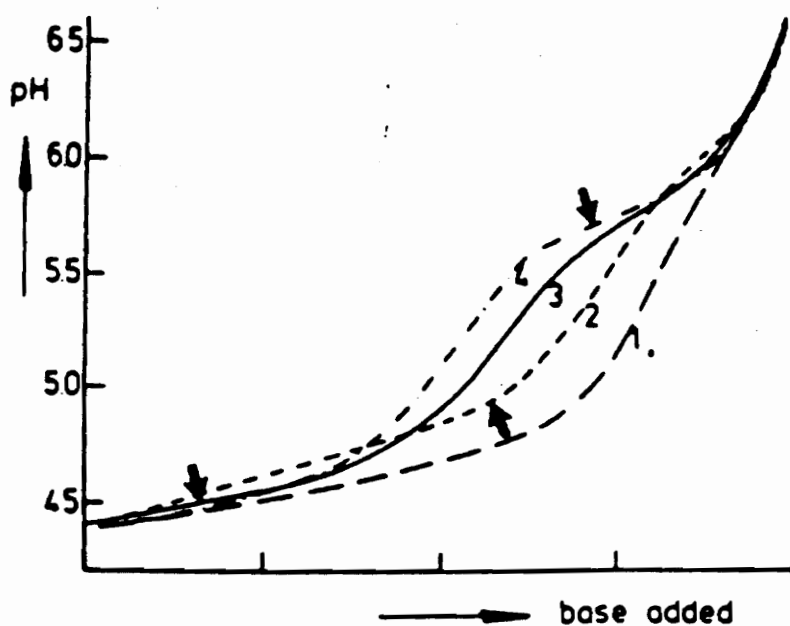


Figure 2. Vermeulen's illustration of the effect of methods of alkali addition on the shape of the pH curve at 25°C. From Vermeulen (20)

line 1) but during a much lower base addition rate, the platform still appears (lines 3 and 4). The appearance of a precipitate is also noted by the arrows in Figure 2 . In the fast addition procedure, a precipitate appeared at a pH value of 2.0. Vermeulen (20) concluded that the inflection point of the second increase in nitrate solutions lies at a OH/Al ratio of about 2.5. Before this point, no precipitate or colloidal particles were observed. Therefore the second platform may be associated with the formation of the solid phase. It was observed using light scattering experiments that indeed visible precipitate is always observed at an OH/Al ratio in excess of 2.5. The inflection point of the third pH increase falls at an OH/Al ratio of three. This determines the free valance point for the neutralization of the Lewis acid Al^{+3} . Vermeulen (20) also noted that if the hydroxyl ion concentration is rapidly and nonuniformly added to the system, a different type of behavior occurred. The solid phase is formed at a OH/Al ratio less than 2.5. This results in a second plateau that is obscured and possibly suppressed (20).

According to Clark (21), Smith and Hem (22) discovered that more polymeric aluminum was formed when the titration of Al^{+3} was carried out at the slowest rate of base addition. During Clark's (21) study of aluminum precipitation, he noticed a delayed upward swing in pH

associated with higher mixing speeds. Clark (21) proposed this is not consistent with the formation of higher ligand number species like aluminum hydroxide ($\text{AlOH}_3(\text{s})$). The earlier upward pH swing at the lower mixing speeds (less than 500 rpm) is associated with the formation of more polymeric species that may buffer less hydroxyl ions from the base. Clark concluded that during lower mixing speeds (less than 500 rpm), almost no aluminum is converted to the solid precipitate. Clark also concluded mixing at different speeds during the titration process causes variations in solid and polymeric species throughout the titration curve, not just in the steady rising region of the titration curve. Therefore the competition between polymeric and solid species is mixing sensitive throughout nearly the entire titration. Clark (21) concluded that intense mixing is only desired if polymeric species are desired.

Snodgrass, et al (10), noted the formation of aluminum fulvate and aluminum hydroxide is accomplished by two different reactions competing for the aluminum. They created a conceptual pathway model for formation of aluminum particles in dilute aluminum solutions. Their model concluded pH as the most important controller of particle formation, and ionic strength as secondary importance. See this source for further details of this study (10).

Many different polymeric forms of aluminum are thought to exist over a wide pH range. At pH values below 10, the solids are found to be either amorphous or microcrystalline (20). At temperatures below 60°C, the material is either amorphous or poorly crystallized bayerite. These precipitates consist of very small particles that are difficult to separate from liquid phase by filtration (20). At pH 10, well crystallized bayerite is then present. If a precipitate is formed at 60°C and pH of 10, gibbsite is formed.

Recycling of sludge (chemical seeding) to induce the formation of more crystalline and less amorphous precipitates was studied by Knocke and Kelley (23). The results showed that less water was incorporated into the metal hydroxide sludge floc matrix when sludge recycling was used. A lower sludge specific resistance to filtration occurred due to an increase in characteristic sludge floc size. Sludge floc density also increased, producing higher dewatered cake solids.

The reversal of titration by adding the acid to the solution was studied by Stol et al (24). The authors showed that if the rate of acid titration is slow enough, it should be possible to obtain complete reversibility. However, at

OH/Al ratios exceeding 2.5, the acid titration curves suggested that the dissolution process is simply not a reverse of the precipitation process. At OH/Al ratios below 0.5, both of the processes are fast. They proposed the slow step in this reverse reaction is the loosening of the bridged bond Al-OH-Al, which is followed by a faster step of water molecule uptake. At OH/Al ratios less than 0.5, mainly monomeric species are present; therefore no bridged hydroxyls are present. Stol et al (24) concluded that singly bound OH ions (not bridged) in monomeric species should react rapidly with the acid. They observed that slow acid kinetics at higher OH/Al ratios could be interpreted as a slow attack of bridged hydroxyls by the acid. Slow kinetics result in the predominance of bridged OH- over individually bound hydroxyls in OH/Al ratios up to 2.5 (24).

Stol et al (24) also observed the effect of increasing ionic strength. Light scattering results testify that increased polymerization on addition of salts is incurred by a more effective screening of the high positive charge of the ionic aggregates by the anions NO_3^- and Cl^- .

METHODS and MATERIALS

The research was performed to evaluate the solids resulting from a precipitation process for the Sodium Bearing Waste (SBW) simulant provided by the Idaho National Engineering Laboratory (INEL). It was proposed that the simulant be treated by base precipitation, and the resulting sludge be conditioned with organic polymers. The precipitation study investigated the manner by which precipitation variables influenced sludge properties. The polymer study entailed observations of the conditioning abilities of various polymers. The Wedge Zone Simulator and the Capillary Suction Time apparatus were the primary methods to evaluate polymer performance. The equipment and materials used in these studies as well as methods employed are described in this section.

Sodium Bearing Waste

The INEL has approximately 1.5 million gallons of liquid radioactive waste in storage. A listing of the representative chemical composition of the Sodium Bearing Waste (SBW), and the SBW simulant used throughout the study is shown in Table 1. The simulant provided by the INEL was created to provide a safer working environment due to the high radioactivity of the SBW. The simulant was stored in

Table 1. Sodium bearing waste chemical composition

	Hot Waste[ppm]	Simulant[ppm]
pH	-0.38	-0.38
specific gravity	1.2	1.2
Acid H+	1.5	2.96
Aluminum +3	14700	17700
Americium-241	1.77×10^{-5}	
Antimony-125	2.4×10^{-4}	
Arsenic +3	3.3	
Barium +2	6.3	
Boron +3	168.3	174
Cadmium +2	206.6	229
Calcium +2	1745.4	1370
Cerium-134	2.79×10^{-5}	
Cesium +1	42.408	10
Chloride -1	815.7	1140
Chromium +3	298.4	306
Cobalt-60	1.42×10^{-4}	
Europium-154/4	2.43×10^{-3}	
Fluoride -1	1200	1800
Iodine-129	142	
Iron +3	1369.5	1530
Lead +2	236.5	212
Manganese	790.5	796
Molybdenum +6	59.5	86
Mercury +2	407.9	570
Nitrate -1	264700	270940
Neptunium-237	1140	
Nickel +2	128.7	104
Phosphate -3	896.5	<871
Plutonium (tot)	4.56×10^{-3}	
Potassium +1	6000	5900
Selenium +4	2.4	
Silver +1	1.9	
Sodium +1	30500	30000
Sulfate -2	3100	1248
Strontium-90	0.561	12
Technetium-99	1.0	
UDS	1600	

two - 20 liter (L) sealed containers for secure storage in the laboratory. Because of the extreme acidic and toxic nature of the simulant, extreme caution was used when working with the waste directly or with any of its related byproducts.

Buchner Funnel Apparatus and Capillary Suction Time

The Buchner Funnel apparatus is commonly used to characterize sludge dewatering by determining the specific resistance to filtration of a sludge. The system apparatus is shown in Figure 3.

The Buchner Funnel apparatus consisted of a cylindrical funnel placed atop a 100 mL graduated cylinder fitted with a two hole rubber stopper. The second opening allowed a vacuum to be fitted to the system. The Buchner Funnel was fitted with a Whatman No. 40, 7 cm diameter ashless filter paper. When the sludge was placed into the funnel and the vacuum started, total suction time and filtrate volume were noted. Cake, total, and dissolved solids were then determined according to *Standard Methods for the Examination of Water and Wastewater* (25).

The other dewatering test performed was the Capillary Suction Time (CST). The CST indicates relative sludge dewatering abilities by measuring sludge water release times.

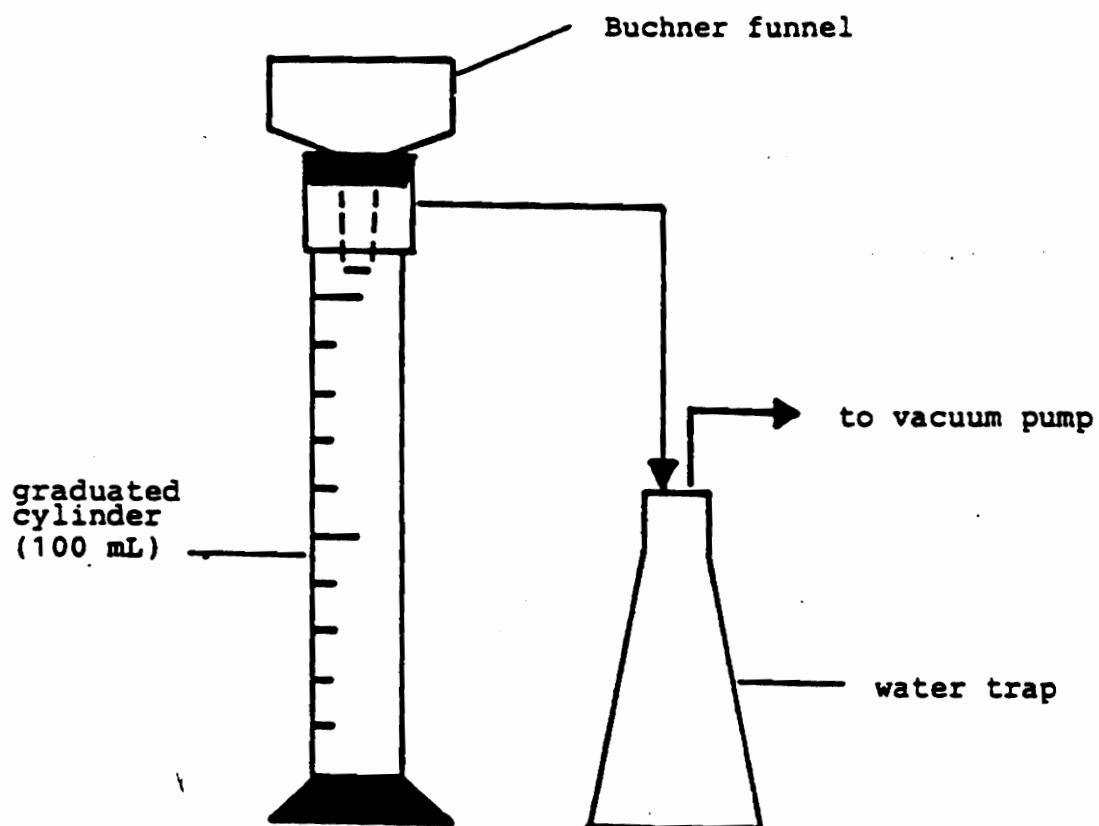


Figure 3. Buchner Funnel apparatus. From Reitz (18)

As previously described by Vesilind (1), the CST device consists of two plastic blocks, a stainless steel collar, a piece of Titron CST chromatography paper, three electrical contacts that are fixed in the upper plastic block, and an electrical timer. Figure 4 shows a diagram of the described configuration. The test starts by pouring approximately 5 mL of sludge into the stainless steel collar. The water begins to flow through the filter paper. After the water interface flows 0.8 cm past the collar edge it makes contact and trips the timer. After the water interface moves another 0.7 cm, it trips another contact which stops the timer. The capillary suction time is then read from the timer and reported in seconds. Sludges that release their water slowly have high CST values. Sludges that readily release their water have low CST values (1).

Sludge Precipitation Procedures

The purpose of this phase of the study was to investigate precipitation conditions that may influence the properties of sludges. The items of interest included:

- Effect of solution pH on sludge characteristics
- Effect of mixing speed on sludge characteristics and calcium and aluminum solubility
- Effect of rate of base addition on sludge characteristics and calcium and aluminum solubility

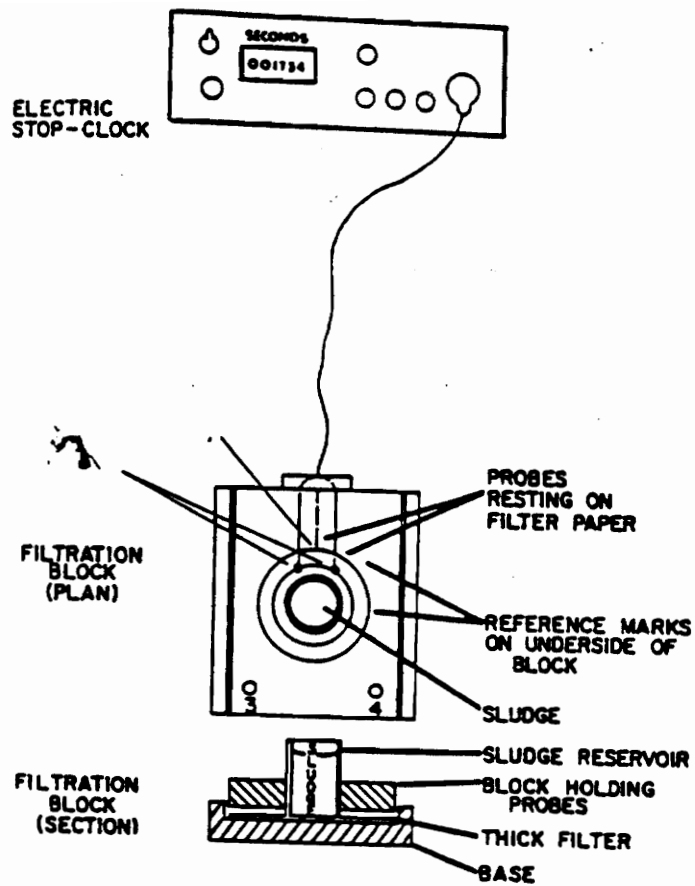


Figure 4. Capillary Suction Time apparatus. From Bandak (12)

- Effect of adding SBW to base (reverse addition) on sludge characteristics
- Effect of calcium spiking the SBW coupled with reverse addition

The previously mentioned procedures involved very similar processes in precipitating the SBW sludge. The next section will describe the standard mixing procedure that was common for most of the precipitation study. The sections following the standard mixing procedure will describe any variations to this procedure needed to perform the study. A summary of the precipitation variations is located in Table 2.

Standard Mixing Procedure

Both a Cole-Palmer variable speed mixer and a high power (1/3 Hp) Sears upright drill press were utilized in this experiment. The lower speed rates were performed with the Cole-Palmer mixer, while the higher rotational speeds utilized the larger mixer.

Two hundred milliliters of SBW was measured in a graduated cylinder and gently poured into the plexiglass baffled mixer previously described in this chapter. The 63.5 mm by 12.7 mm metal paddle was attached to the mixing motor device, and the mixer was adjusted to the proper

Table 2. Summary of chemical precipitation mixing procedure variables

Procedure	Mixer rpm	Base Addition Time	Solution pH	Special Notes
Mixing Speed	50-3000	10 min	9.5	mixing speed changed for each test
Base Addition	430	0-1200 min	9.5	base addition rate changed for each test
Reverse Addition	100	1,8,17 min	9.5	SBW added to base
Spiked Reverse Addition	100	10 min	9.5	Ca(OH) ₂ spiked SBW added to base
pH Study	430 & 1870	10 min	5.0-10.0	base added until proper pH reached

mixing rotational speed (between 50 and 3000 rpm). While the mixer was rotating, two molar sodium hydroxide (base) was added at a rate such that a sludge pH of 9.5 could be reached within 10 minutes. Precipitation pH 9.5 was initially chosen because of high metals removal. The probe of the pH meter was placed into the sludge after the solution color changed from blue to brown. The mixing and base addition was stopped when the solution pH reached 9.5.

If the CST needed to be determined, sludge was withdrawn from the mixing vessel using a pipette fitted with a suction bulb. The withdrawn sludge was then transferred to the CST apparatus and the corresponding CST value determined.

For specific resistance determinations, 50 mL of the sludge was withdrawn from the mixing vessel and transferred to the Buchner Funnel apparatus. The sludge was poured into the top of the holding apparatus, above a clean Whatman No. 40, 7 cm diameter ashless filter paper. A vacuum of 20 psi was applied to the sludge. The time for the filtrate volume (10, 15, 20, 25, and 30 mL) to accumulate in the graduated cylinder was recorded.

The cake that was accumulated atop the ashless filter paper was carefully removed and analyzed for moisture content. Approximately 10 mL of filtrate was analyzed for total suspended solids. These two analysis were performed

according to the procedure described in *Standard Methods for the Examination of Water and Wastewater* (25).

The remaining sludge supernatant liquor was vacuum filtered through a 0.45 μm glass filter to remove any remaining suspended material. The filtered sample was then poured directly into an acid washed, 200 mL storage container. The sample was acidified with concentrated nitric acid until the solution pH was at or below 2.0 and then stored for a metals analysis.

pH Study

The solution pH was varied to see what effect this had on the SBW sludge characteristics and metal removal efficiencies. The removal of calcium and aluminum were of particular interest due to their high initial concentration in solution and to their ability to promote clogging of the ion exchanger located downstream in the proposed treatment process. The mixing procedure was similar to the standard mixing procedure except for a few differences. Two different mixing speeds were used: 430 and 1870 rpm. A complete set of data was obtained for each of the mixing speeds. The base was added to the acid at a rate of one drop per second, with a maximum addition time of 10 min. The titration was halted when the proper solution pH was reached. The range of pH values studied were between pH 5.0

and pH 10.0, at 0.5 pH unit intervals. Also, a metals analysis of the supernatant liquor was performed by Atomic Adsorption.

Mixing Speed Study

The mixing speed study incorporated most of the procedures previously described. A wide range of impeller rotational speeds was utilized to determine the effect of mixing speed on the SBW precipitation. The rotational speeds used were between 50 and 3000 rpm, with 3000 rpm being the highest rotational speed achievable using the laboratory equipment available. The base was added dropwise until the pH of the solution reached 9.5. The entire addition was completed within 10 minutes.

Base Addition Study

The base addition study also incorporated much of the standard mixing procedure previously detailed. The two molar (2M) sodium hydroxide (NaOH) was added at different rates to determine the effect of base addition on the precipitation of SBW sludge. The impeller mixing speed was 430 rpm. The time of base addition ranged from immediate addition to 1200 minutes. During each of the tests, the rate of base addition was kept constant throughout the entire time period.

Reverse Addition Study

The addition of SBW dropwise to the base was studied to determine what effect this reverse addition would have on the characteristics of the precipitates and the precipitation process. Approximately 150 mL of 2M NaOH was placed in the baffled mixing vessel and stirred at 100 rpm. The acid was added to the base at such a rate that the solution pH of 9.5 was reached in either 1, 8, or 17 minutes. The remaining standard mixing procedure was then followed.

Spiked Reverse Addition Study

This procedure involved spiking the SBW with known amounts of calcium hydroxide ($\text{Ca}(\text{OH})_2$), and adding this spiked mixture to the base as described in the reverse addition study. The effects of calcium spikes on the precipitation process were observed. The impeller mixing speed was kept constant at 100 rpm. The acid was added to the base at such a rate that the solution pH of 9.5 was achieved in 10 minutes. The amount of spiked $\text{Ca}(\text{OH})_2$ dissolved into the SBW ranged from 0.5 times to 10 times the initial calcium concentration (130 mg to 2500 mg of $\text{Ca}(\text{OH})_2$ per 100 mL SBW) in the SBW.

Mineql+ and Minteqa2 Chemical Equilibrium Modeling

Chemical equilibrium modeling of the SBW was performed by Mineql+ and Minteqa2. Both programs provided chemical equilibrium data from theoretical SBW titrations with sodium hydroxide.

Mineql+ was developed by William Schecher and Drew McAvoy (26) at The Procter and Gamble Company. This program was originally developed to solve mass balance expressions using equilibrium constants. Mineql+ uses the Minteqal thermodynamic database with additional data from the original Mineql database. Minimization of Gibbs Free Energy and chemical speciation solves the complex chemical equilibrium problems.

Minteqa2 is a geochemical equilibrium speciation model capable of computing equilibria among dissolved, absorbed, solid, and gas phases. Minteqa2 was developed by Jerry Allison, David Brown, and Kevin Novo-Gradac (27) at the Environmental Research Laboratory of the U.S. Environmental Protection Agency.

A summary of input conditions and molar concentrations of the species used are displayed in Table 3.

Table 3. Mineql+ and Minteqa2 initial input conditions

Component	Initial Molarity [M/L]
H ₂ O	0.61
H ⁺	1.0e-4
Al ⁺³	0.65
Ca ⁺²	0.0342
Cl ⁻	0.0321
Fe ⁺³	0.0274
K ⁺	0.151
Mn ⁺²	0.0145
Na ⁺	1.30
NO ₃ ⁻	4.37
PO ₄ ⁻³	0.00917
SO ₄ ⁻²	0.0130

- Solution temperature kept constant at 25°C
- Ionic Strength corrections made automatically
- pH varied from 4 to 10

Polymer Preparation

A variety of polymers were used in this study. Polymers of various mole charges, ionic strengths, and cationic and anionic charges were used.

Stock polymer solutions were prepared in advance of the chemical sludge conditioning and were kept refrigerated for a maximum of five days. The stock solutions were prepared with distilled water. The polymer solutions were in liquid form. The solutions were prepared by adding the appropriate volume of distilled water into the plastic jar and injecting the polymer with a plastic 10 mL syringe. A 0.5% by weight polymer solution was used. The solutions were then mixed with the caged impeller powered by the variable speed motor. The rotational speed of the impeller was high enough to cause a mild vortex to form within the polymer solution. The solution was mixed for 30 minutes. The 0.5% solution created a polymer by volume equal to 10,000 mg/l.

Mixing Apparatuses

Several different mixing apparatuses were used. During the polymer addition phase of the study, a Cole-Palmer variable speed jar test apparatus was used. The motor rotated a 63.5 mm by 12.7 mm metal paddle inside a 500 mL unbaffled, circular, plexiglass vessel.

When generating the SBW sludge for the polymer study, a Sears 13 inch, five speed, one-third horse power upright drill press was utilized. The large mixer rotated a 63.5 mm by 12.7 mm metal paddle. A cylindrical, plexiglass, baffled mixing chamber measuring 94.0 mm in diameter and 216 mm high was used to mix the sludge. Four, 12.7 mm baffles positioned 90 degrees apart were positioned lengthwise in the cylindrical mixing chamber.

For most of the precipitation study, a Cole-Palmer variable speed stirring motor mounted on a ring stand and positioned above the baffled mixing chamber was used. The speed of the motor was controlled by a Fischer Scientific variable speed auto transformer wired to the Cole-Palmer mixing controller. Again, the motor rotated a 63.5 mm by 12.7 mm metal paddle. The rpm of the mixer for a given mixer setting was measured with a General Radio Strobotac strobe light.

Wedge Zone Simulator

The wedge zone, free drainage zone, and high pressure zone of a belt filter press were simulated with a Wedge Zone Simulator (WZS). The design was similar to a field testing unit developed by the Aris Andritz Company and described by Burgos (19).

The simulator consisted of a pneumatic cylinder fitted over a box type dewatering chamber. The entire chamber rested on two 10 cm x 10 cm x 25.4 cm blocks to provide clearance for a 250 mL graduated cylinder. The pneumatic cylinder (Ashcroft A38) pressure was regulated with a standard air pressure regulator. The on-off operation of the pneumatic cylinder was accomplished by a dual action pneumatic switch (Atlas Copaco VA 15 HB2-5).

The actual dewatering chamber consisted of a square plexiglass box, 10 cm square by 8.5 cm deep. The box was open at the top and the bottom was sealed with a 1.5 mm rubber gasket. Both the gasket and the plexiglass bottom were drilled with a matrix arrangement with 3 mm holes for the drainage of the filtrate. The box bottom was fitted with a piece of actual filter belt fabric placed over the holes. The top ram component of the dewatering chamber was similar to the bottom, but smaller so it would fit tightly into the first box. A piece of filter fabric was placed on top of the sludge sample before the top box was placed inside the bottom. This setup effectively sandwiched the sludge between the two pieces of filter fabric (19).

The pressure applied to the sludge in the WZS was a function of pressure applied to the pneumatic cylinder. A conversion factor of 0.31 psi applied to the sludge per psi gauge applied to the cylinder was determined by Reitz (18).

The pressure used in the WZS polymer experiments was 20 psi gauge, translating to 6.2 psi applied to the sludge.

Polymer Experimental Procedures

Polymer conditioning experiments were used to determine the effectiveness of polymers on SBW sludge dewatering. The Wedge Zone Simulator and the Capillary Suction Time were used to determine the effect of polymers on dewatering. Other sludge measures included cake solids content of the dewatered sludge, filtrate solids of the supernatant, and free drainage volume of the filtrate. The free drainage volume was the volume of filtrate to pass through the bottom piece of filter fabric within one minute under gravity (19).

The sludge was produced in approximately 800 mL aliquots. Three hundred milliliters of the SBW was emptied into the plexiglass baffled mixing chamber. A 500 mL pipette filled with two molar sodium hydroxide (base) was placed above the mixing vessel, and one drop of base per second was added to the mixing chamber. A mixing speed of 1170 rpm was used to ensure adequate interaction between the SBW and the added base. This rate was rapid enough to allow the pH of the sludge solution to reach 9.5 in approximately 15 minutes. When the solution changed colors from blue to brown, the probe of the Fisher Accunet pH Meter Model 610 was placed inside the mixing chamber. This probe was placed

into the solution during this stage of the titration so it would not be damaged by the very acidic conditions and to extend the operational life of the probe. When the pH reached 9.5, the mixer was stopped, and the mixing vessel was removed from the large mixer.

A series of simple tests were performed in order to determine the optimal mixing conditions for polymer conditioning. The procedure involved adding various doses (6.2, 8.7, and 12.5 mg/kg) of a medium molecular weight anionic polymer to the 100 mL sludge sample, and mixing at a specific rpm (50, 75, and 100 rpm) for a maximum of 10 minutes. At various time intervals, the mixer was stopped and sludge removed for CST testing. The data obtained was used to create graphs of CST versus mixing time (see Figures 33, 34, and 35). Based on the data, a mixing time of 2 minutes and a mixing speed of 100 rpm was selected.

Conditioned sludges were tested using the WZS. One hundred milliliter samples of conditioned sludge were poured directly onto the filter fabric in the bottom dewatering chamber located in the WZS. The drainage time measurements began when the conditioned sludge contacted the filter fabric. The cumulative volume of the filtrate was measured in a 100 mL graduated cylinder located below the filtrate funnel at times of 10, 30, 50, and 60 seconds. Between the

30 and 60 second readings, the other piece of filter fabric was placed on top of the sludge in the lower box. The upper box was then placed on top of the second piece of filter fabric. After one minute of free drainage, an applied pressure was exerted by the pneumatic cylinder onto the upper box of the dewatering chamber. Filtrate volume continued to be measured at 30 second time intervals for 4 minutes, at which the pressure was stopped and the test completed. The total cycle time was 5 minutes.

Solids determination for the filter cake and the filtrate were determined with the procedure described in *Standard Methods for the Examination of Water and Wastewater* (25).

Centrifuge Procedure

High speed centrifugation was studied using a laboratory centrifuge. Previously mixed SBW sludge (100 mL) was conditioned with each of the polymers used in the previous polymer conditioning study. The optimal dose of each of the polymers was used. Approximately three 10 mL samples of the conditioned sludge were then poured into centrifuge tubes, and inserted into a Beckman Model J-21C high rate laboratory centrifuge. The samples were rotated at 15000 rpm for 10 minutes. The resulting cake solids

content was then determined according to *Standard Methods for the Examination of Water and Wastewater* (25).

RESULTS and DISCUSSION

Data obtained during this research were significant in that they clearly indicate the effects of mixing speed, base addition, and polymer addition on the properties of chemical sludges. The data showing the effects of various parameters on the characteristics of sludges will be presented and discussed in the following order:

- pH
- Base (2M NaOH) addition rates
- Reverse base addition
- Reverse base addition incorporated with a calcium hydroxide ($\text{Ca}(\text{OH})_2$) spike addition
- Mineql+ and Minteqa2 equilibrium modeling
- Sludge Conditioning

CHEMICAL PRECIPITATION

pH Study

This portion of the study focused on the effects of precipitation pH on the sludge characteristics and metals removal. The removal of calcium and aluminum was studied because of concern about the possibility of these metals clogging the proposed ion exchanger downstream. The sludge

characteristics studied included specific resistance, CST, and dissolved species removal efficiency.

The base was added to the SBW at a constant rate until the predetermined solution pH was reached. The pH range during this procedure was between pH 5.0 and 10.5. The entire procedure was completed using two different mixing speeds: 430 and 1870 rpm. Each precipitation pH test was conducted separately opposed to increasing the pH over a range and collecting samples over a range of pH values. In this way, the time for precipitation was equal for all tests.

The data for specific resistance as a function of precipitation pH for the mixing speed of 430 rpm are shown in Figure 5. At the low solution pH values, the specific resistance low. The sludge improved more as the pH increased, providing an minimum specific resistance between pH 8.0 and 9.0. The lowest specific resistance value was 3.5×10^{11} m/kg. Since the highest specific resistance achieved was 8.0×10^{11} m/kg, the sludge exhibits good dewatering characteristics regardless of solution pH. It should be noted that with most sludge characterizations, some variability was seen in the samples where pH was varied. While procedures were maintained as consistent as possible, variations occurred, possibly because of localized pH variations.

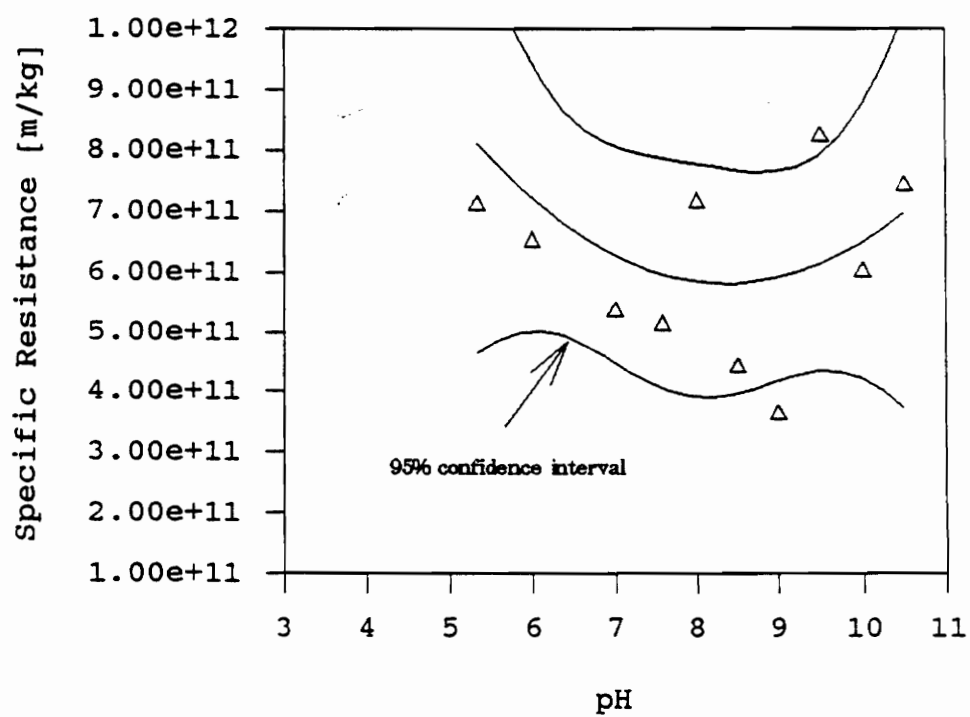


Figure 5. Effect of solution pH on specific resistance for 430 rpm mixing speed at 10 min 2M NaOH addition time

The specific resistance results for the 1870 rpm mixing speed are displayed in Figure 6. These results are more variable than those obtained at the 430 rpm mixing speed, with the best sludge produced at a pH of 9.5.

The cake solids data are presented in Figures 7 and 8. For both mixing speeds, the highest cake was achieved at the lower range of pH values (between pH 5.5 and 7.0). As the solution pH increased, the cake solids decreased to below 20%.

The supernatant liquor samples remaining after each of the samples were analyzed for several metals. A list of soluble metal concentrations is shown in Tables 4 and 5. The residual calcium concentrations in the liquor supernatant are displayed in Figure 9. Both mixing speeds provided identical results. At the lowest solution pH, the amount of soluble calcium species in solution was highest. As the pH increased, the amount of calcium steadily decreased, until trace amount remained at pH 10.0.

Mercury results are shown in Figure 10. The removal is very efficient at pH levels above 9.0. Apparently mixing plays a critical role at lower solution pH. The lower mixing speed removes less mercury, although the reason behind this could not be determined. Boron (Figure 11) removal is effective

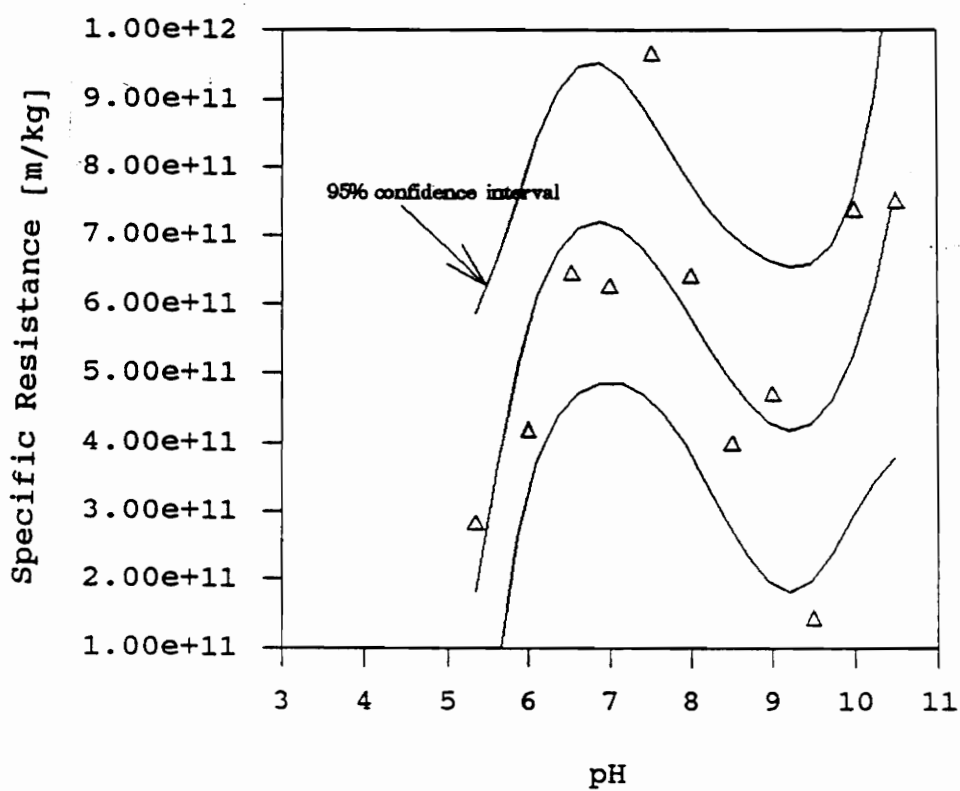


Figure 6. Effect of solution pH on specific resistance for 1870 rpm mixing speed at 10 min 2M NaOH addition time

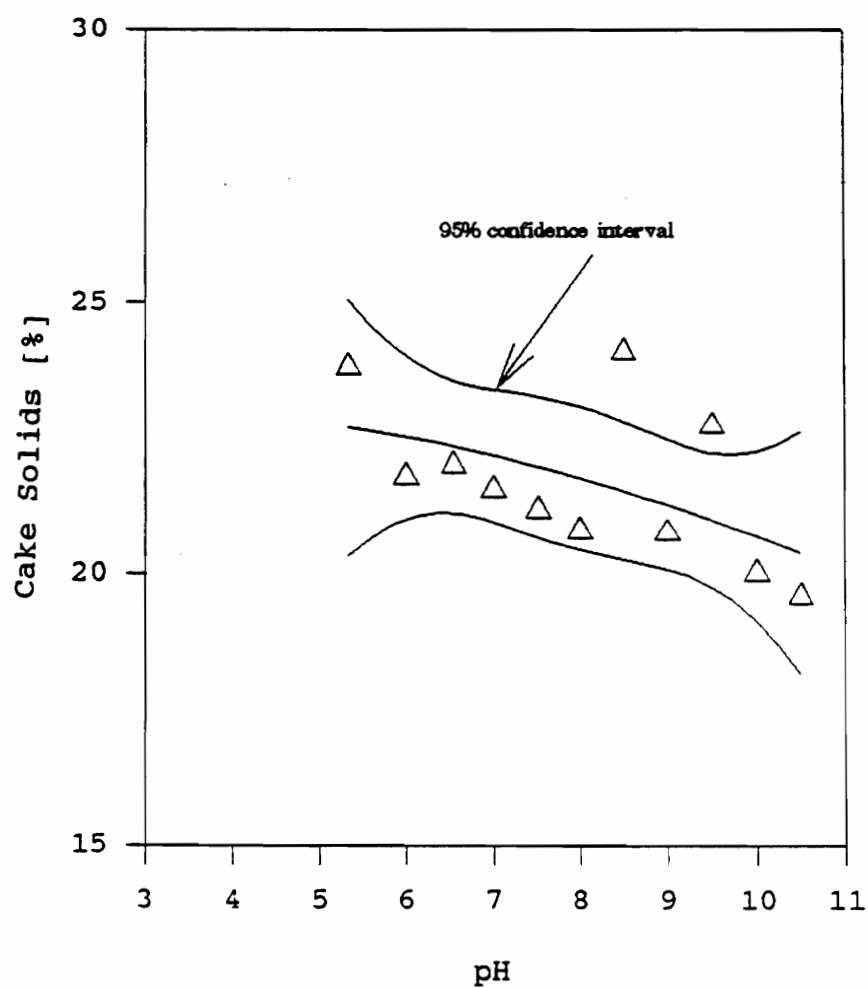


Figure 7. Effect of solution pH on cake solids concentration for 430 rpm mixing speed at 10 min 2M NaOH addition time

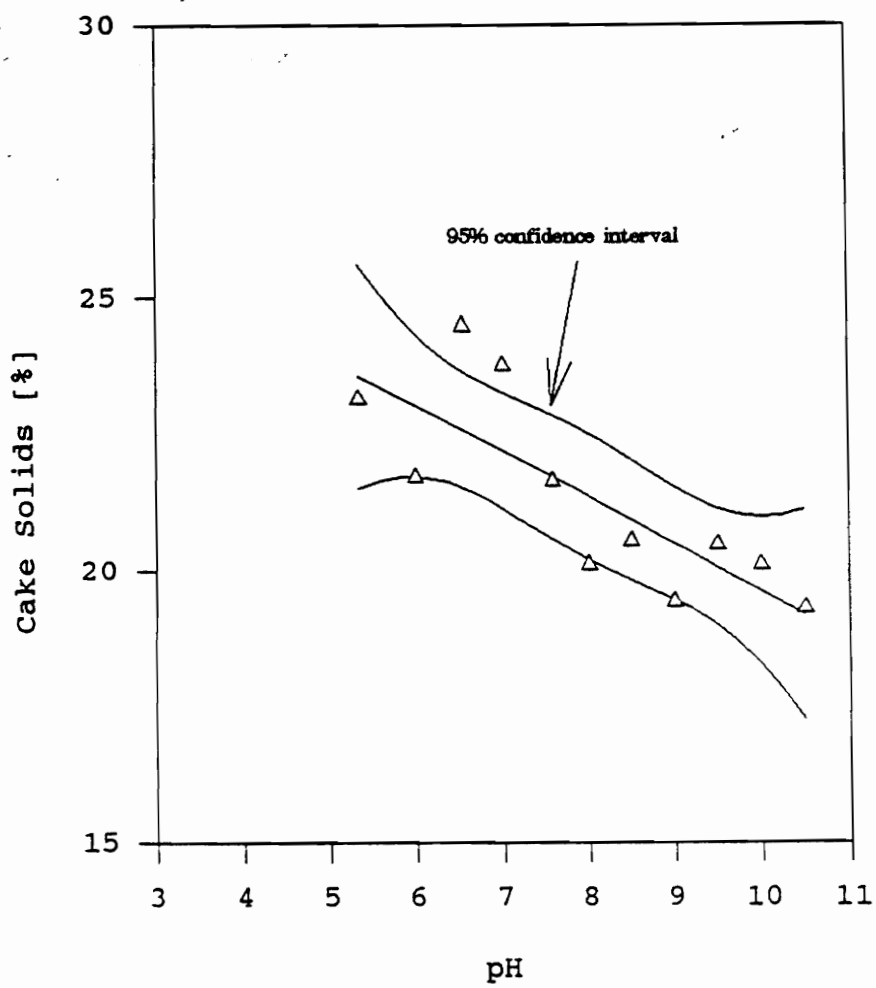


Figure 8. Effect of solution pH on cake solids concentration for 1870 rpm mixing speed at 10 min 2M NaOH addition time

Table 4. Results of the metals analysis during the precipitation pH study

pH	Ca ⁺²		Hg ⁺²	
	430 rpm	1870 rpm	430 rpm	1870 rpm
5.3	42.5	42.3	48.8	5.3
6.0	40.5	39.5	22.6	1.0
6.5	41.1	39.5	7.9	0.43
7	38.3	36.8	19.7	0.76
7.5	32.8	34.0	2.9	3.0
8.0	20.7	29.4	5.3	7.3
8.5	22.8	29.5	2.9	2.5
9.0	17.4	17.1	1.0	0.72
9.5	10.0	12.2	0.5	0.15
10.0	5.0	3.6	0.13	<0.01
10.5	2.1	1.6	0.05	<0.01

pH	Mo [mg/l]		B ⁺³ [mg/l]	
	430 rpm	1870 rpm	430 rpm	1870 rpm
5.3	<0.01	<0.01	41.2	43.0
6.0	<0.01	<0.01	30.3	24.0
6.5	<0.01	<0.01	17.5	13.9
7	<0.01	<0.01	10.3	7.5
7.5	<0.01	<0.01	0.06	2.5
8.0	<0.01	<0.01	<0.01	<0.01
8.5	<0.01	<0.01	<0.01	<0.01
9.0	<0.01	<0.01	<0.01	<0.01
9.5	<0.01	<0.01	0.66	<0.01
10.0	0.32	0.029	7.7	10.3
10.5	1.16	0.94	19.2	24.2

Table 5. Results of metals analysis during precipitation pH study

pH	Ni [mg/l]	Mn [mg/l]	Cd [mg/l]	Pb [mg/l]	Fe [mg/l]
5.0	17.45	470	32.0	8.1	0.6
6.0	6.1	346	8.95	2.0	0.6
7.0	1.4	75	0.9	2.0	0.6
8.0	1.9	18.9	0.6	2.7	1.0
8.5	1.85	34.8	0.7	2.6	1.0
9.0	2.1	4.9	0.5	2.6	0.9
9.5	2.1	0.1	0.5	2.3	0.9
10.0	2.2	0.1	0.4	2.3	0.9
10.5	2.2	0.1	0.5	2.2	1.0
11.0	2.3	0.1	0.5	2.4	1.1

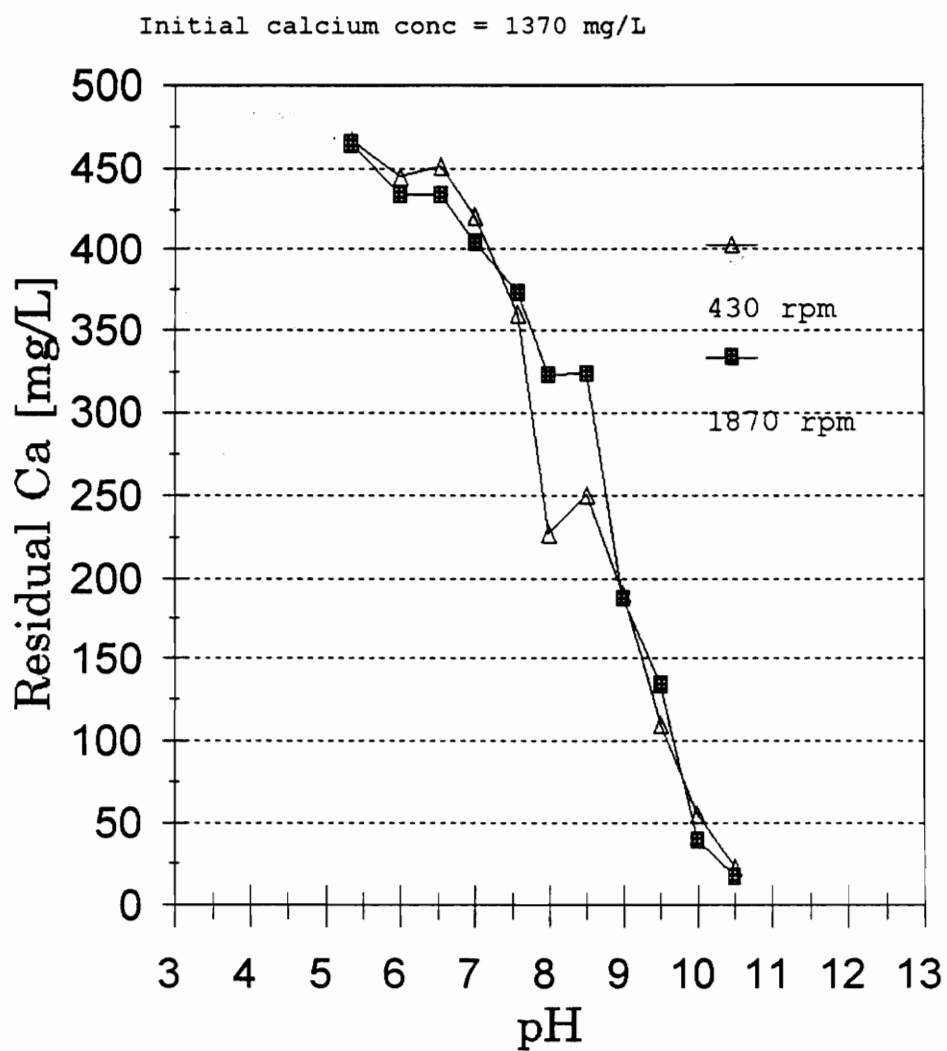


Figure 9. Effect of solution pH on residual calcium concentration for 430 and 1870 rpm mixing speeds at 10 min 2M NaOH addition time

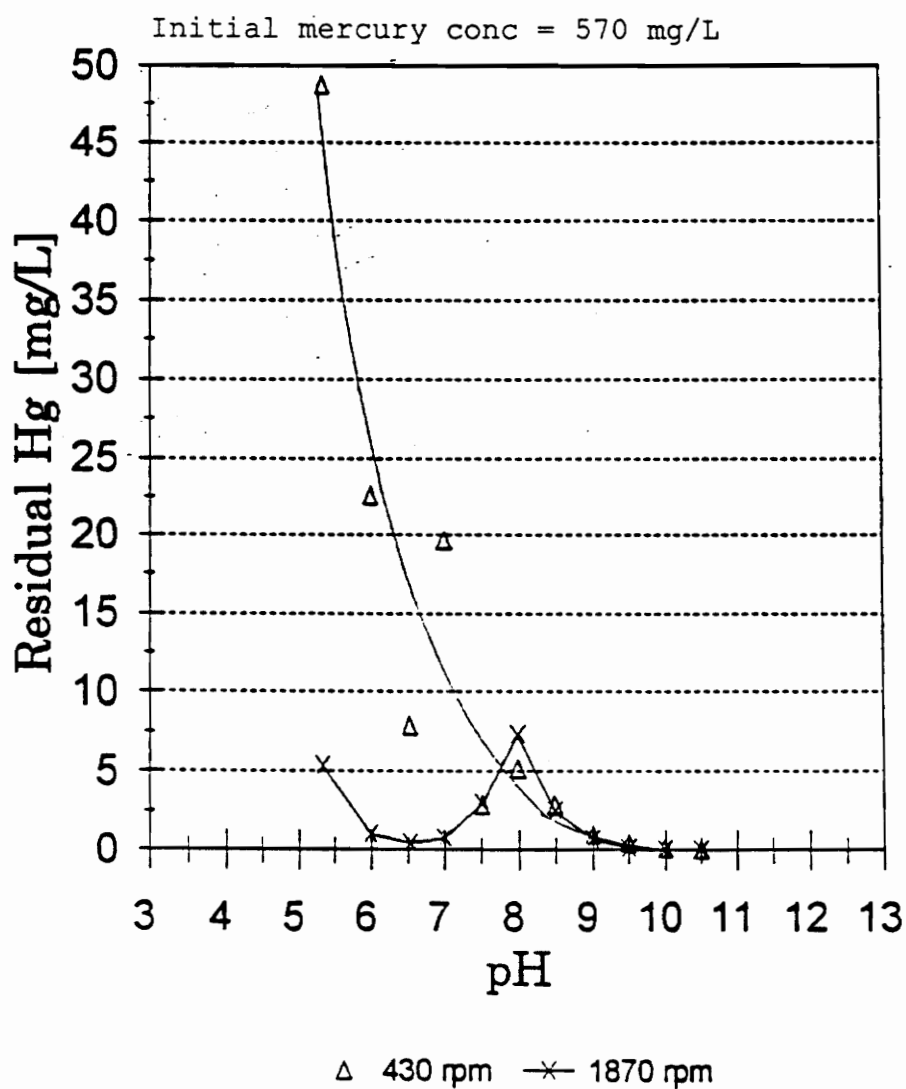


Figure 10. Effect of solution pH on residual mercury concentration for 430 and 1870 rpm mixing speeds at 10 min 2M NaOH addition time

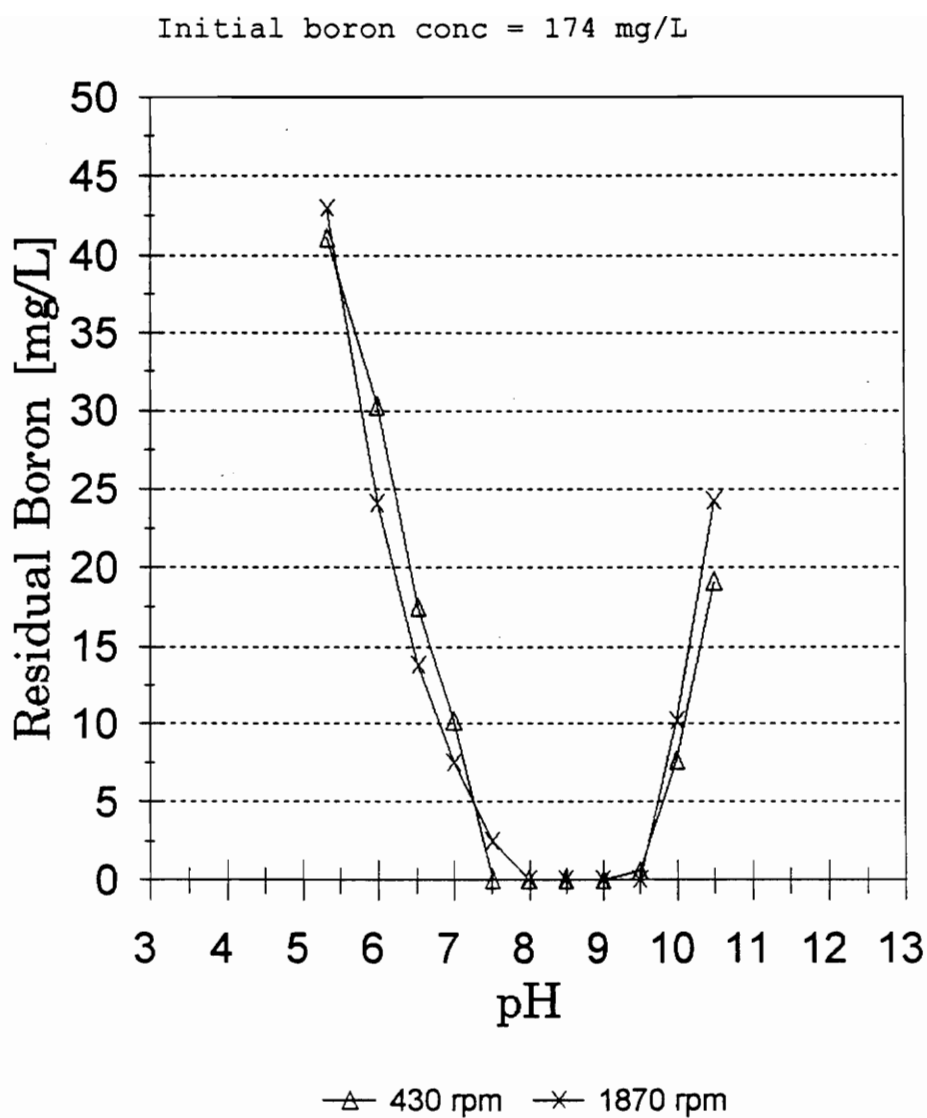


Figure 11. Effect of solution pH on residual boron concentration for 430 and 1870 rpm mixing speeds at 10 min 2M NaOH addition time

over the pH range of 7.5 to 9.5. Molybdenum (Figure 12) removal is effective below pH 9.5. Nickel (Figure 13), manganese (Figure 14), cadmium (Figure 15), and lead (Figure 16) appear to be efficiently removed above pH of 5.0. Iron (Figure 17) appears to be unaffected by solution pH.

The sludge exhibits good dewatering characteristics regardless of solution pH. The main concern is associated with metals removal, and precipitation pH in the range of 8.5 to 9.5 provides the most effective removal of metals in solution.

Mixing Speed Study

The purpose of this portion of the study was to determine the effect of impeller mixing speed on sludge characteristics and metal precipitation efficiencies for the sodium bearing waste. Both a high powered (1/3 Hp) Sears upright drill press and a Cole-Palmer variable speed mixer were utilized, along with the baffled mixing chamber described previously. The solution pH was brought to 9.5 with 2M NaOH, and this solution pH was achieved in a 10 minute time period. Both the target pH and base concentration were recommended by the Idaho National Engineering Laboratory. The specific resistance and CST results for the mixing speed study are displayed in Figures 18 and 19. In general, as the mixing speed increased, the

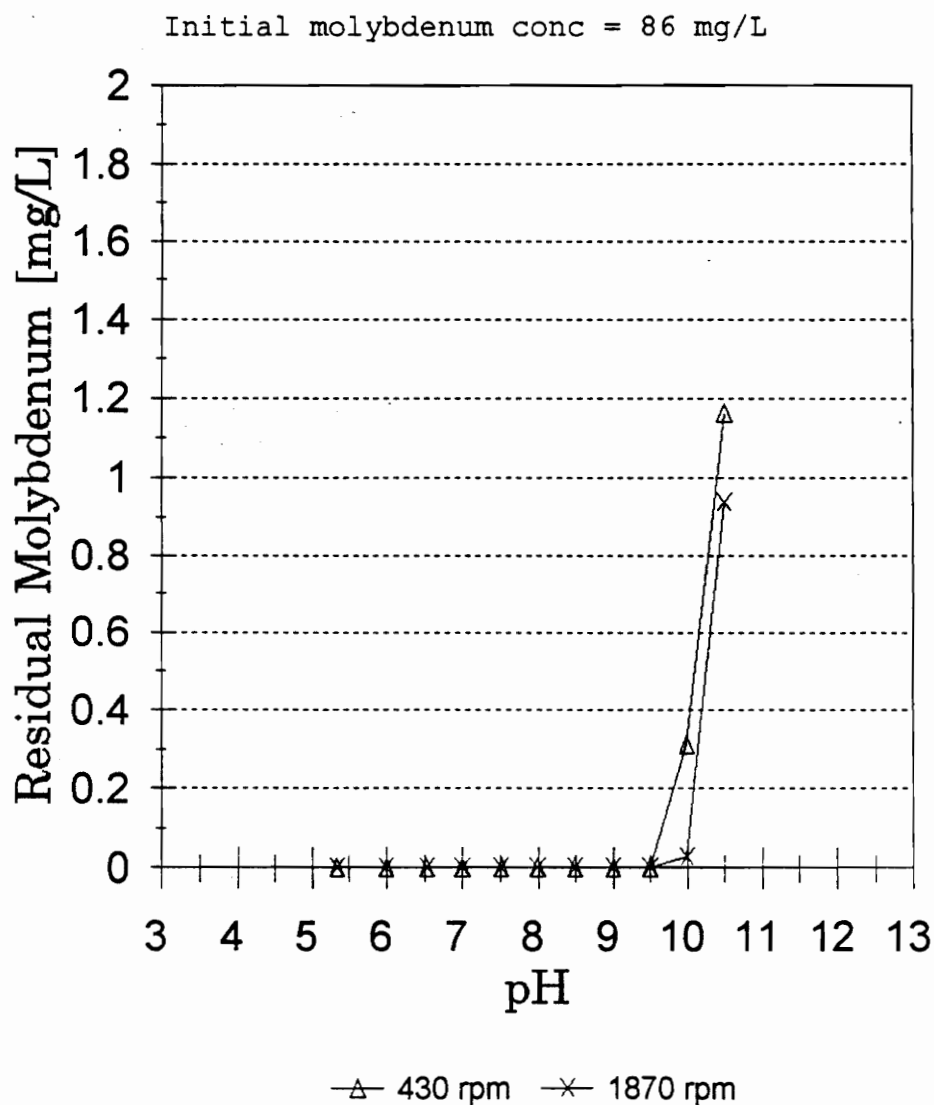


Figure 12. Effect of solution pH on residual molybdenum concentration for 430 and 1870 rpm mixing speeds at 10 min 2M NaOH addition time

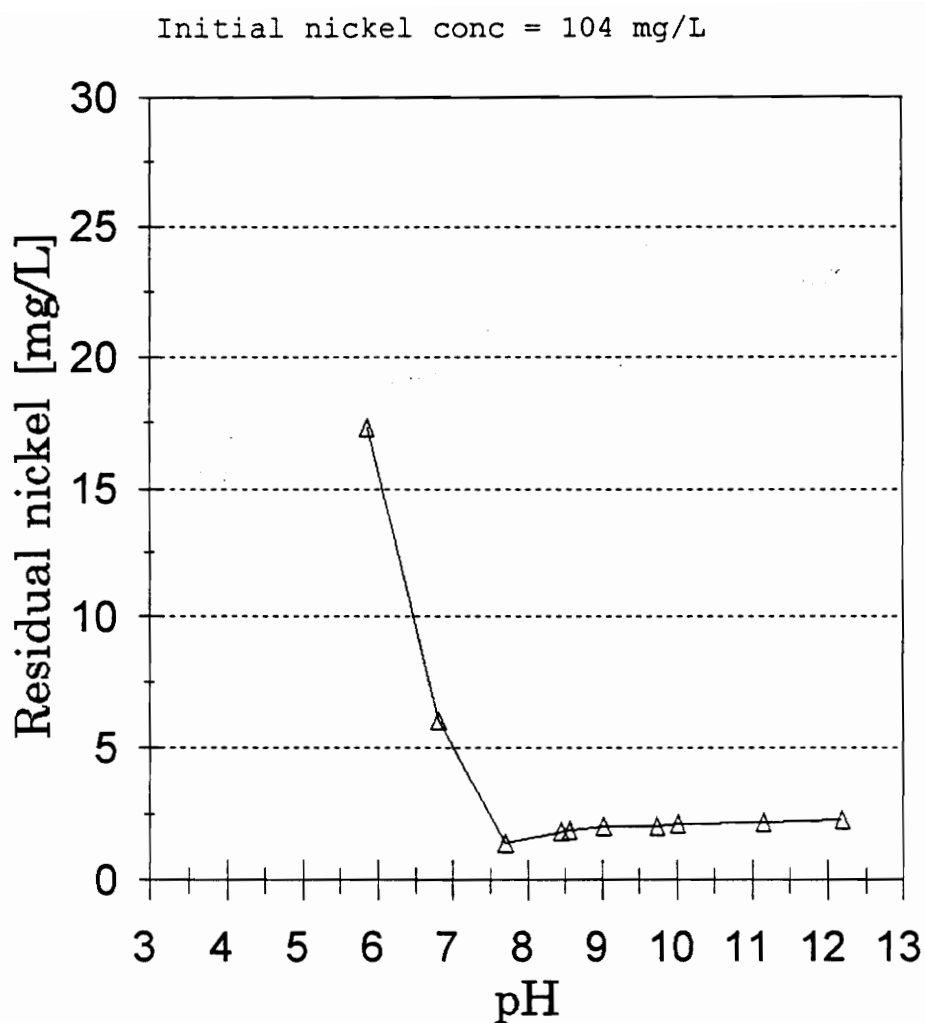


Figure 13. Effect of solution pH on residual nickel concentration for 430 rpm mixing speeds at 10 min 2M NaOH addition time

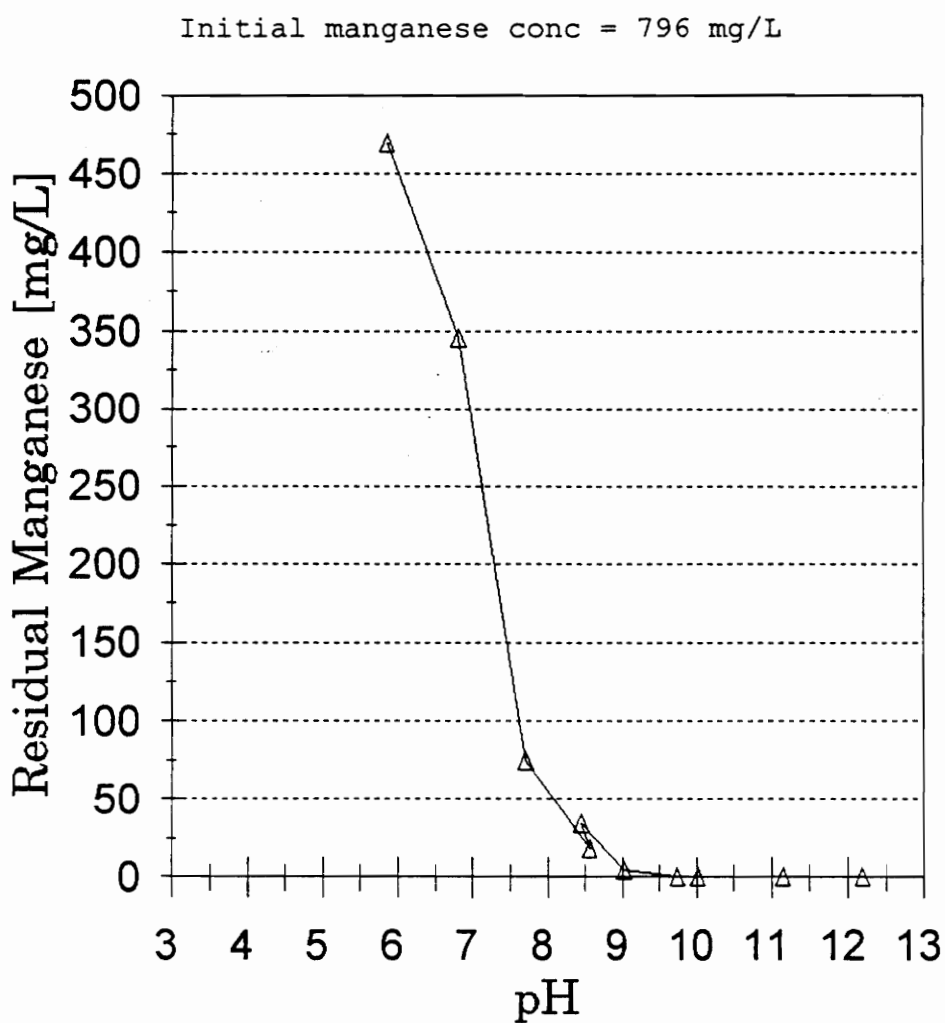


Figure 14. Effect of solution pH on residual manganese concentration for 430 rpm mixing speeds at 10 min 2M NaOH addition time

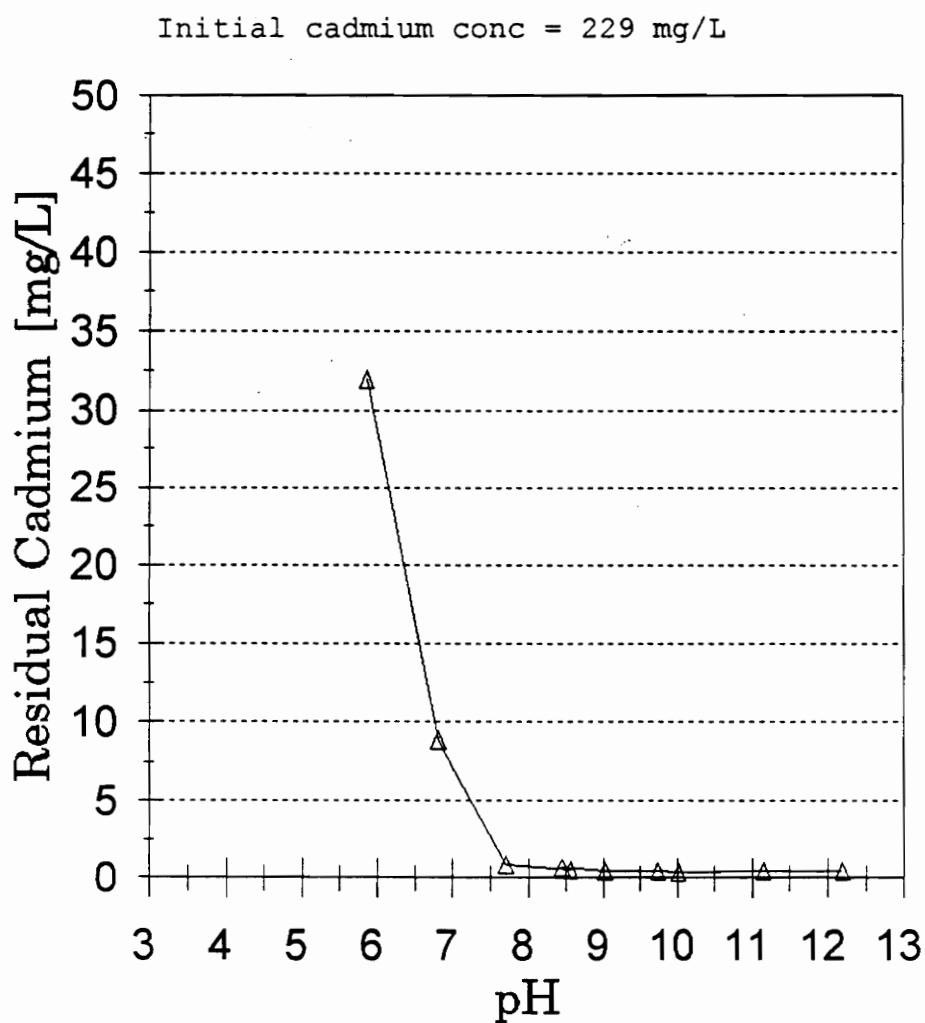


Figure 15. Effect of solution pH on residual cadmium concentration for 430 rpm mixing speeds at 10 min 2M NaOH addition time

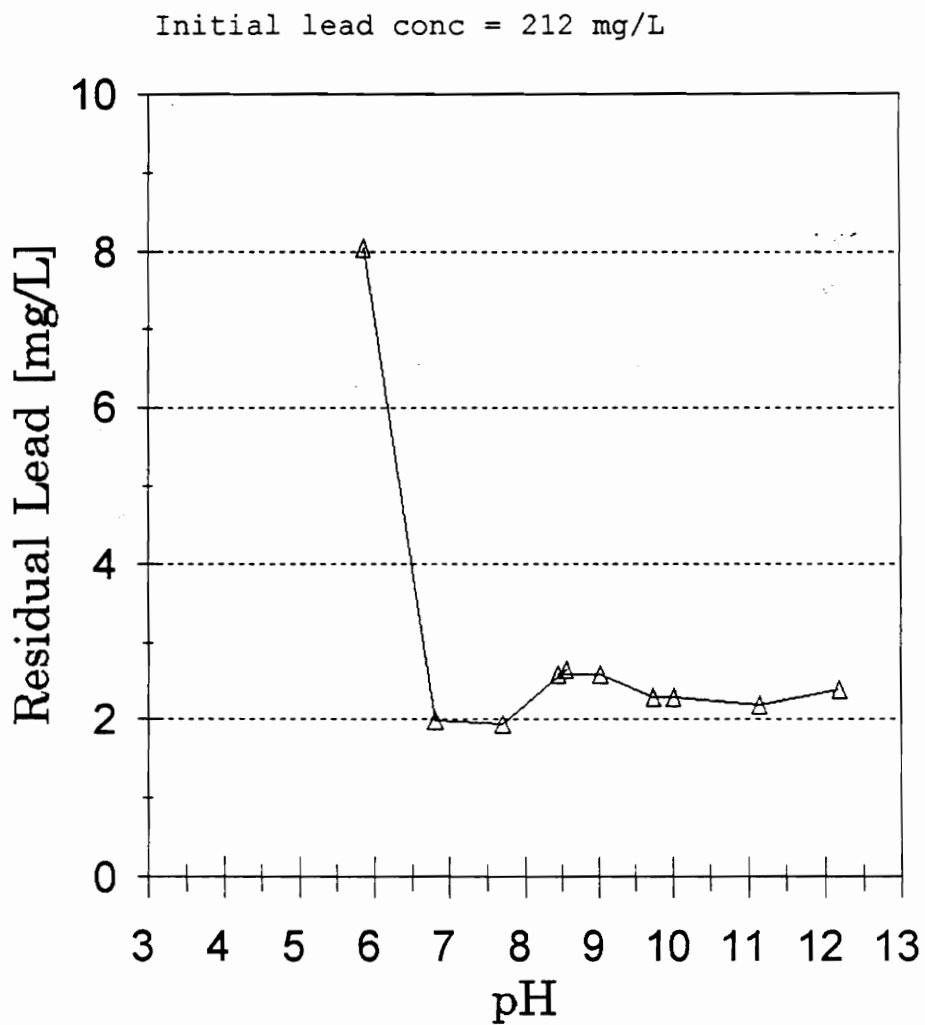


Figure 16. Effect of solution pH on residual lead concentration for 430 rpm mixing speeds at 10 min 2M NaOH addition time

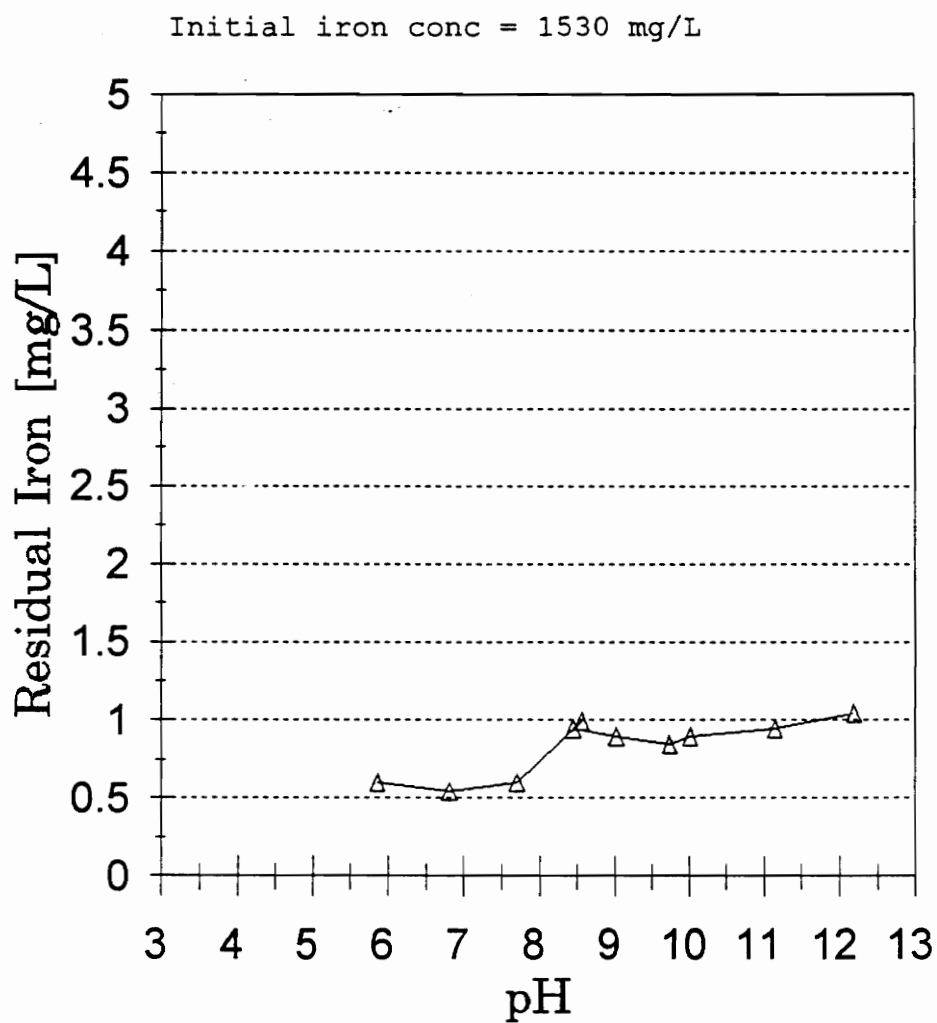


Figure 17. Effect of solution pH on residual iron concentration for 430 rpm mixing speeds at 10 min 2M NaOH addition time

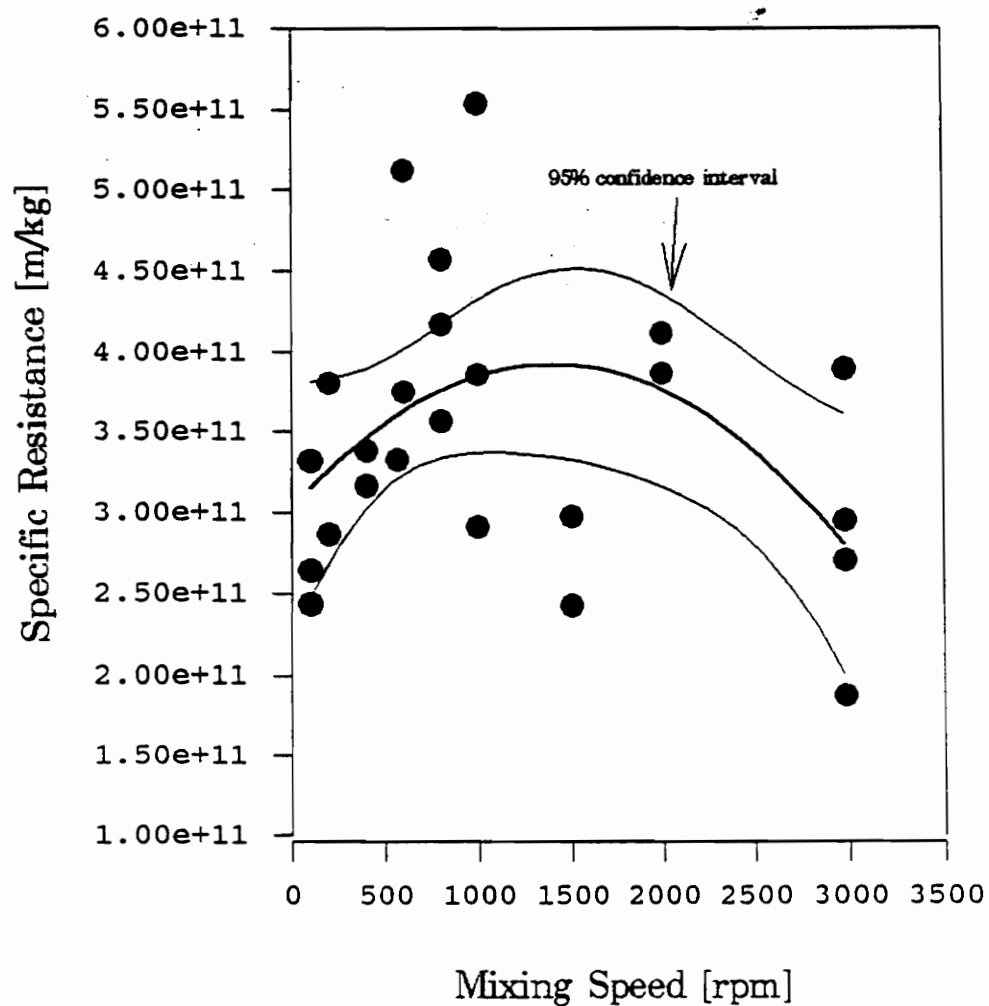


Figure 18. Effect of solution mixing speed on the specific resistance for 10 minute 2M NaOH addition

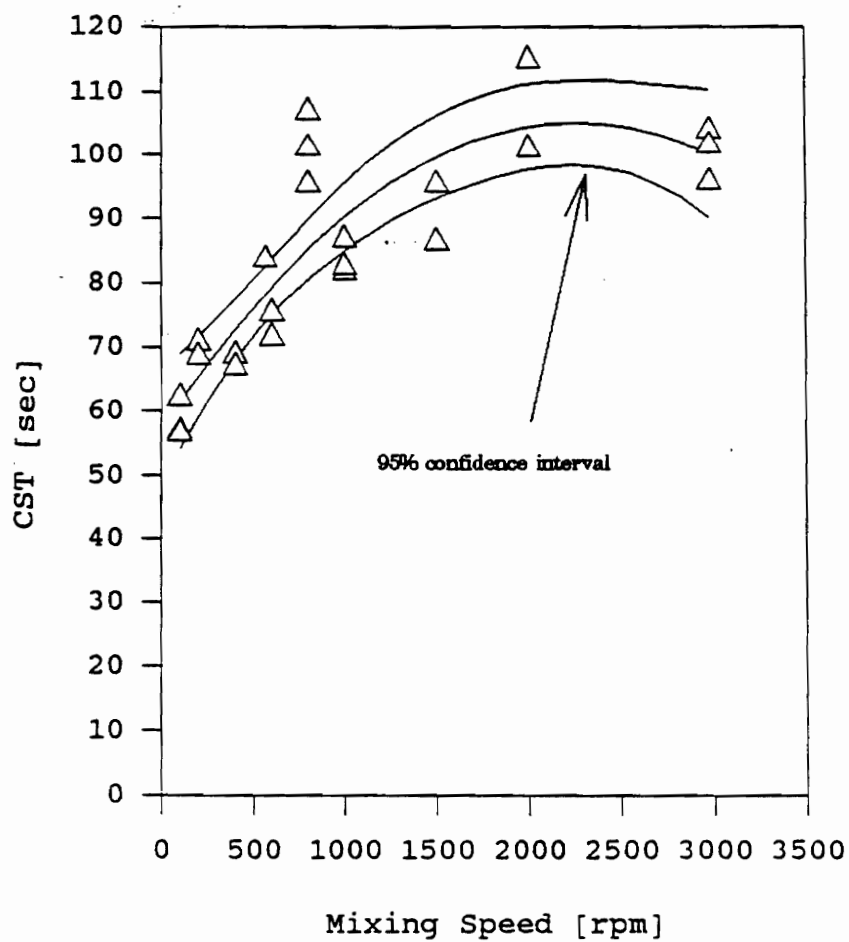


Figure 19. Effect of solution mixing speed on CST for 10 minute 2M NaOH addition

specific resistance associated with the sludge increased up to a mixing speed of 1500 rpm. At speeds above 1500 rpm, the specific resistance declined. Since the mixer used could not obtain speeds higher than 3000 rpm, the trend suggesting that the sludge improved at higher mixing speeds could not be verified although duplicate tests at 3000 rpm suggested that the decline in specific resistance was real. Even at the highest specific resistance values obtained, the sludge demonstrates good dewatering characteristics. The CST data shown in Figure 19 demonstrate results similar to the specific resistance data. Again, the best sludges tended to be those formed during the lower mixing speeds (between 100 and 500 rpm). However, the sludge does not improve at the highest mixing speed studied.

These results differ from the findings by Clark and Flora (15). They concluded that at higher mixing speeds, smaller floc fragments are created. These fragments enable the sludge to have worse dewatering characteristics. Knocke (8) stated that a decrease in mean particle size causes an increase in the specific resistance to filtration. The data does not show this trend of increasing specific resistance at the highest mixing speeds, where the most particle shearing would take place. It would have been beneficial to continue the study using higher mixing speeds.

The solution cake solids concentrations were obtained as part of the Buchner Funnel Test procedure (Figure 20). The highest cake solids concentration was measured at the lowest mixing speed tested, but the data indicated that cake solids are generally not affected by impeller rotational speed. The cake solids concentration was consistently above 20% at all mixing speeds.

Supernatant liquor samples remaining from each of the mixing experiments were analyzed for calcium and aluminum and these results are presented in Figures 21 and 22. At the slower mixing speeds, the residual calcium was consistently above 40 mg/l. As the impeller mixing speed increased, calcium concentration decreased to 15 mg/l at the 2000 rpm mixing speed. Above 2000 rpm, calcium increased. The aluminum was a mirror image of the calcium data. The best aluminum removal efficiency occurred at the lowest and the highest mixing speeds studied. The solution at the lowest mixing speeds contained 100 mg/l of aluminum. The highest mixing speed also produced low aluminum levels. It should be noted that overall removal efficiencies of both calcium and aluminum are both very good regardless of mixing speeds used. Variability associated with the specific resistance possibly is due to localized precipitation. A similar variability was also observed during Vermeulen's (20) chemical mixing study.

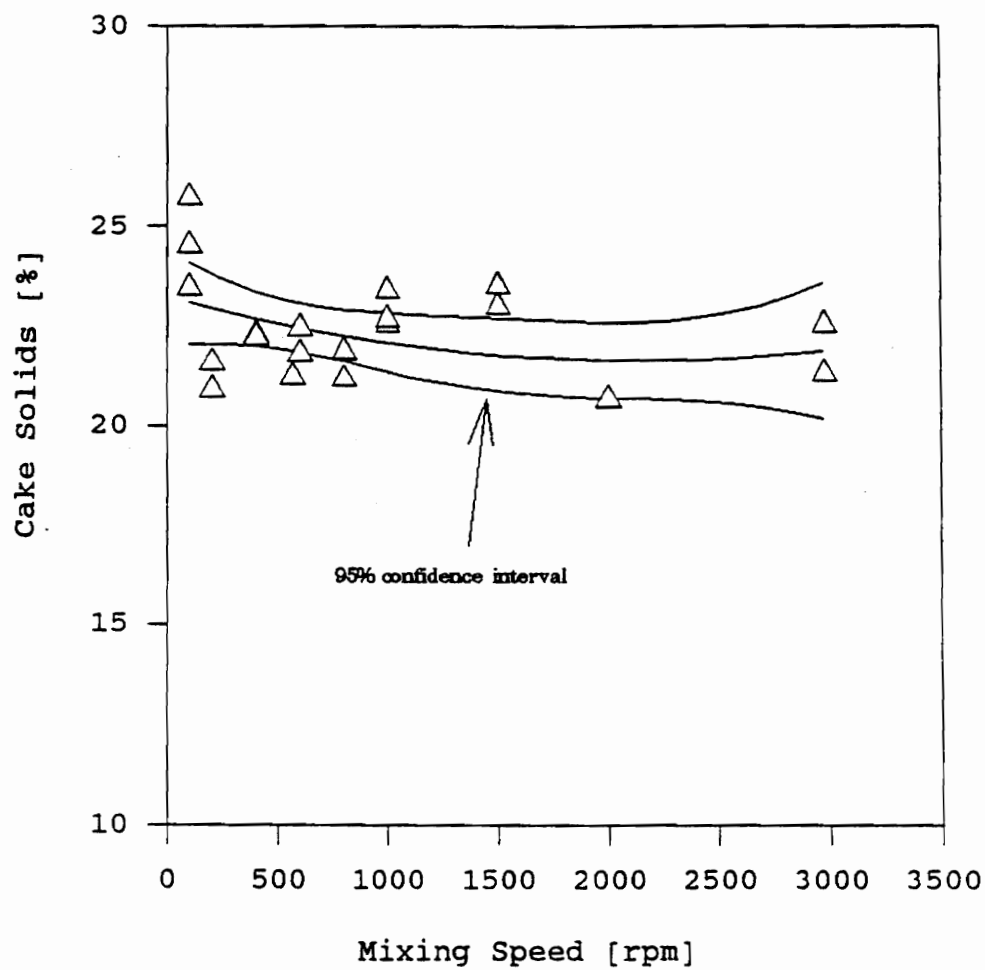


Figure 20. Effect of solution mixing speed on cake solids concentration for 10 minute 2M NaOH addition

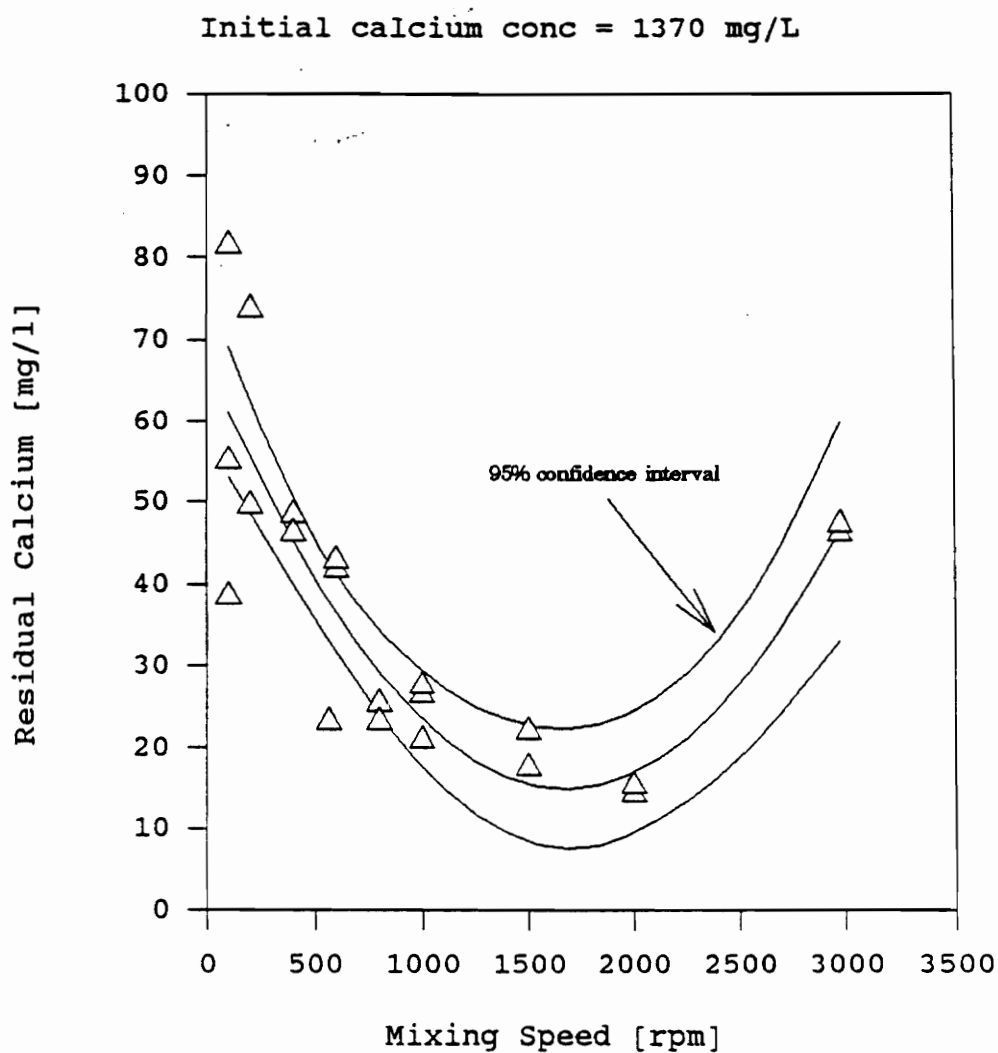


Figure 21. Effect of solution mixing speed on residual calcium for 10 minute 2M NaOH addition

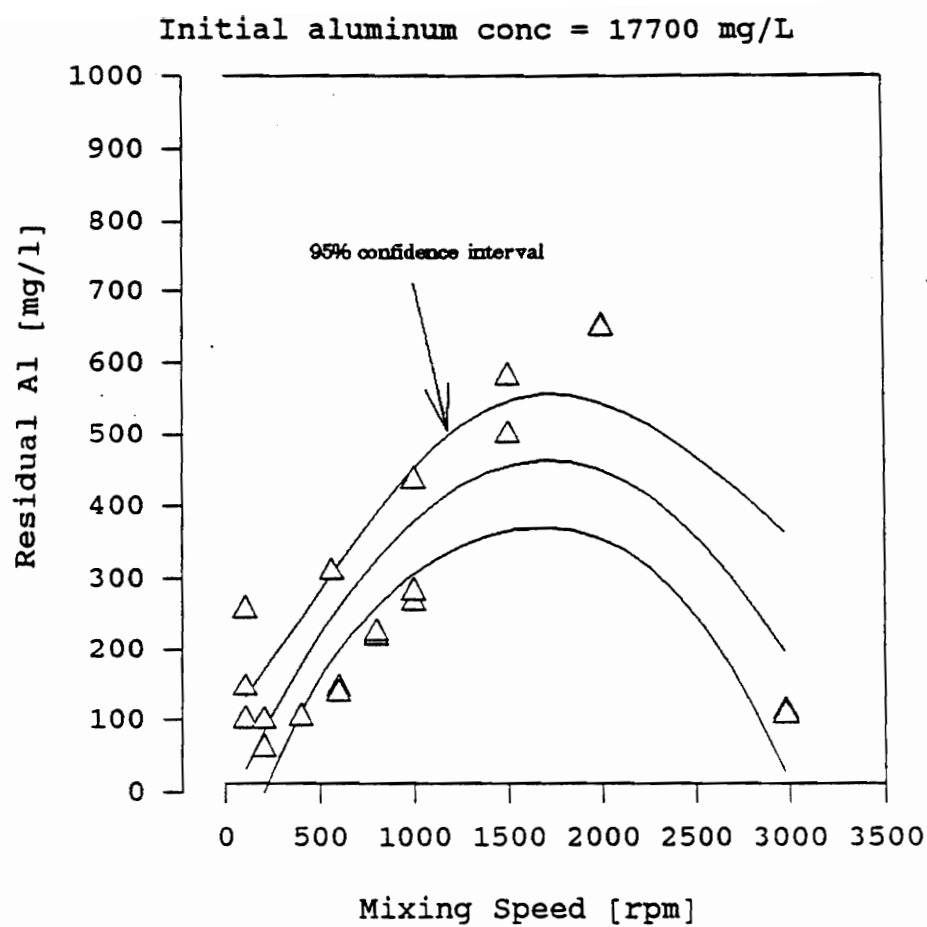


Figure 22. Effect of solution mixing speed on residual aluminum for 10 minute 2M NaOH addition

It appears that variations in calcium and aluminum precipitation are related to sludge properties as measured by the specific resistance. As more aluminum is removed from the solution, the specific resistance increases. The converse is true with calcium removal. As calcium is removed from solution, the specific resistance decreases. Presently, this study cannot explain the relationships between these parameters.

Aluminum removal data does correlate well with the findings of Clark et al (21). It was proposed that lower mixing speeds (500 rpm) formed more polymeric species which tend to "buffer" less of the hydroxyl ions from the added base. Clark stated at higher mixing speeds, more solid was formed, thus this solid buffered more hydroxyl ions. It was also noted in his study that at lower mixing speeds (500 rpm), virtually no aluminum was converted to the solid product. According to Figure 22 the best conversion of the aluminum species was at the lower mixing speeds.

During sludge mixing, when the solution pH was raised to 4.0, the mixture periodically formed a gel-like precipitate. This usually occurred when mixing speeds below 500 rpm were used. The concern with the formation of the gel-like precipitate was inadequate mixing and more particle shearing. Higher mixing speeds prevented the solution from solidifying by keeping the mixture in constant motion.

In summary, this portion of the study demonstrates the importance of mixing speed on the characteristics of the SBW sludge and the metal content of the solution. Lower mixing speeds provide the best aluminum removal and create a sludge with the best dewatering characteristics. However, overall removal efficiencies of both calcium and aluminum and sludge specific resistance are good regardless of mixing speed. Higher mixing speeds helped prevent the solution from forming a gel-like precipitate during the titration.

Base Addition Study

The rate of base addition was studied to see how this effects the removal efficiency of the SBW species. Specific resistance to filtration and capillary suction time were performed to observe the effect base addition has on the dewatering characteristics of the sludge.

Two molar sodium hydroxide was dripped into the mixing vessel containing the SBW at a predetermined constant rate until a solution pH of 9.5 was reached. The range of base addition times were from immediate addition to 20 hours. The impeller mixing speed was kept constant at 430 rpm. When mixing was complete, the sludge specific resistance, filter cake solids, and dissolved metal content were determined.

To determine optimal base addition times, both CST and specific resistance to filtration were performed to determine the corresponding dewatering characteristics. The specific resistance to filtration results are displayed in Figure 23. Addition times greater than 500 minutes produced the best dewatering rates. As the addition time increased, the specific resistance increased slightly. However, the data were variable and inconsistent at the lower addition times due to high localized hydroxyl ion concentrations (20). Overall, the specific resistance indicates good dewatering characteristics regardless of base addition time. A specific resistance value of 4.0×10^{11} m/kg is indicative of an easily dewatered sludge.

CST versus base addition time for the precipitated sludge is also shown in Figure 24. Again, the base addition times greater than 500 minutes provided the best precipitation characteristics. Addition times less than 200 minutes provided CST values all above 50 seconds. The results of both the specific resistance to filtration and CST both indicate the best sludge is created at higher addition times (greater than 500 min) or slower rates of base addition.

The effect of base addition rate on calcium removal is displayed in Figure 25. The best removal rates occurred at the most rapid base addition rates. However, the data were

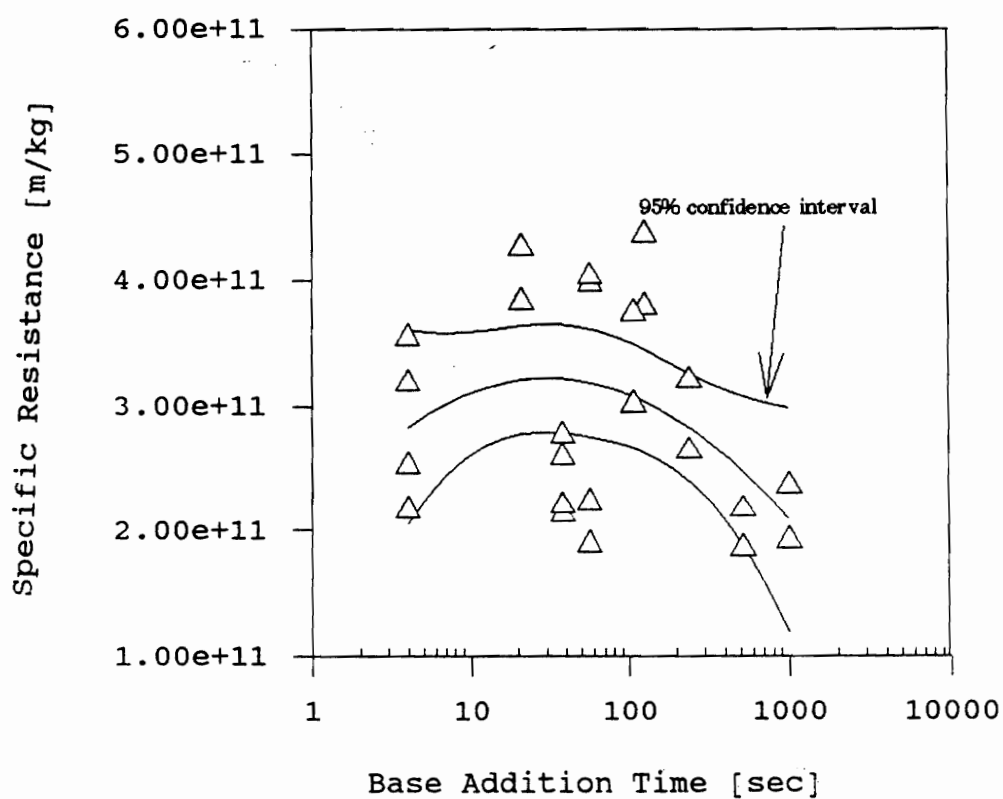


Figure 23. Effect of 2M NaOH addition time on solution specific resistance for 430 rpm mixing speed

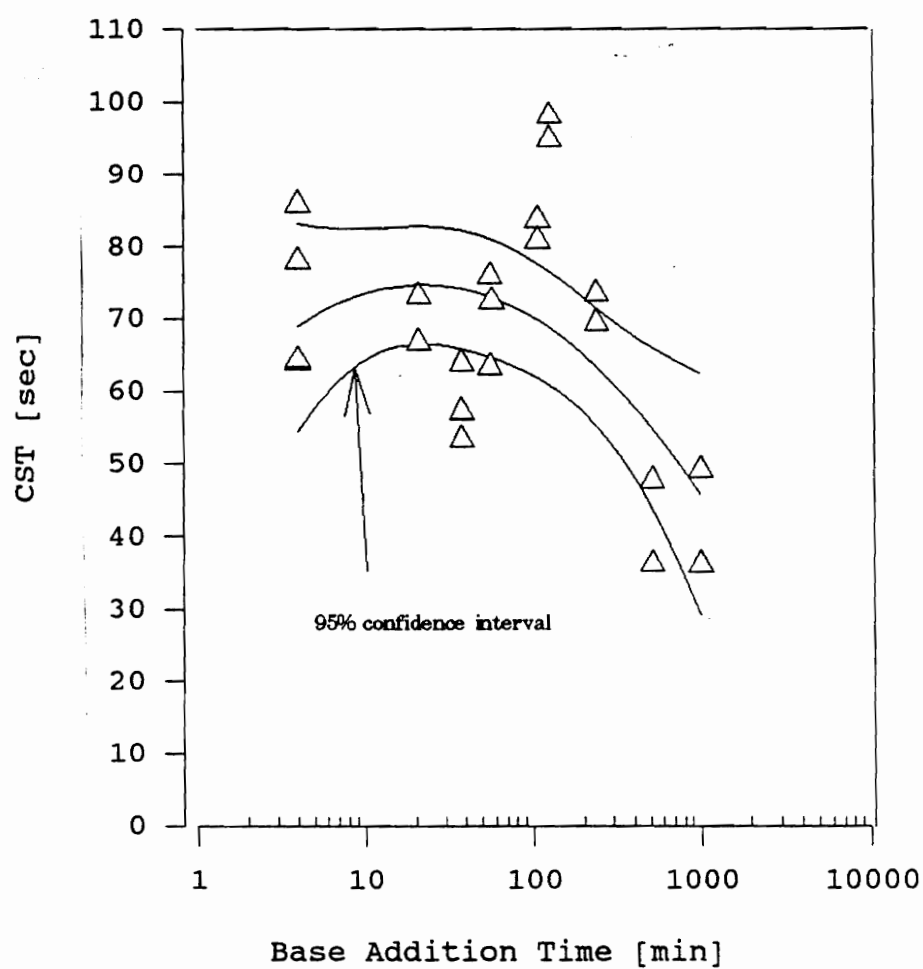


Figure 24. Effect of 2M NaOH addition time on the solution CST for 430 rpm mixing speed

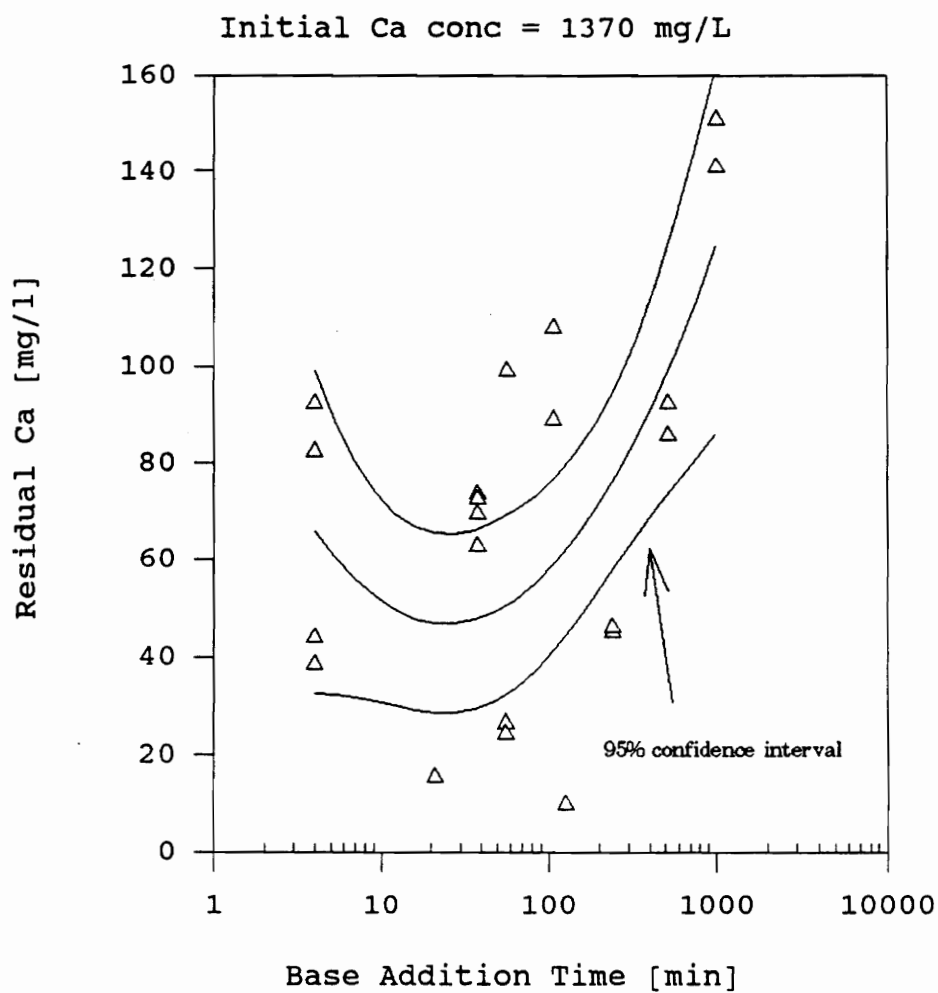


Figure 25. Effect of 2M NaOH addition time on the residual calcium for 430 rpm mixing speed

highly variable at rapid addition rates. The high variability associated with the rapid base addition could be caused by the 0.45 micrometer glass filter not effectively capturing the calcium. Periodically during the procedure, white precipitate remained in solution, easily passing through the glass filter. The overall trend in Figure 25 shows shorter base addition times produce better calcium removal rates.

The cake solids data (Figure 26) shows that the solids concentration increased as addition time increased. The cake solids concentration was consistently between 20% and 25%.

The results show that the best dewatering characteristics occur at the slower base addition rates. These slow addition times provide the best dewaterability characteristics, although the sludge, regardless of addition time, possesses good dewatering characteristics. The best calcium removal efficiency occurred at the fastest base addition times.

Reverse Addition Study

The addition of SBW to the base rather than addition of base to the SBW was studied to see what effects this may have on the sludge properties. A specific goal was to see if calcium aluminate, a dense, crystalline solid would be

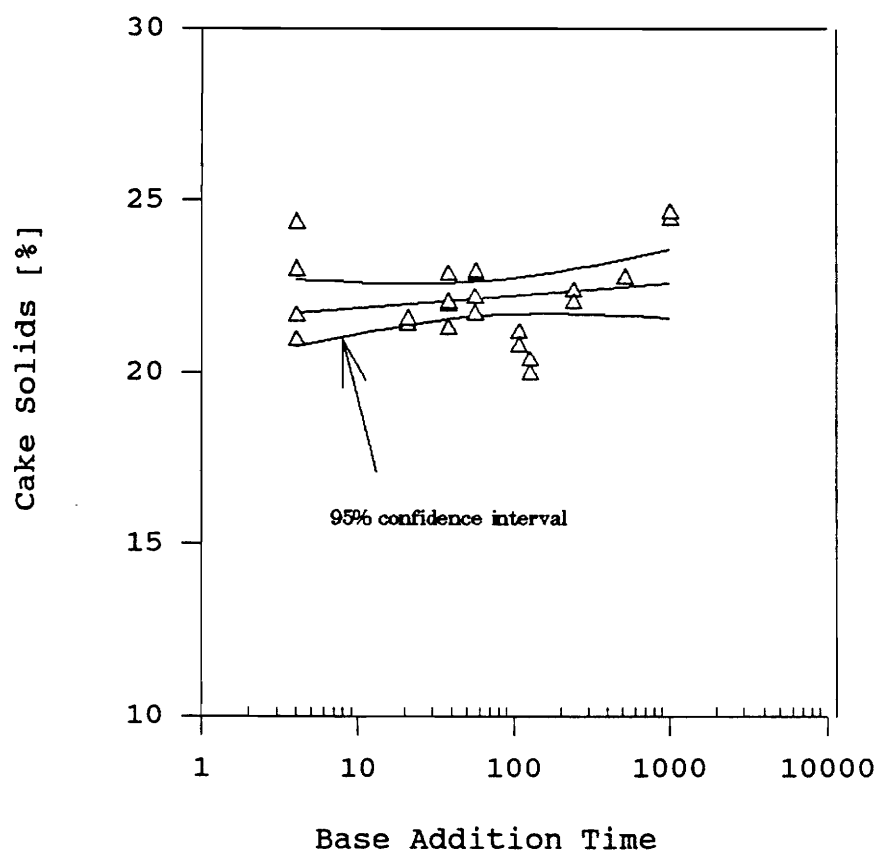


Figure 26. Effect of 2M NaOH addition time on cake solids concentration for 430 rpm mixing speed

formed and thereby provide a better sludge than the aluminum hydroxide. Specific resistance to filtration was performed to observe the effect base addition has on the dewatering characteristics of the sludge.

The SBW was carefully dripped into the mixing vessel containing 2M NaOH until the solution pH was 9.5. The SBW addition time was either 1, 8, or 17 minutes. The mixing impeller was rotated at 100 rpm. When mixing was complete, the Buchner Funnel test was performed to determine the specific resistance, cake solids, and dissolved solids of the sludge. The remaining supernatant liquor was filtered with a 0.45 micrometer glass filter and acidified with concentrated nitric acid and metals were analyzed.

The specific resistance and calcium concentration are shown in Figure 27. The specific resistance of the solution remains constant regardless of the SBW addition time. A specific resistance value of 5.0×10^{11} m/kg indicates a sludge dewateres more slowly than sludges created by adding base to acid. The residual calcium remaining in the supernatant also remained relatively constant, regardless of the SBW addition time. A calcium residual of 30 mg/l indicates this process does an exceptional job of removing calcium from solution since the initial calcium concentration was 1370 mg/L.

Initial calcium conc = 1370 mg/L

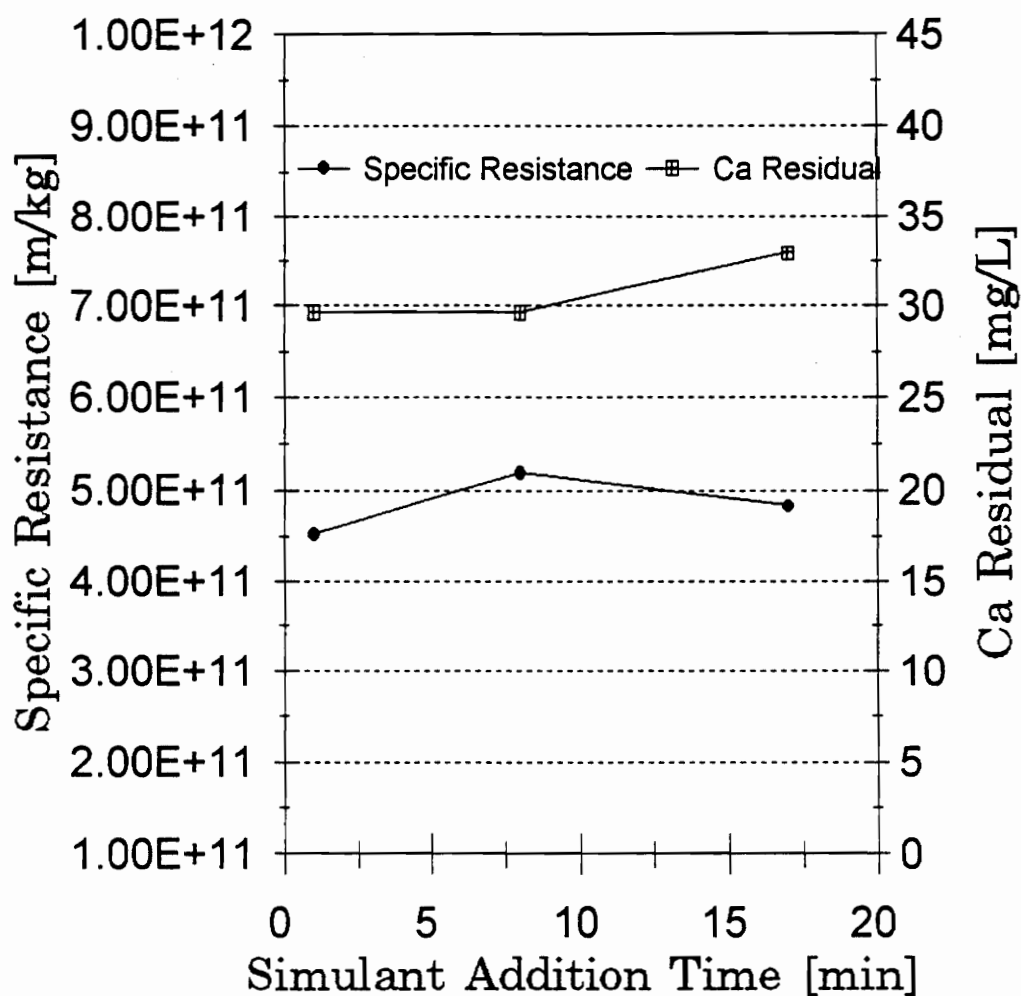


Figure 27. Effect of SBW simulant addition time (1, 8, and 17 min) on the specific resistance and residual calcium concentration during reverse addition study for 100 rpm mixing speed

Specific resistance and aluminum concentrations are displayed in Figure 28. As addition time increased, the amount of dissolved aluminum species remaining in solution decreased. However, this amount of aluminum removal was no better than removals during the mixing speed or base addition studies.

In summary, the process of adding the SBW to the base produced a sludge which had poorer dewatering characteristics than the sludge created by adding the base to the SBW. Also, removal rates of calcium and aluminum were no better. Therefore, the process of reverse addition is not recommended.

Spiked Reverse Addition Study

The process of adding the SBW with added calcium was studied to see what effects this procedure has on the sludge properties. The rationale was to see if additional calcium would promote more calcium aluminate formation. Specific resistance to filtration was performed to observe the effect base addition has on the dewatering characteristics of the sludge.

The procedure was the same as the reverse addition procedure previously described, except that the SBW incorporated different initial concentrations of calcium. These spikes were used to see if additional calcium could

Initial aluminum conc = 17700 mg/L

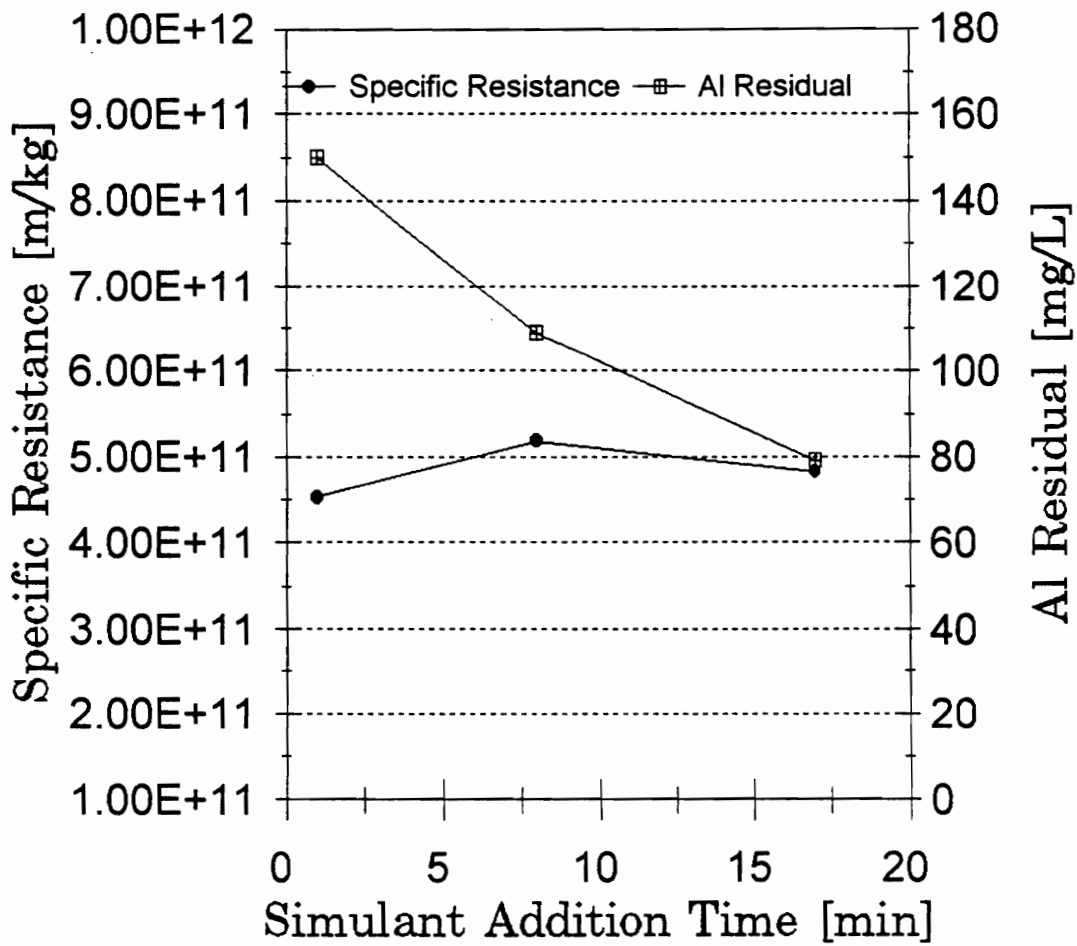


Figure 28. Effect of SBW simulant addition time (1, 8, and 17 min) on the specific resistance and residual aluminum during reverse addition study for 100 rpm mixing speed

change sludge properties by promoting calcium aluminate precipitation.

The results of the study are presented in Figures 29 and 30. As seen in Figure 29, as the initial calcium concentration increased, the dewatering characteristics improved considerably. The best sludge, with an initial calcium species concentration of 15,070 mg/l, produces a specific resistance below 2.0×10^{11} m/kg. It appears that calcium addition provides a better sludge. However, the amount of residual calcium in solution increases with an increase in the initial calcium concentration. The residual aluminum (Figure 30) concentration changed somewhat, generally increasing as calcium was added. The response of solution aluminum to calcium addition is the opposite of what was expected.

These results support the findings of Knocke and Kelley (23). They found that seeding a sludge by recycling sludge solids to encourage crystal formation improved dewatering rates. They found that a larger and denser floc was created, causing a 20 fold decrease in specific resistance values.

While calcium addition, combined with reverse addition provided a better sludge, the residual calcium and aluminum in solution increased. With the increase in calcium and aluminum concentrations in solution, the INEL needs to

Initial calcium conc = 1370 mg/L

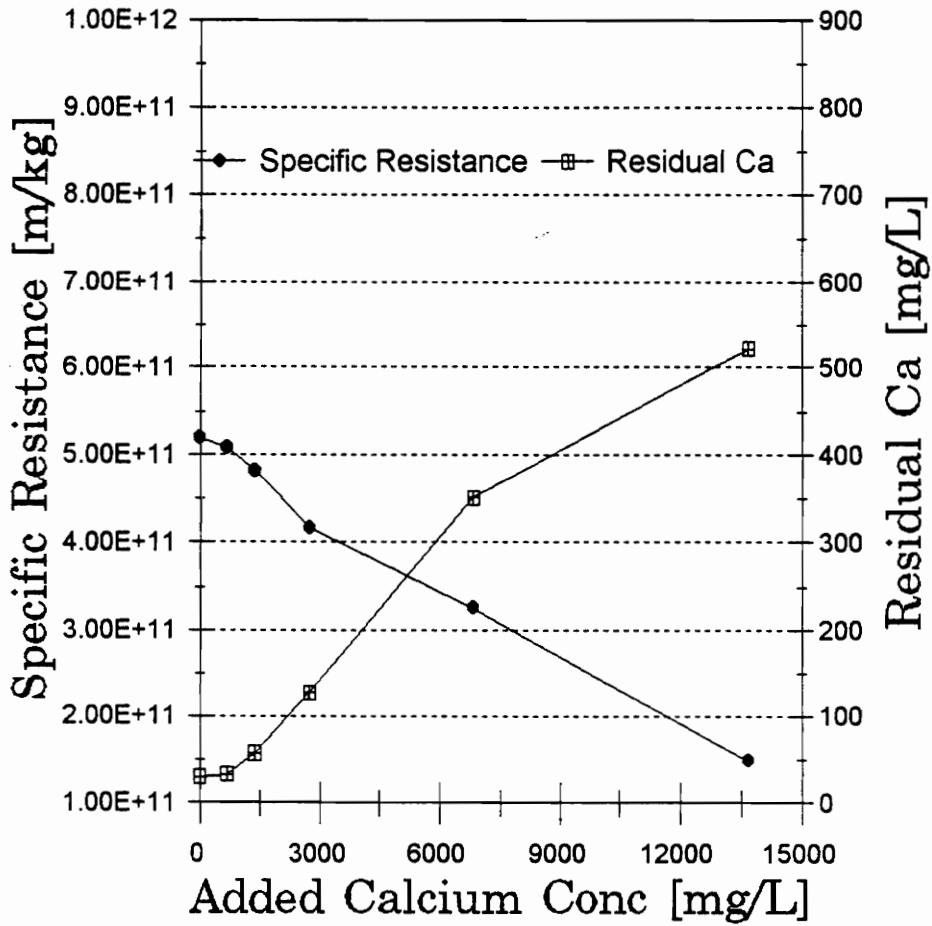


Figure 29. Effect of initial calcium concentration on the solution specific resistance and residual calcium concentration during the spiked reverse addition study for 100 rpm mixing speed and 10 min spiked SBW addition time

Initial aluminum conc = 17700 mg/L

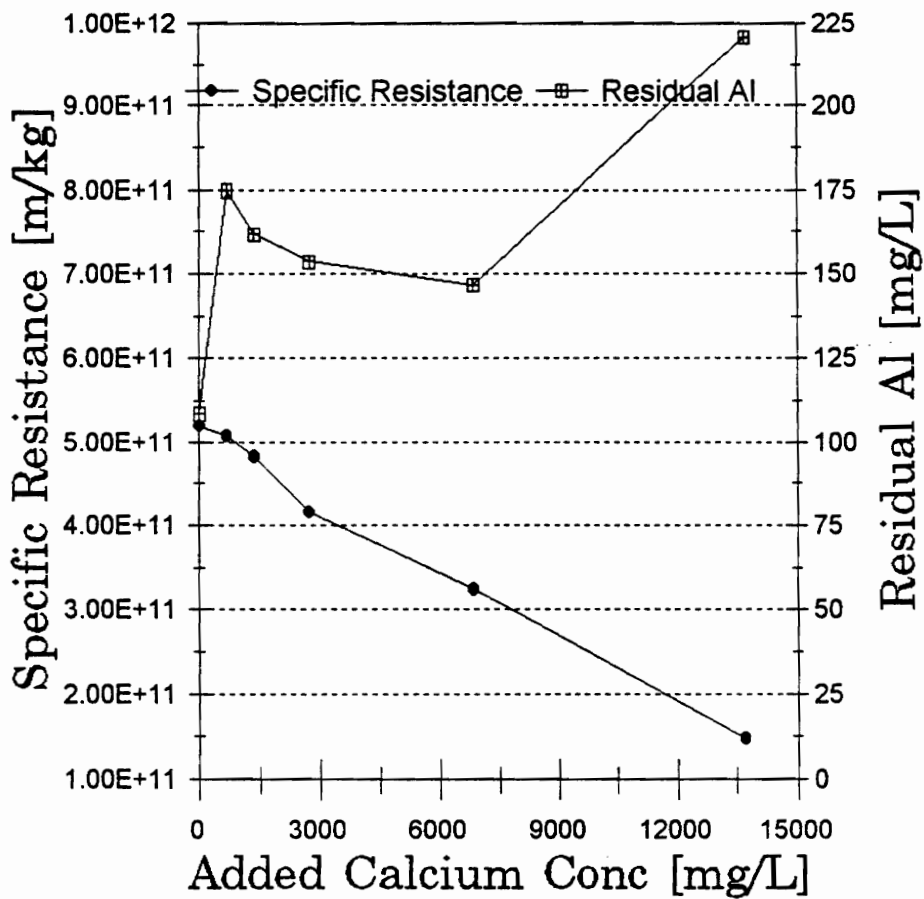


Figure 30. Effect of initial calcium concentration on the solution specific resistance and residual aluminum concentration during the spiked reverse addition study for 100 rpm mixing speed and 10 min spiked SBW addition time

determine compatibility with the downstream processes (ion exchange). Although the results are promising, further study is also needed to see if this process can be made more efficient for calcium and aluminum removal.

Mineql+ and Minteqa2 Chemical Equilibrium Modeling

Chemical equilibrium modeling was performed using Mineql+ and Minteqa2 computer models. The initial input variables and constants are presented in Table 3. Due to model non convergence, only twelve species could be used.

Calcium specie concentrations as a function of solution pH is shown in Figure 31. Initially, all the calcium in solution is Ca^{+2} . As the pH increases, solid gypsum is formed. Gypsum accounts for 16% of the calcium at pH 6.0. At higher pH, $\text{Ca}_5\text{OH}(\text{PO}_4)_3$ precipitates, theoretically removing over 44% of the calcium found initially in solution.

Residual calcium as a function of solution pH is shown in Figure 32. Both observed (using pH study under 1870 rpm mixing speed) and modeled (Mineql+ and Minteqa2) total calcium concentrations are displayed. The theoretical calcium includes calcium phosphate and gypsum precipitation.

Major differences exist between the two models as shown in Figure 32. Mineql+ shows calcium decreasing above pH 4.0, while Minteqa2 does not predict calcium removal until

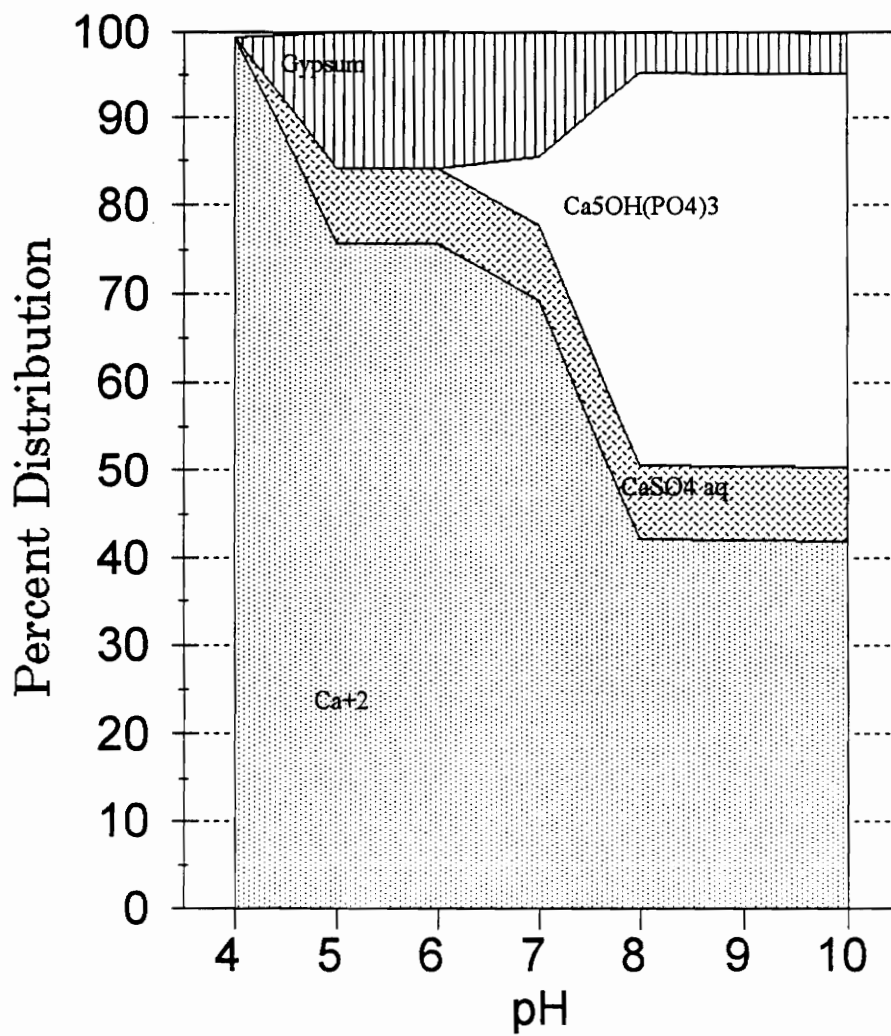


Figure 31. pH versus percent distribution of calcium species according to Minteqa2

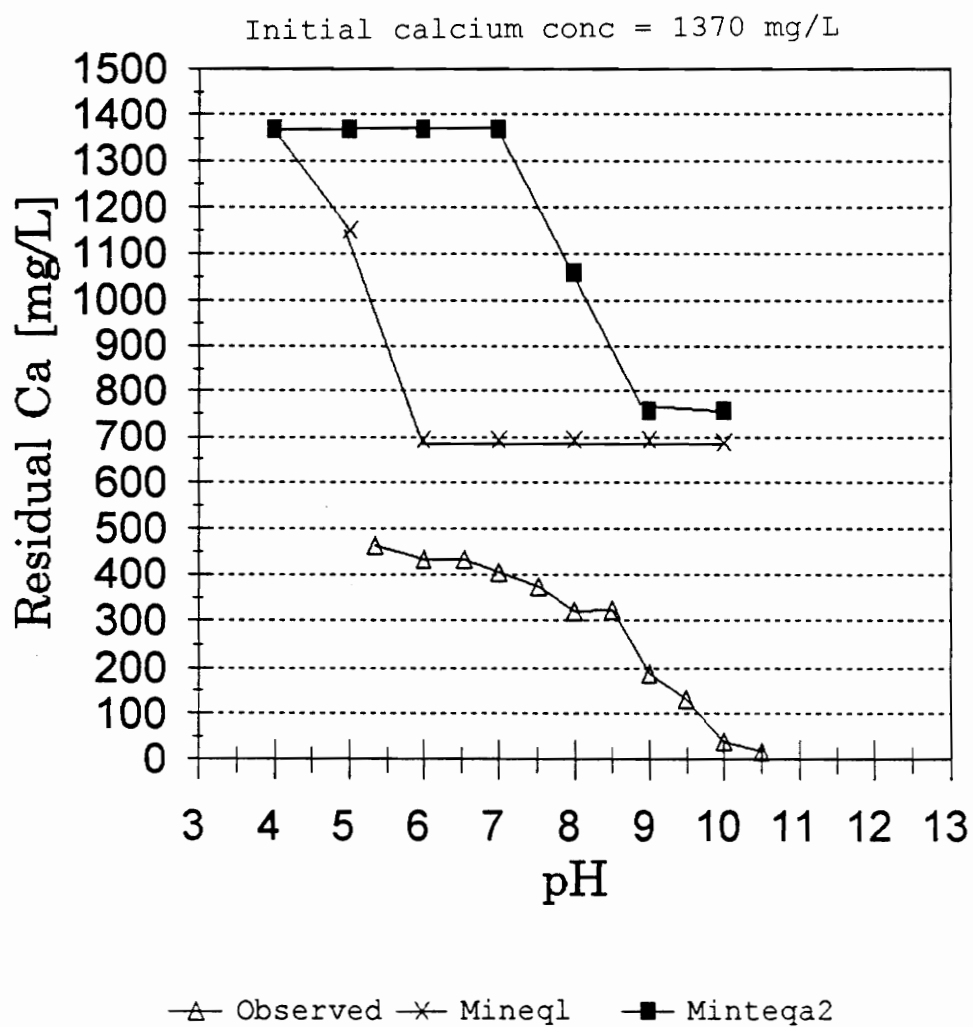


Figure 32. Effect of solution pH on residual calcium for 1870 rpm mixing speed (observed), Mineql+, and Minteqa2

pH 7.0. These differences may be due to a number of factors. Ionic strength was calculated by each model, and the possibility exists that each model used different ionic strengths when calculating equilibrium conditions. The two models do use similar databases for equilibrium constants, but discrepancies may exist. When observing the solids production of the two models, Minteqa2 provided a larger database. The difference in predicted solids include: Ferrihydrite, Hydrapatite, Mirabilite, Strengite, Portlandite, Lepidocrocite, and $\text{Fe}_2(\text{SO}_4)_3$. The inclusion of these solids may account for the differences between these models.

The differences between the observed and predicted is also large. All three of the data points display decreasing calcium concentration as the pH increases. However, the pH where the calcium begins to decrease and the total amount of removal are all different. Several explanations exist to explain these differences.

Coprecipitation could be occurring in the actual process and the computer modeling may not be including this process with the chemical equilibrium data. Knocke (9) observed the effects of coprecipitation on mixed metal sludges. He noted species were removed under conditions that would not typically remove the species. Calcium concentrations in the observed are much lower than

predicted, thus coprecipitation may be occurring. Mixing conditions may also play an important role in chemical precipitation. The models do not take into effect the mixing conditions or the rate of base addition during the simulated titration. As observed previously, each of these play an important role in final solution equilibrium.

The data shown in Figure 32 provide information about the differences between the observed and predicted values of calcium during chemical precipitation. Removal rates of calcium are much higher than expected. Coprecipitation may be occurring, but to what extent is not known. It would have been interesting to see if other species behaved in similar manner.

The remainder of the results are located in Appendix B. A summary of molar distribution of components among each of the SBW components is included, along with percent distribution diagrams for dissolved and solid species.

It appears the programs do not model SBW properly. By calculating the calcium concentrations and comparing them to the observed values, the models underestimate calcium removal. A more detailed metals analysis would be needed to prove the validity of the models. The SBW appears to be too complex for either model to accurately predict chemical equilibrium.

SLUDGE CONDITIONING

Polymer Experiments

This section of the research focused on the dewatering and polymer conditioning of Sodium Bearing Waste (SBW) sludge. The effects of polymer mixing parameters (impeller rpm and total mixing time) were evaluated. Bench-scale Wedge Zone Simulation (WZS) tests, and centrifugation studies were conducted in order to evaluate the performance of each of the polymers. The polymers were judged on their ability improve the dewatering rate and produce a high quality filtrate. When choosing polymers for sludge conditioning, these measures were used along with the polymer dose that was required to achieve optimum conditions. Because the relationship between specific polymer properties and the ability of these polymers to condition the SBW sludge is not very well understood, a variety of mole charges and charge densities were used.

The first phase of the study involved observing the effects of mixing time and impeller mixing rate (rpm) on the conditioning of the sludge. Freshly prepared sludge samples of 100 mL (pH = 9.5) were placed into the jar test mixing apparatus, and rotational speeds of 50, 75, and 100 rpm were tested. Doses of 6.2, 8.7, and 12.5 mg/kg of a 0.5%

solution of an anionic medium molecular weight polymer were added to the sludge. At various predetermined time intervals, samples of the sludge were removed from the mixing chamber, and CST of the sample was determined.

The effect mixing time and dose on the CST associated with the sludge at a mixing speed of 50 rpm is shown in Figure 33. At a mixing time of one minute, all three of the doses had a high CST value. This high CST most likely occurred because not enough mixing time was allowed to induce proper interparticle contacts between the sludge and the polymer. As the mixing time increased to 2 minutes, the sludge improved, and as the mixing time increased past 2 minutes, all three of the sludges deteriorated. The optimum dose appears to be 12.5 mg/kg when mixed for 2 minutes. This is consistent with the findings of Novak and O'Brien (2), who stated that excess mixing causes floc rupture or rupture of polymer surface bonding when conditioning occurs under intense or prolonged mixing. This floc rupture will cause more small fragments within the mixture and dewatering rates of the sludge will decrease due to a decreased cake porosity (12).

The graph shown in Figure 34 presents the results of the 75 rpm mixing study. The 6.2 and 8.7 mg/kg doses at the one minute mixing time interval appear to be underdosed. As

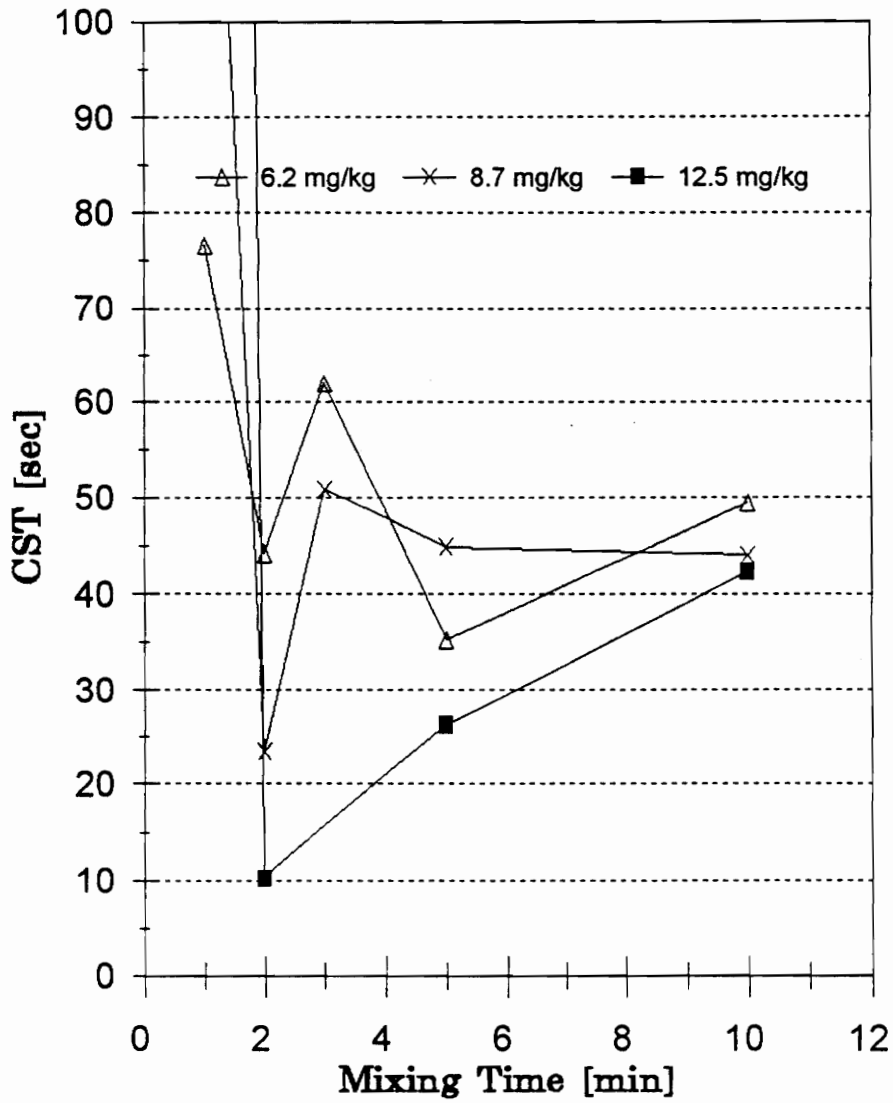


Figure 33. Effect of mixing time on CST for 6.2, 8.7, and 12.5 mg/kg doses of A-M-30% polymer for 50 rpm mixing speed

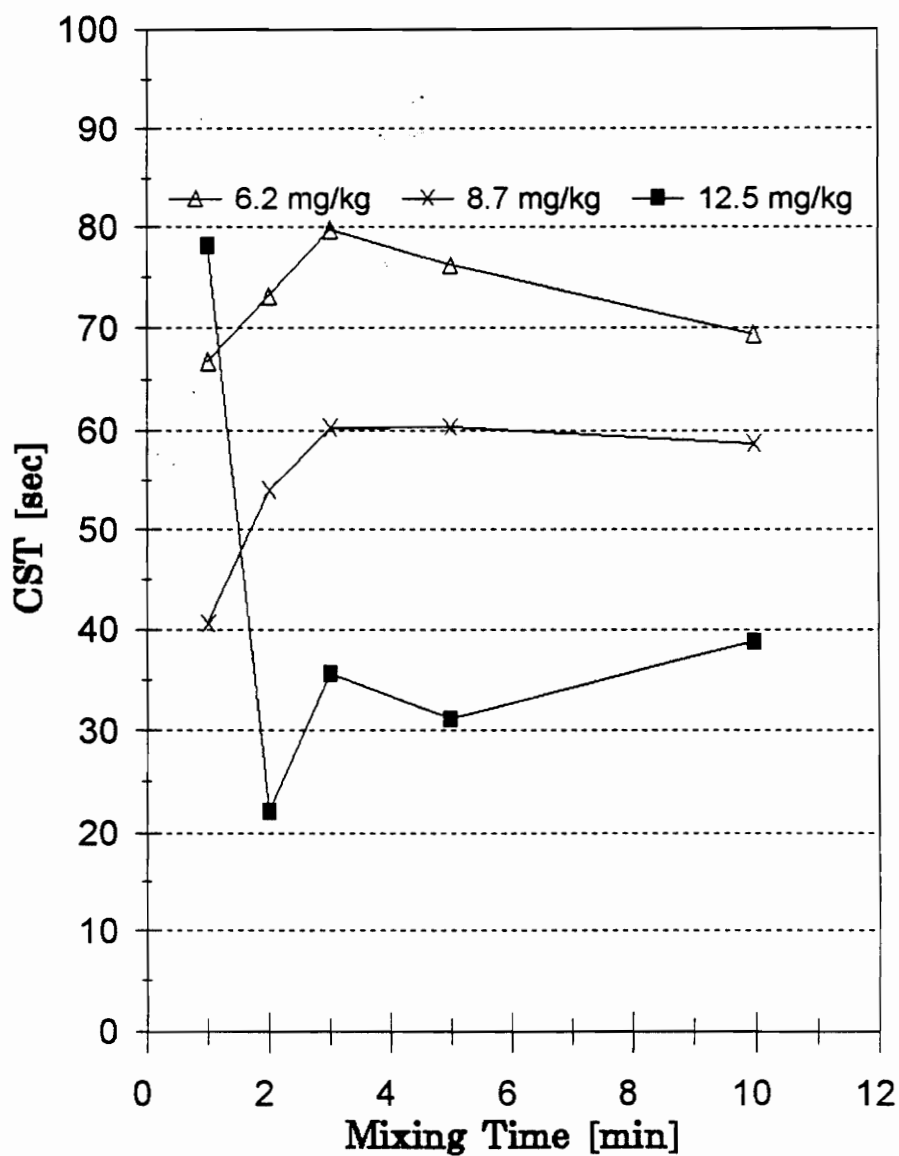


Figure 34. Effect of mixing time on CST for 6.2, 8.7, and 12.5 mg/kg doses of A-M-30% polymer for 75 rpm mixing speed

the mixing time increased for both of the doses, the CST value generally increased. The 12.5 mg/kg dose at the 1 minute mixing time had the highest CST value, but as mixing continued, the sludge improved substantially, reaching a minimum at the 2 minute mixing time. The results of the 100 rpm mixing study are shown in Figure 35. The trend in the data are similar to the 75 rpm results, indicating that the 12.5 mg/kg dose is optimal and 2 minutes of mixing provides the best dewatering conditions at this dose.

The graphs show a general trend of deteriorating sludge as mixing time increased past two minutes. This could be caused by a shearing or folding in the polymer chains or could be the result of metal hydroxide flocs deteriorating. From these results, a standard mixing procedure using a mixing time of 2 minutes along with a sample mixing speed of 100 rpm were used throughout the rest of the polymer study.

Wedge Zone Simulator Study

This phase of the research involved testing the performance of the various polymers using the bench-scale Wedge Zone Simulator (WZS). The WZS simulates the wedge zone and press cycle of a belt filter press.

The SBW sludge samples were prepared according to the procedure listed previously in the methods and materials chapter. Operating conditions of the WZS included using 100

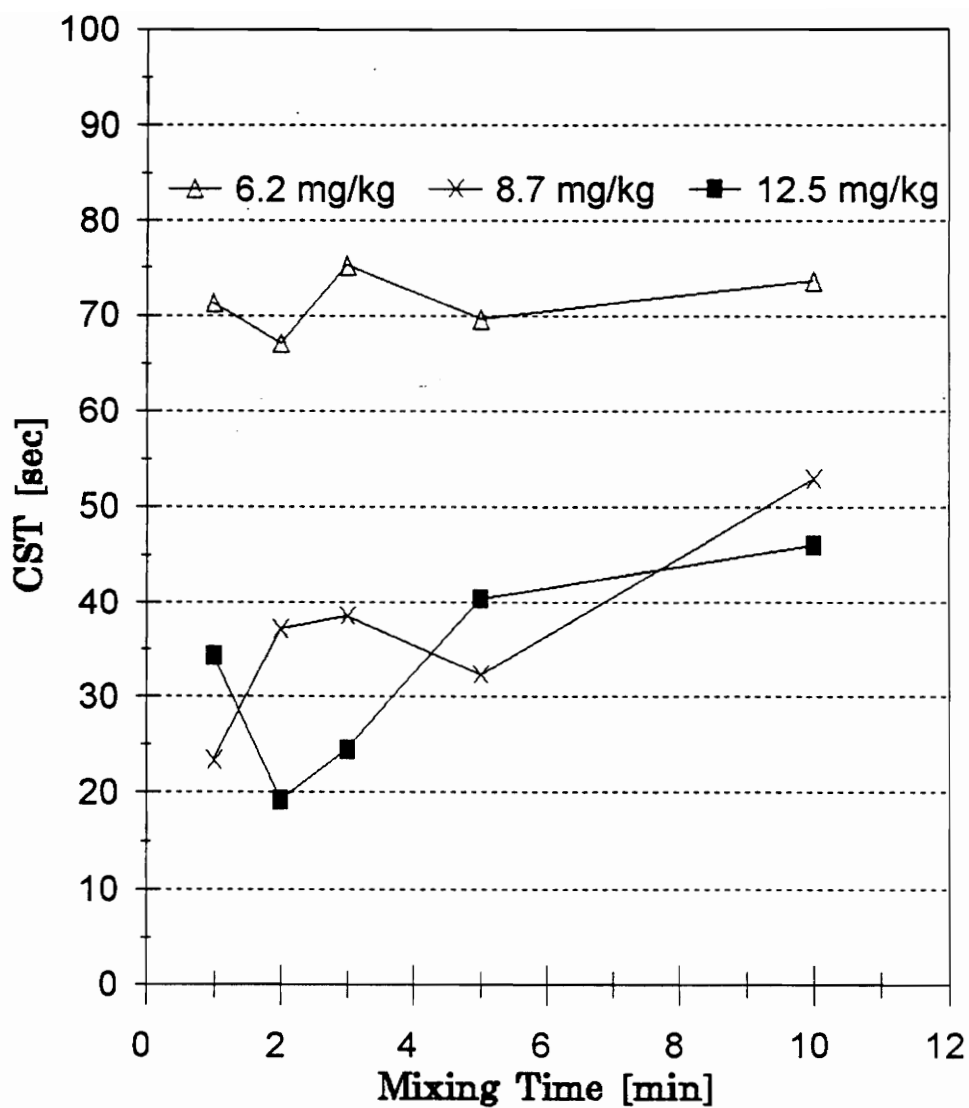


Figure 35. Effect of mixing time on CST for 6.2, 8.7, and 12.5 mg/kg doses of A-M-30% polymer for 100 rpm mixing speed

mL of conditioned sludge and loading the pneumatic cylinder to 20 psi gauge (translating to 6.2 psi applied to the sludge). The conditioned polymer sludge was placed on top of the filter fabric in the bottom to the dewatering chamber in the WZS and the measured time of the test was started at this instant. The free drainage volume was measured at times of 10, 30, 50, and 60 seconds. At 60 seconds, the pressure was applied, and continued for 4 minutes. Filtrate volume continued to be measured at 30 second intervals for the 4 minutes. The total cycle time of the test was 5 minutes.

Optimal dose, cake solids, and filtrate solids data for the polymer tests are shown in Table 6. Cake solids and filtrate solids for each polymer defined the optimal dose.

In order to better evaluate each polymer, two graphs were created from the data obtained from the WZS procedure. The first graph shows capillary suction time as a function of polymer dose. The second graph shows filtrate solids and sludge cake solids as a function of polymer dose.

The conditioning response of polymer A-M-13% (anionic medium molecular weight with a 13% mole charge) is displayed in Figure 36. As the polymer dose increased to 10 mg/kg, the solids removal rate improved considerably. The dose of 10 mg/kg was the optimal dose due to the outstanding

Table 6. List of optimal dose, cake solids, and filtrate solids for each polymer as determined by WZS and CST

Polymer	C-M- 30%	C-L- 30%	A-L- 7%	A-M- 13%	A-M- 20%	A-M- 30%	A-H- 50%
Optimal Dose (mg/kg)	11.0	6.2	29.4	10.0	17.4	11.2	15.6
Cake Solids (%)	22.0	23.6	20.2	23.3	21.9	21.5	22.3
Filtrate Solids (mg/l)	10407	6212	3489	2727	6485	5427	4334

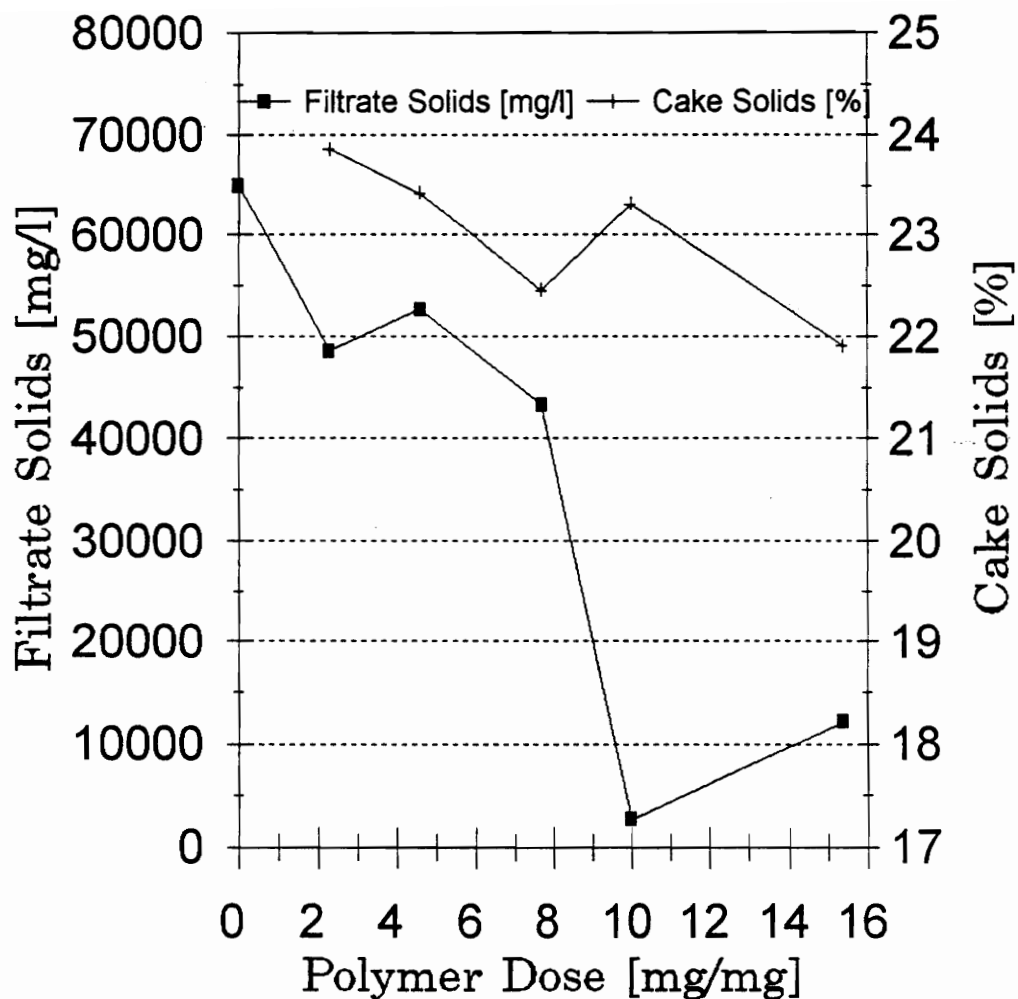


Figure 36. Filtrate solids and cake solids versus A-M-13% polymer dose determined by WZS for 100 rpm mixing speed and 2 min mixing time

filtrate quality and high cake solids concentration. As the polymer dose was increased to 15.4 mg/kg, the filtrate solids concentration deteriorated.

The CST plotted as a function of dose (Figure 37) indicated an optimal polymer dose of 4.6 mg/kg. This conflicts with the 10 mg/kg optimal dose determined by the WZS tests.

The value of the CST is in comparing polymers. The best polymer (lowest dose, lowest CST) should also be best for other dewatering processes, even though the CST does not predict the optimum dose. While the optimal dose according to CST for A-M-13% is significantly underestimated, the optimal doses according to CST for the other polymers was consistently overestimated.

Polymer A-M-30% (anionic medium molecular weight with 30% mole charge) produced good dewatering characteristics. As can be seen in Figure 38, the cake solids content remained consistently above 20% when the sludge was properly dosed. The filtrate solids was low for both the 11.2 mg/kg and the 13.7 mg/kg doses. The CST data shown in Figure 39 for polymer A-M-30% indicated the optimal dose of 11.2 mg/kg. The optimal dose of 11.2 mg/kg was chosen due to the low CST value, low filtrate volume, and high cake solids.

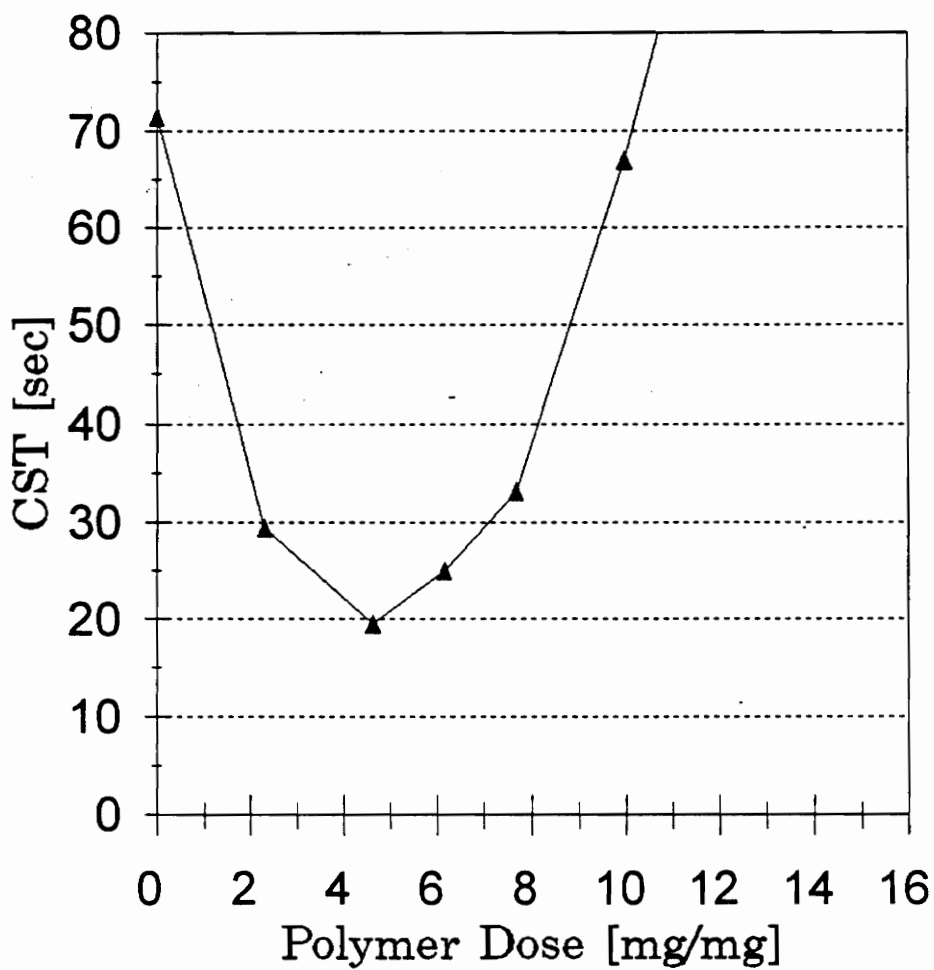


Figure 37. Effect of A-M-13% polymer dose on CST for 100 rpm mixing speed and 2 min mixing time

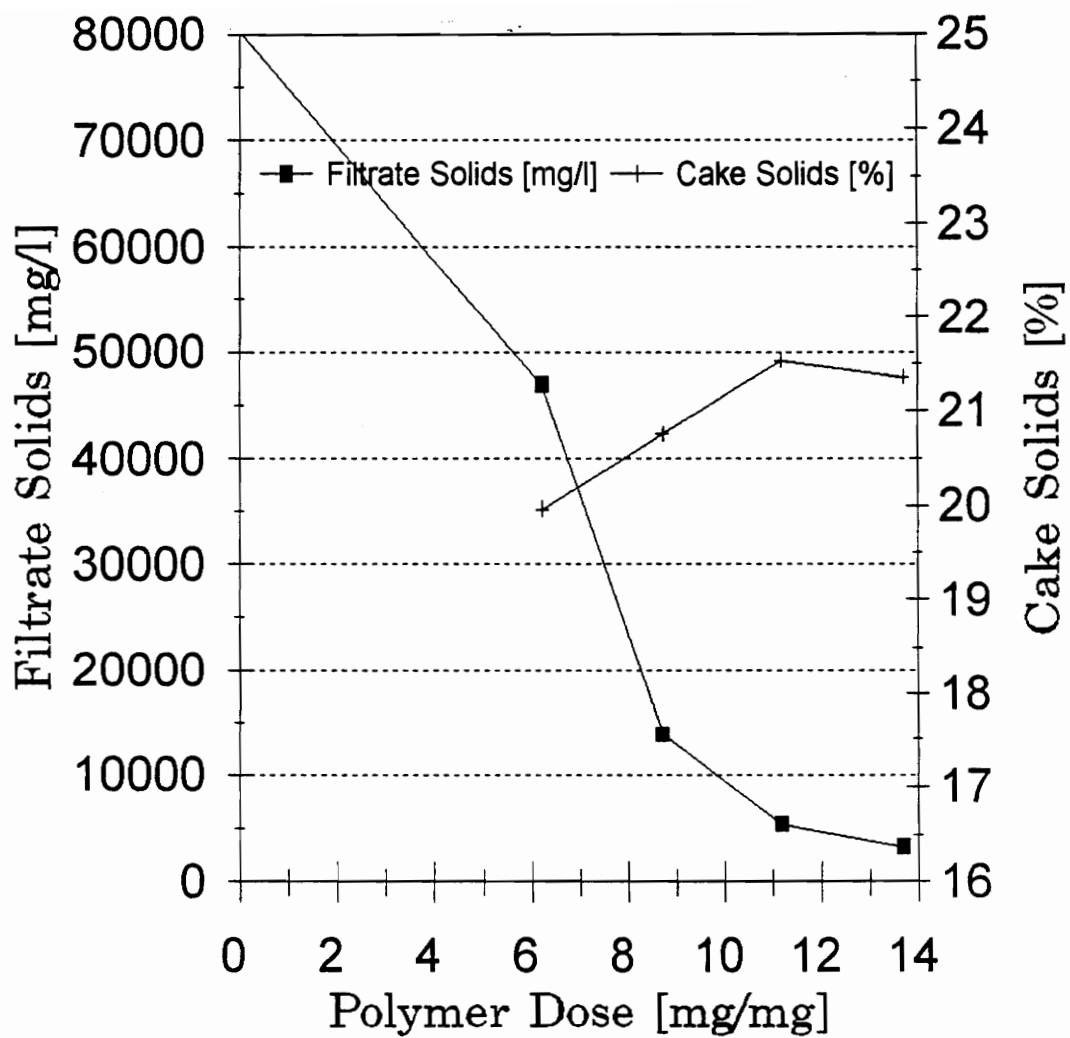


Figure 38. Filtrate solids and cake solids versus A-M-30% polymer dose determined by WZS for 100 rpm mixing speed and 2 min mixing time

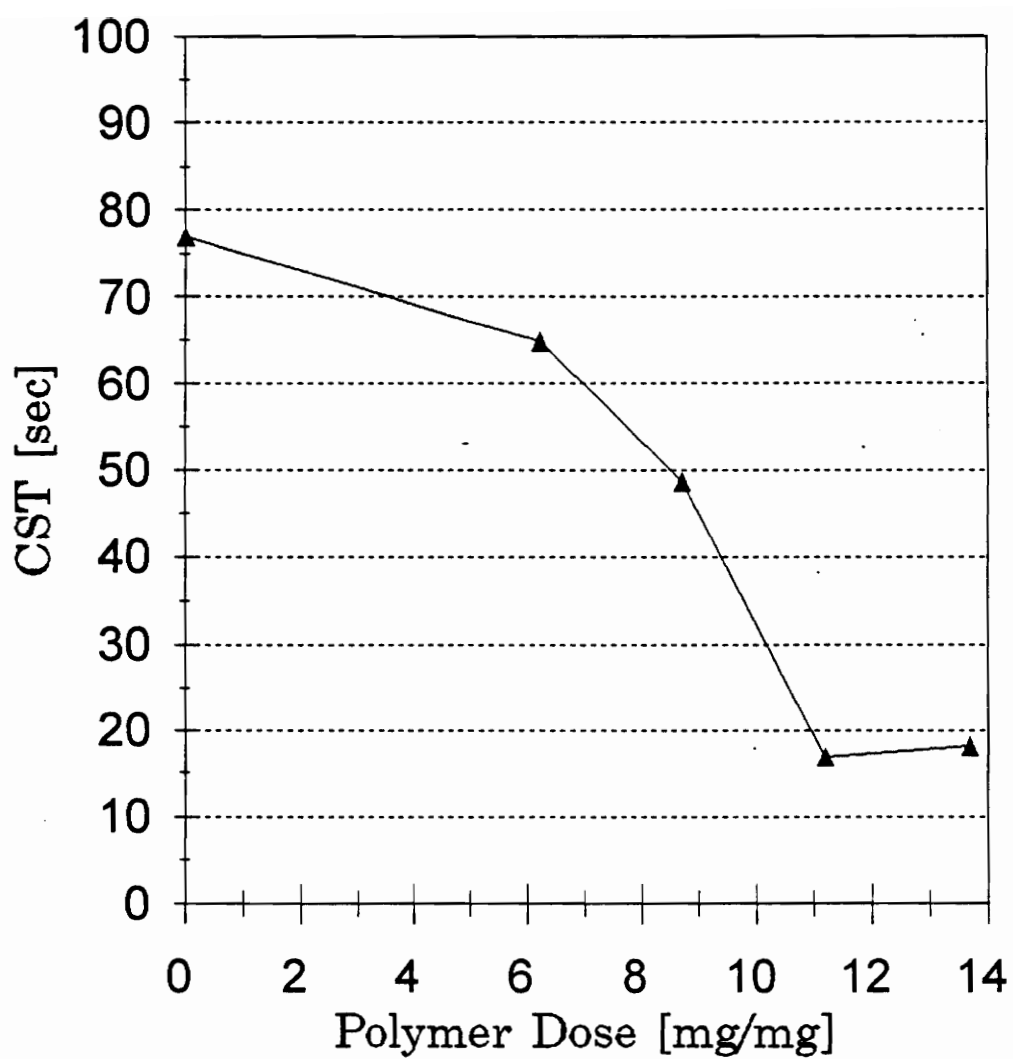


Figure 39. Effect of A-M-30% polymer dose on CST for 100 rpm mixing speed and 2 min mixing time

A-H-50% (anionic high molecular weight with 50% mole charge) results are shown in Figures 40 and 41. The optimal dose based on filtrate quality was selected as 15.6 mg/kg. The cake solids at this dose was above 22%. CST data (Figure 41) also indicated a polymer optimal dose of 15.6 mg/kg.

The other anionic polymers were not as effective, typically requiring much more polymer to achieve similar results. The optimal dose for polymer A-L-7% (anionic low molecular weight with 7% mole charge) was 33.7 mg/kg, which was more than three times higher than the optimal doses for A-M-30% and A-M-13%. Polymer A-M-20% (anionic medium molecular weight with 20% mole charge) behaved in a similar fashion. The results of these polymers can be found in Appendix A.

The majority of the cationic polymers also performed poorly. The performance of C-L-1% (cationic low molecular weight with a 1% mole charge) had poor filtrate quality and a low filter cake solids concentration. Therefore, the data are not included. Polymers C-L-30% and C-M-30% (cationic low and medium molecular weight with 30% mole charge) produced acceptable filtrate solids removal rates (Figures 42 and 44); however, the optimal CST never was below 40 seconds (Figures 43 and 45). It appears both of the

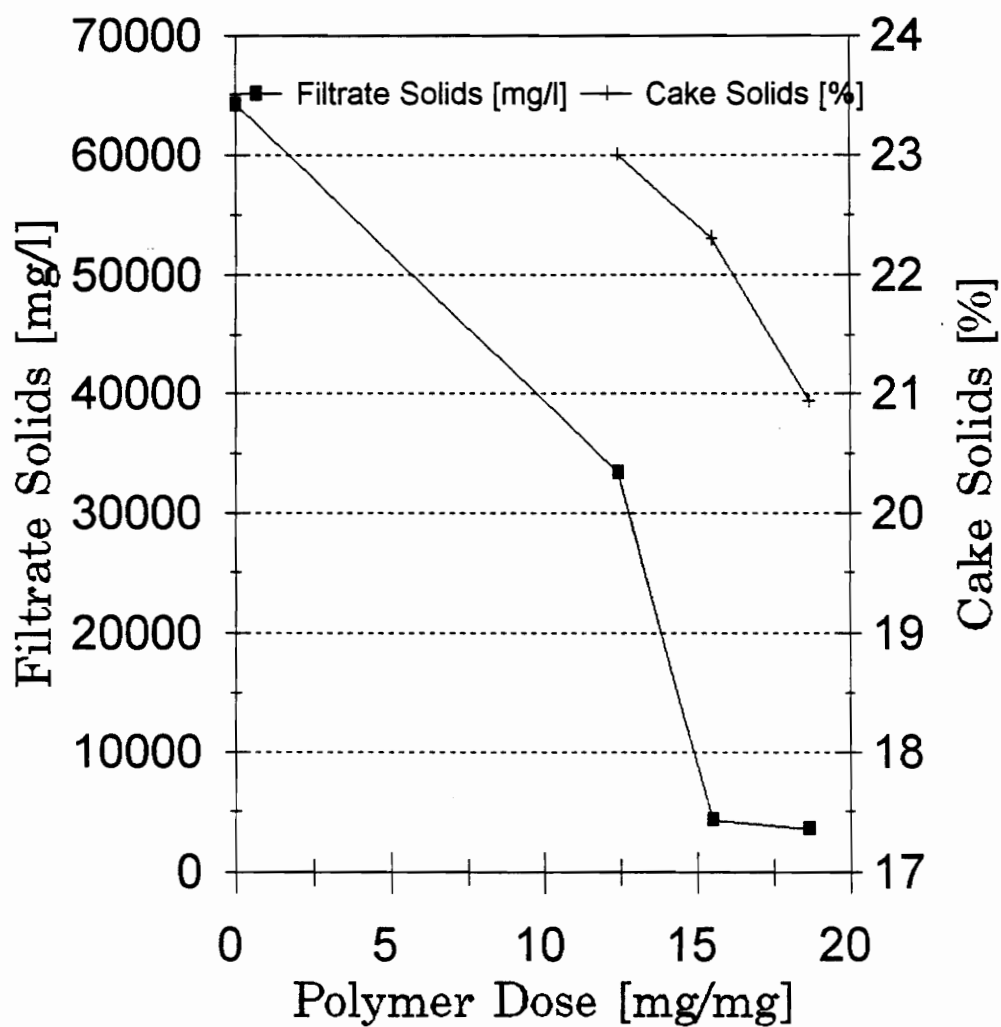


Figure 40. Filtrate solids and cake solids versus A-H-50% polymer dose determined by WZS for 100 rpm mixing speed and 2 min mixing time

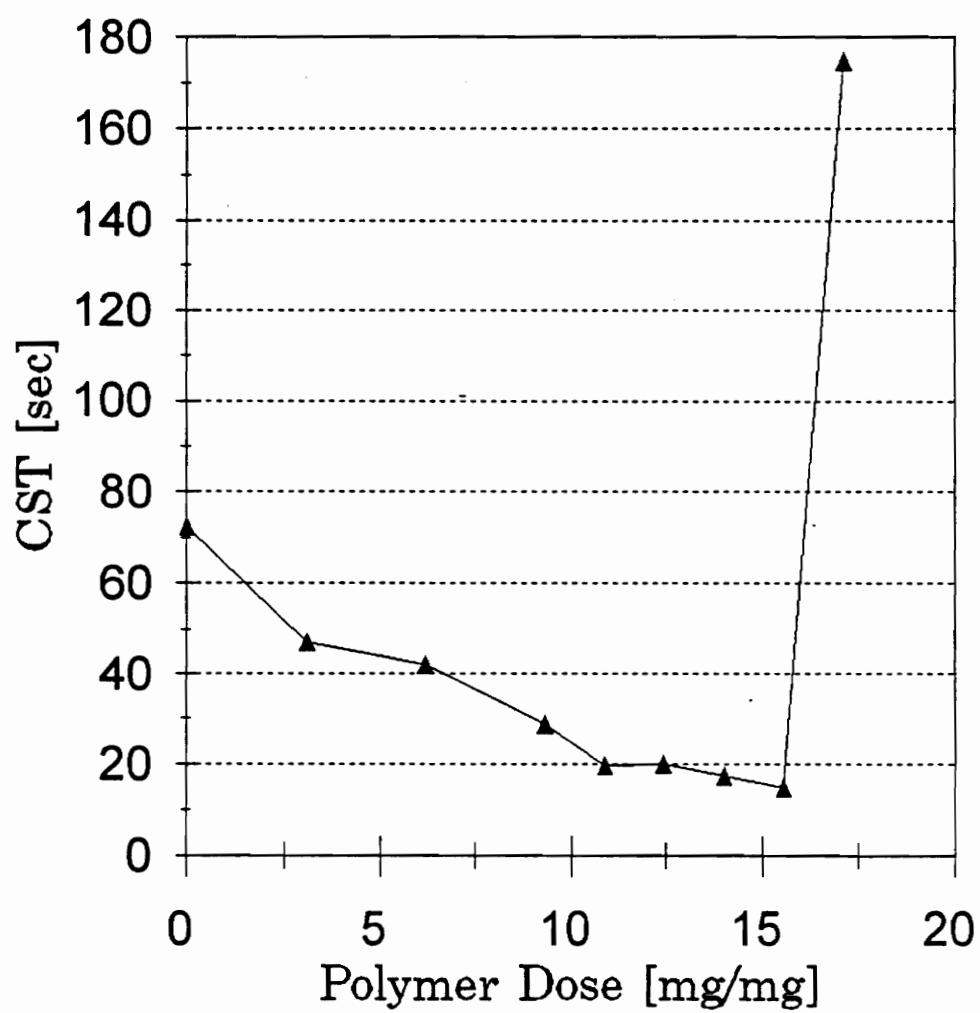


Figure 41. Effect of A-H-50% polymer dose on CST for 100 rpm mixing speed and 2 min mixing time

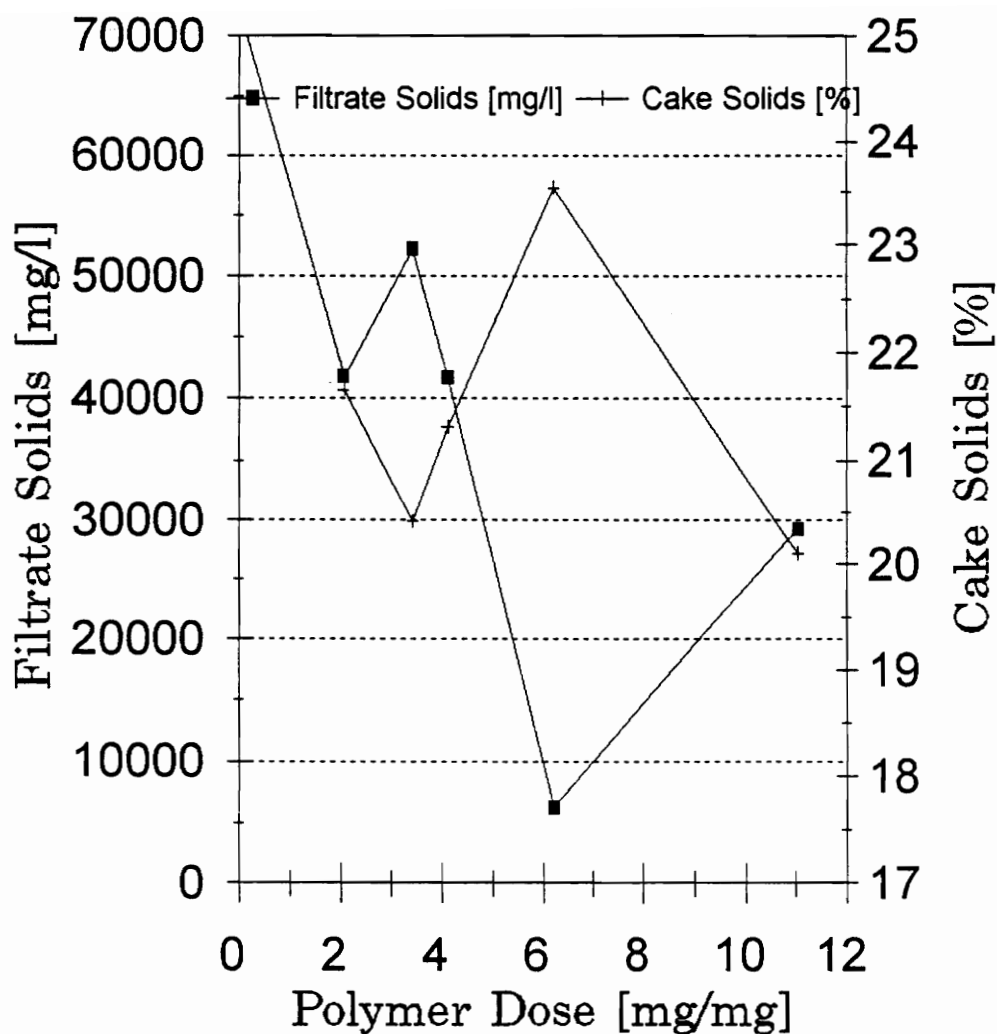


Figure 42. Filtrate solids and cake solids versus C-M-30% polymer dose determined by WZS for 100 rpm mixing speed and 2 min mixing time

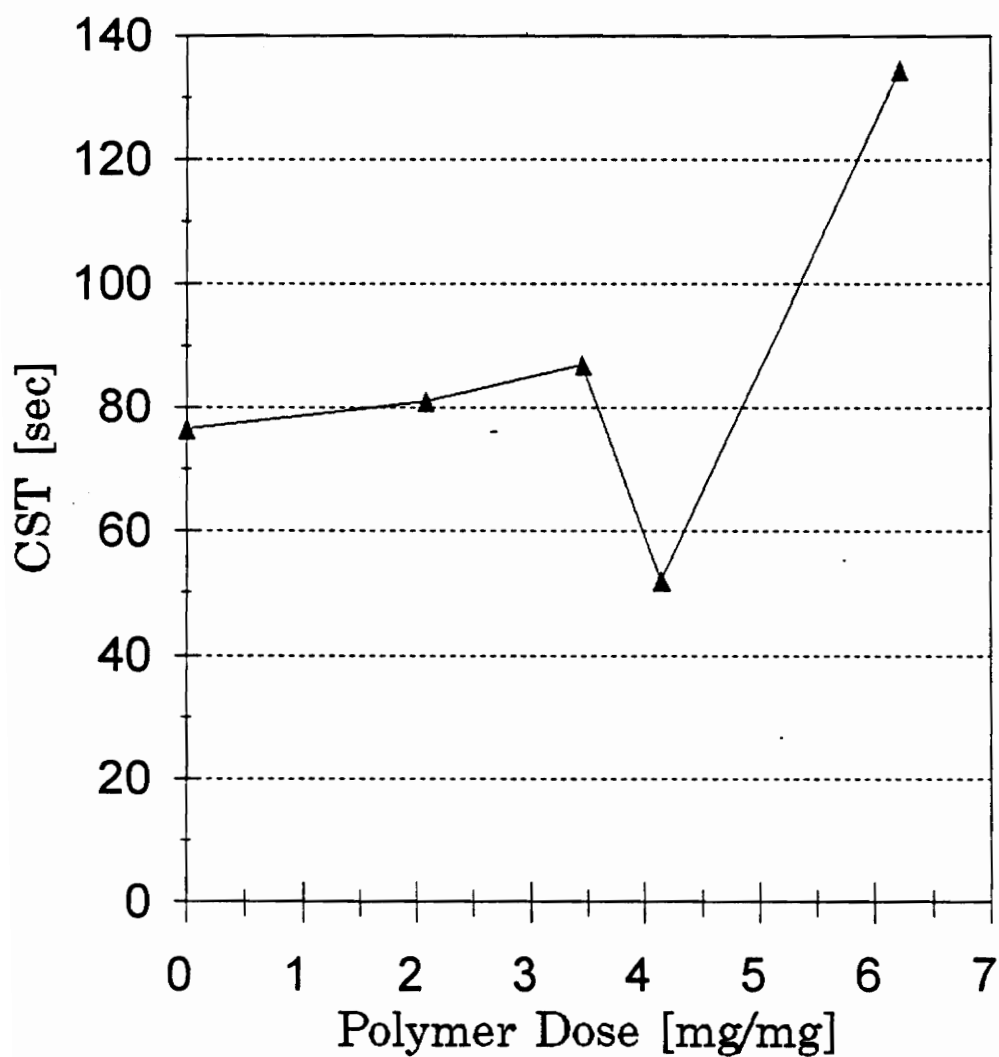


Figure 43. Effect of C-M-30% polymer dose on CST for 100 rpm mixing speed and 2 min mixing time

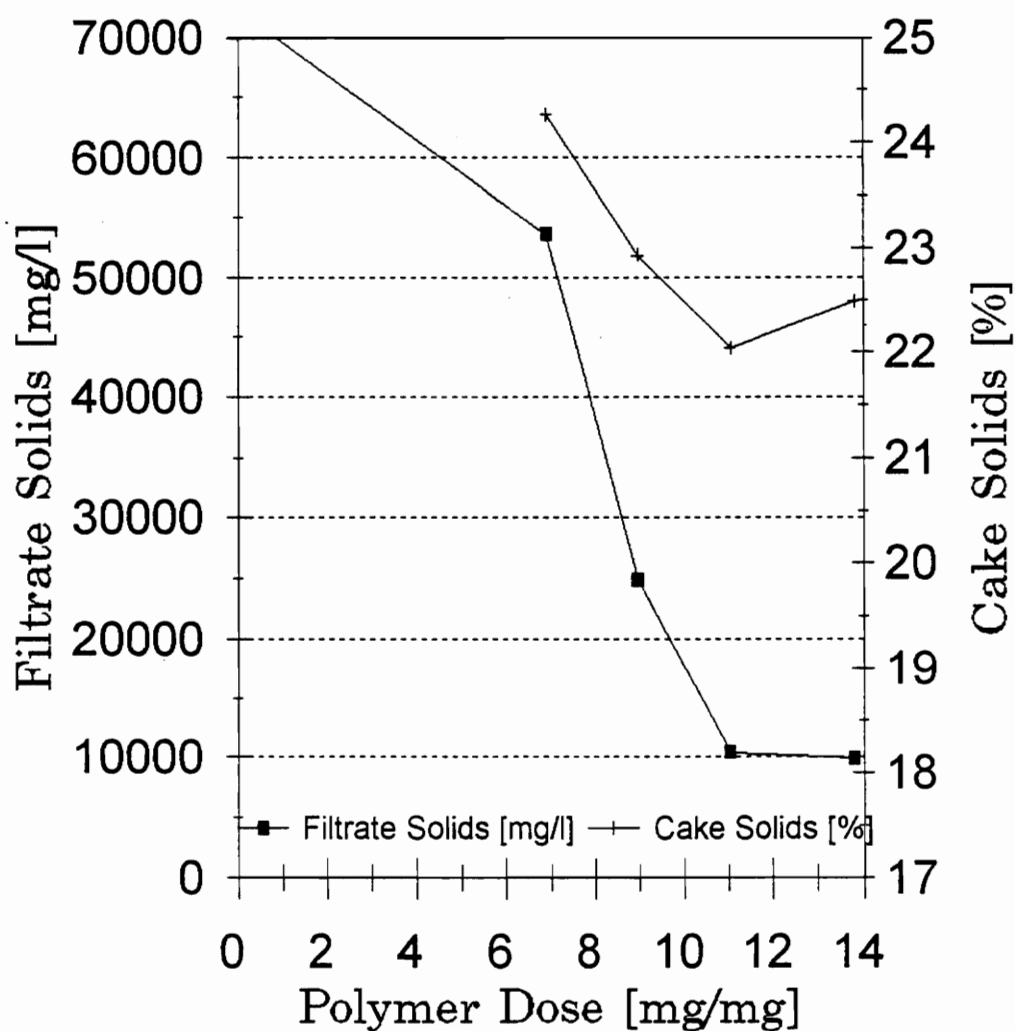


Figure 44. Filtrate solids and cake solids versus C-L-30% polymer dose determined by WZS for 100 rpm mixing speed and 2 min mixing time

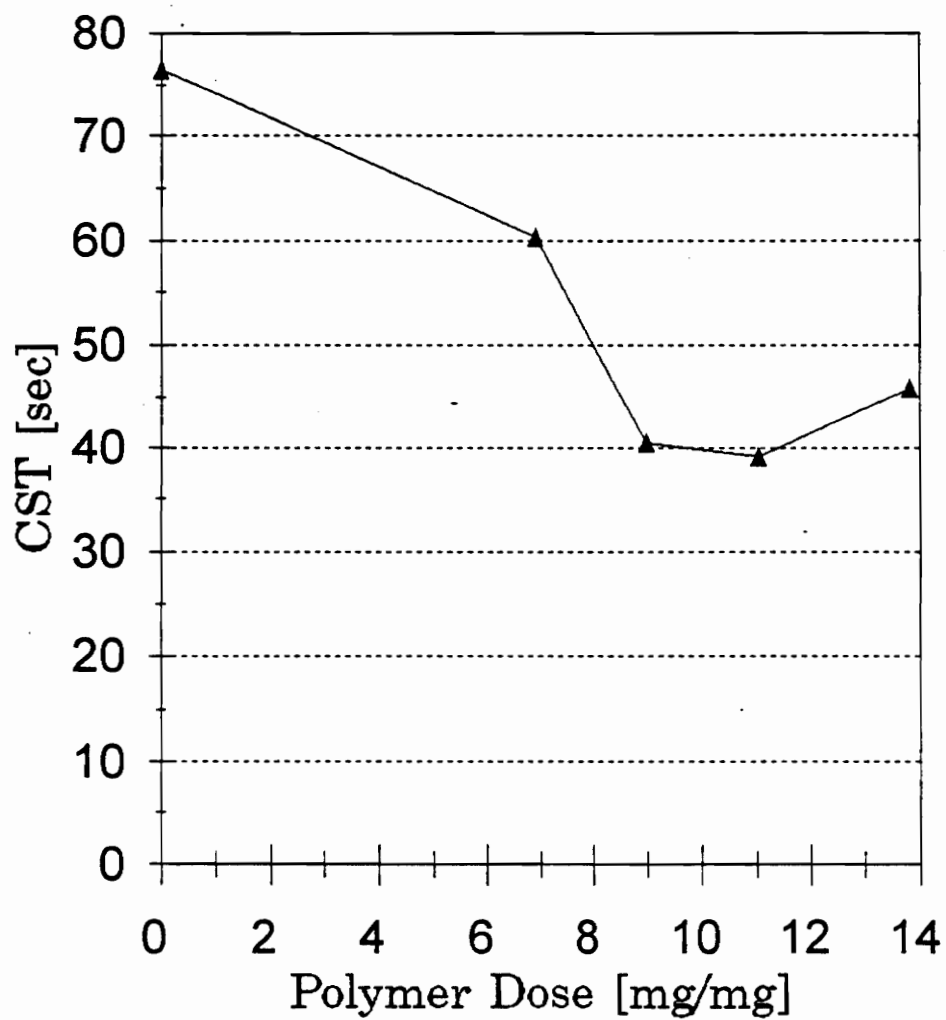


Figure 45. Effect of C-L-30% polymer dose on CST for 100 rpm mixing speed and 2 min mixing time

cationic polymers condition the sludge well compared to the performance of the medium molecular weight anionic polymers.

The sludge, conditioned at the optimal dose achieved for each of the polymers, was then subjected to high speed (15,000 rpm) centrifugation using a laboratory centrifuge. The results of the cake solids for each of the polymers during high speed centrifugation and WZS, along with unconditioned sludge cake solids, are shown in Figure 46. Typical unconditioned sludges during the mixing speed and precipitation pH study produced cake solid concentrations between 20% and 22%. All of the polymers produced a cake solid that would indicate satisfactory performance (above 20%). This indicates a high rate laboratory centrifuge could be possibly incorporated into the SBW sludge dewatering process and the cake solids produced will be similar to those from a belt filter press. Polymers A-M-30%, A-H-50%, and C-L-30% produced high cake during both of the processes. Overall, both dewatering mechanisms produced similar cakes. The cake solids concentration was consistently above 20%. However, cake solids from unconditioned sludges were also consistently above 20%. This data indicates that cake solids concentrations may not improve with the addition of conditioning polymers. The true benefit of polymer addition appears to be in aiding the

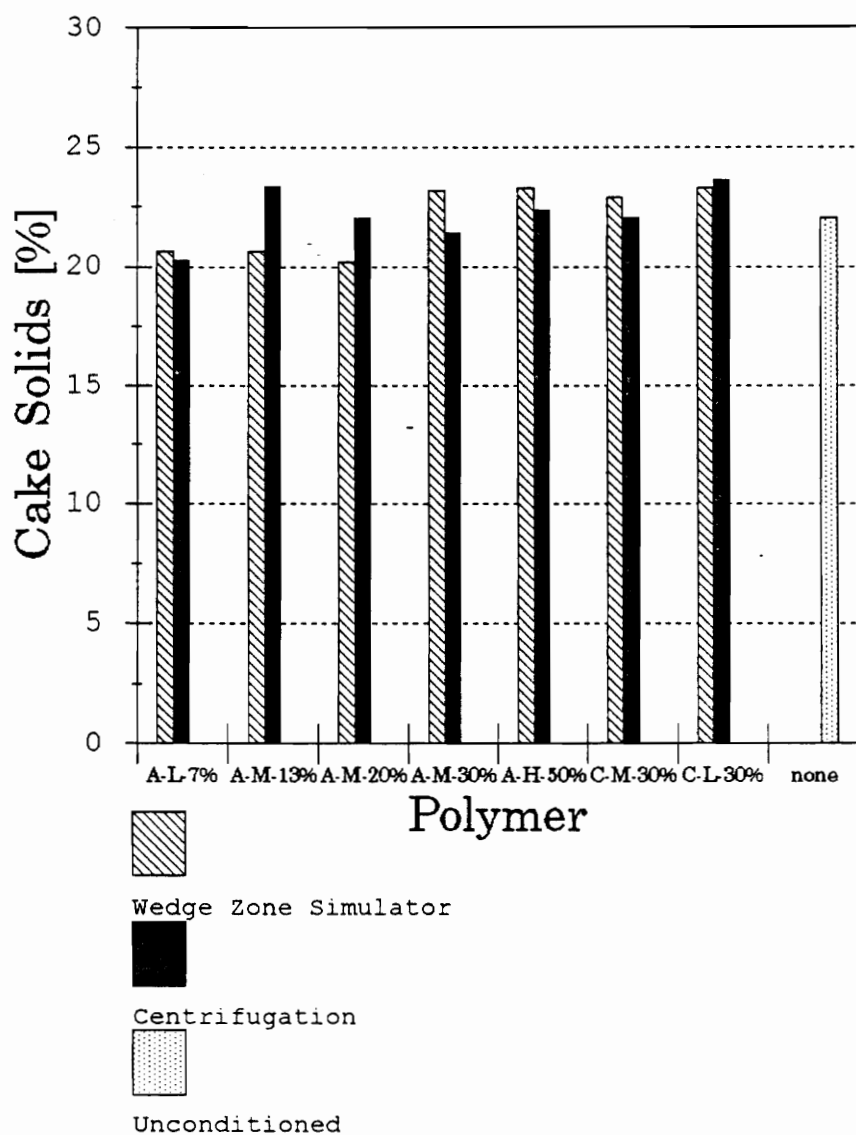


Figure 46. Cake solids concentration obtained from WZS and high speed laboratory centrifuge for the optimal dose of each polymer

sludge dewatering process, not in improving the sludge filter cake.

A summary polymer performance is displayed in Figures 47 and 48. The capture efficiency of most of the polymers was well above 90%, excluding polymers C-M-30% and C-L-1%. When polymer dose is included (Figure 48), A-M-13% and C-L-30% provided the best results. The low required dose, coupled with a very effective capture efficiency and high cake solids make these polymers most suited for conditioning the SBW sludge. Other anionic polymers (A-M-20%, A-M-30%, and A-H-50%) also performed favorably. It can be concluded that the performance of these polymers is similar to conditioning results of other chemical sludges such as water treatment plant (alum) sludges (19, 14, 11). The SBW sludge performs like most other chemical sludges with regard polymer conditioning.

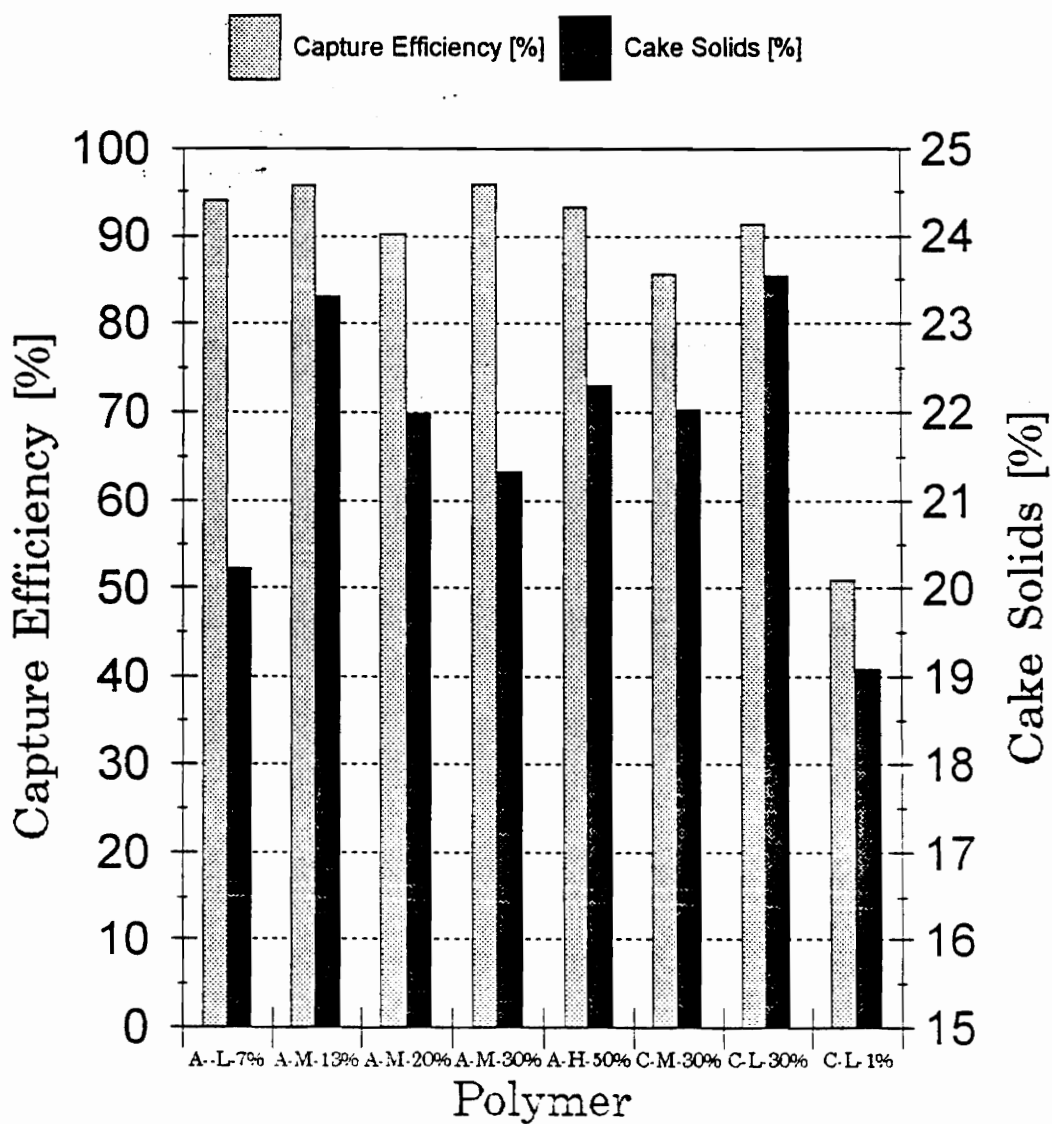


Figure 47. Capture efficiency and cake solids concentration for the optimal dose of each polymer determined by WZS

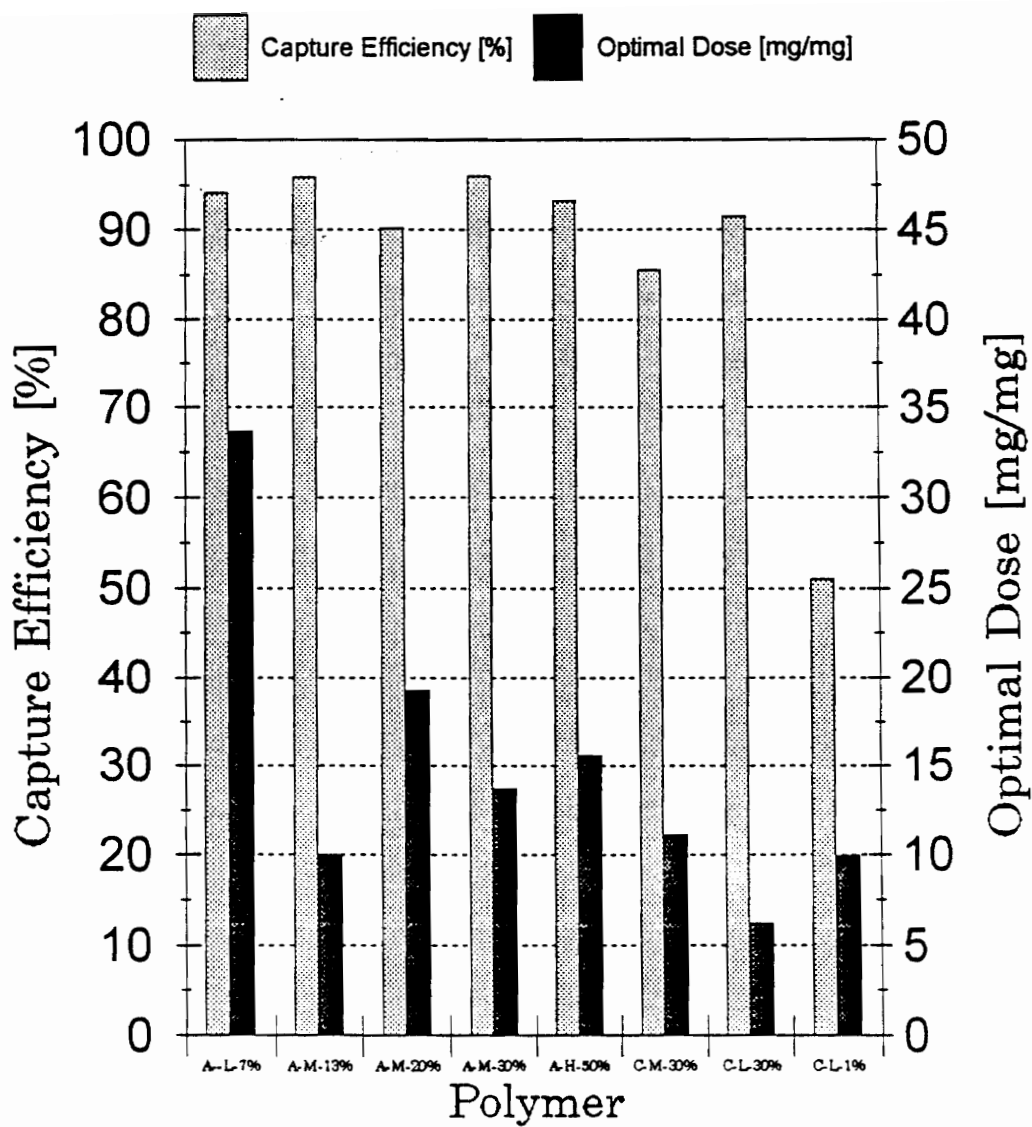


Figure 48. Capture efficiency and optimal dose for each polymer determined by WZS

Summary and Conclusions

The purposes of this study were to develop a chemical precipitation procedure that would treat the radioactive sodium bearing waste (SBW) and to evaluate the use of polymers for sludge conditioning. Several chemical precipitation variables were studied to determine the effect on the resistance to filtration, metals removal rate, and filter cake solids concentration. Polymer conditioners were evaluated base on their ability to produce a low specific resistance to filtration, low capillary suction time, and high cake solids concentration. The wedge zone simulator (WZS) was utilized to simulate belt filter press performance.

Precipitating the SBW at pH between 8.5 and 9.5 maximized the amount of solids removal and provided the least resistance to filtration. Mixing intensity and base addition rates play an important role in chemical precipitation. The data show imparting a high mixing intensity only marginally improves the filtration characteristics of the sludge. Slow base addition rates (less than 1 mL per second) provides benefit to solution precipitation by reducing specific resistance. Reversing the titration by adding the SBW to the base provides lower sludge specific resistance, however, more metals remain in solution. It should be noted that the SBW sludge,

regardless of the precipitation procedures used, possesses good dewatering characteristics with regards to specific resistance and CST.

The polymer experiments showed that anionic medium to high molecular weight and cationic low molecular weight organic polymers provided the best sludge conditioning. The performance of low molecular weight anionic polymers, along with most cationic polymers, did not reduce the specific resistance to filtration to satisfactory levels. Cake solids from both WZS and high speed centrifugation during optimal polymer dosing were typically above 20%.

Based on the results of this study, the following conclusions were made:

1. The SBW sludge can be efficiently precipitated with sodium hydroxide.
2. Changes in mixing speeds and base addition rates can impart changes in the SBW sludge characteristics during chemical precipitation.
3. The optimal solution precipitation pH effective metals removal and good sludge characteristics is between pH 8.5 and 9.5.
4. The addition of calcium, coupled with addition of SBW to a base solution, provides lower specific resistance and higher calcium concentrations in solution.

5. The SBW sludge can be effectively conditioned using medium to high molecular weight anionic and cationic polymers, provided adequate contact times and mixing speeds are used.
6. High speed centrifugation produces cakes solids concentrations above 20% for properly conditioned sludges.
7. The wedge zone simulator results suggest that belt filter press could adequately dewater a properly conditioned SBW sludge, producing filtrates less than 5000 mg/l and cakes solids concentrations greater than 20%.

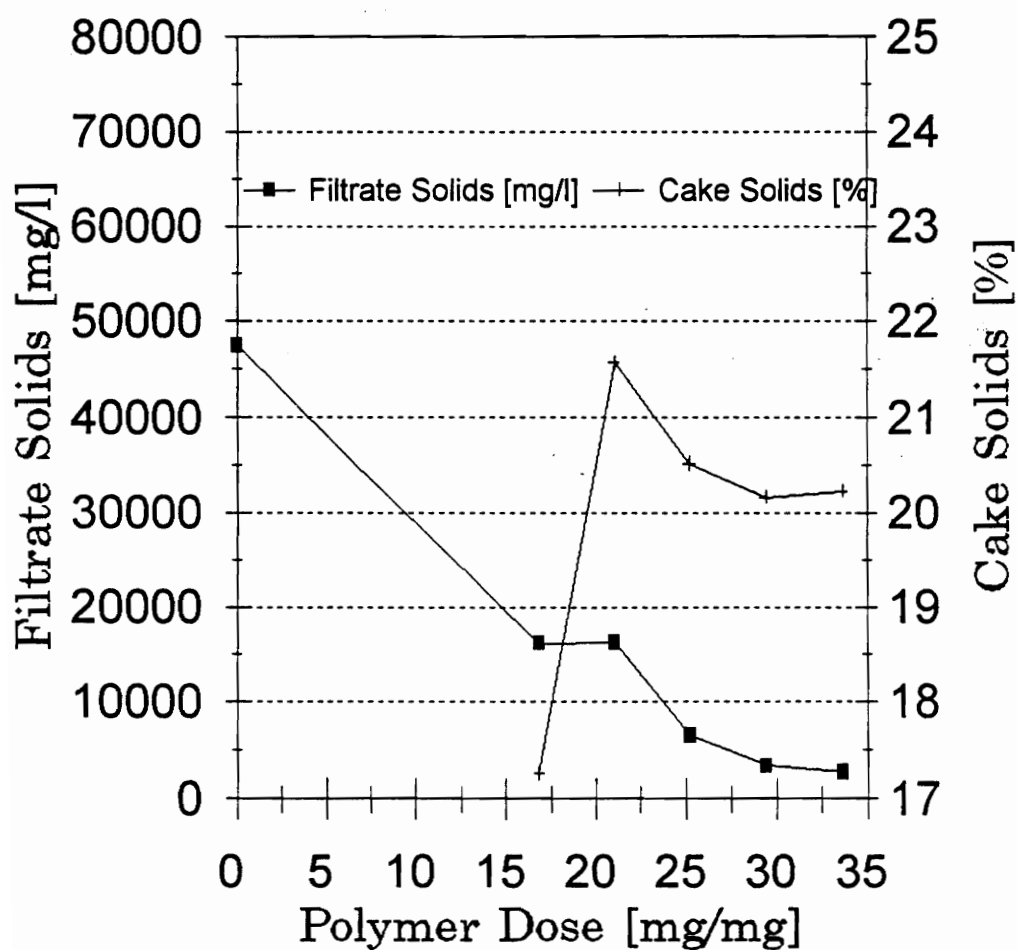
BIBLIOGRAPHY

1. Vesilind, P. A., "Capillary Suction Time as a Fundamental Measure of Sludge Dewaterability." *Journal Water Pollution Control Federation*, 60(2); pp 215-220, (1988)
2. Novak, J. T., and O'Brien, J. H., "Polymer Conditioning of Chemical Sludges." *Journal Water Pollution Control Federation*, 47(10); pp 2397-2410, (1975)
3. Christiansen, G. L. and Dick, R. I., "Specific Resistance Measurements: Nonparabolic Data." *Journal Environmental Engineering Division American Society of Civil Engineers*, 111(3); pp 243-247, (1985)
4. Novak, J. T., and Knocke, W. R., "Discussion of Specific Resistance Measurements: Nonparabolic Data." *Journal Environmental Engineering Division American Society of Civil Engineers*, 113, pp 649-650, (1987)
5. Karr, P. R., and Keinath, T. M., "Limitations of the Specific Resistance and CST Tests for Sludge Dewaterability." *Filtration and Separation*, Nov/Dec 1978, pp 543-544
6. Baskerville, R. C., and Gale, R. S., "A Simple Automatic Instrument for Determining the Filterability of Sewage Sludges." *Journal Water Pollution Control Federation*, 67(3); pp 233-241, (1968)
7. Sato, T., and Ruch, R., "Stabilization of Colloidal Dispersions by Polymer Adsorption." Dekker, New York, New York, p. 155, (1980)
8. Knocke, W. R., Ghosh, M. M., and Novak, J. T., "Vacuum Filtration of Metal Hydroxide Sludges." *Journal Environmental Engineering Division American Society of Civil Engineers*, 106(2); pp 363-376, (1980)
9. Knocke, W. R., "The Characterization of Metal Hydroxide Suspensions." *PhD Dissertation*, University of Missouri - Columbia, (1979)

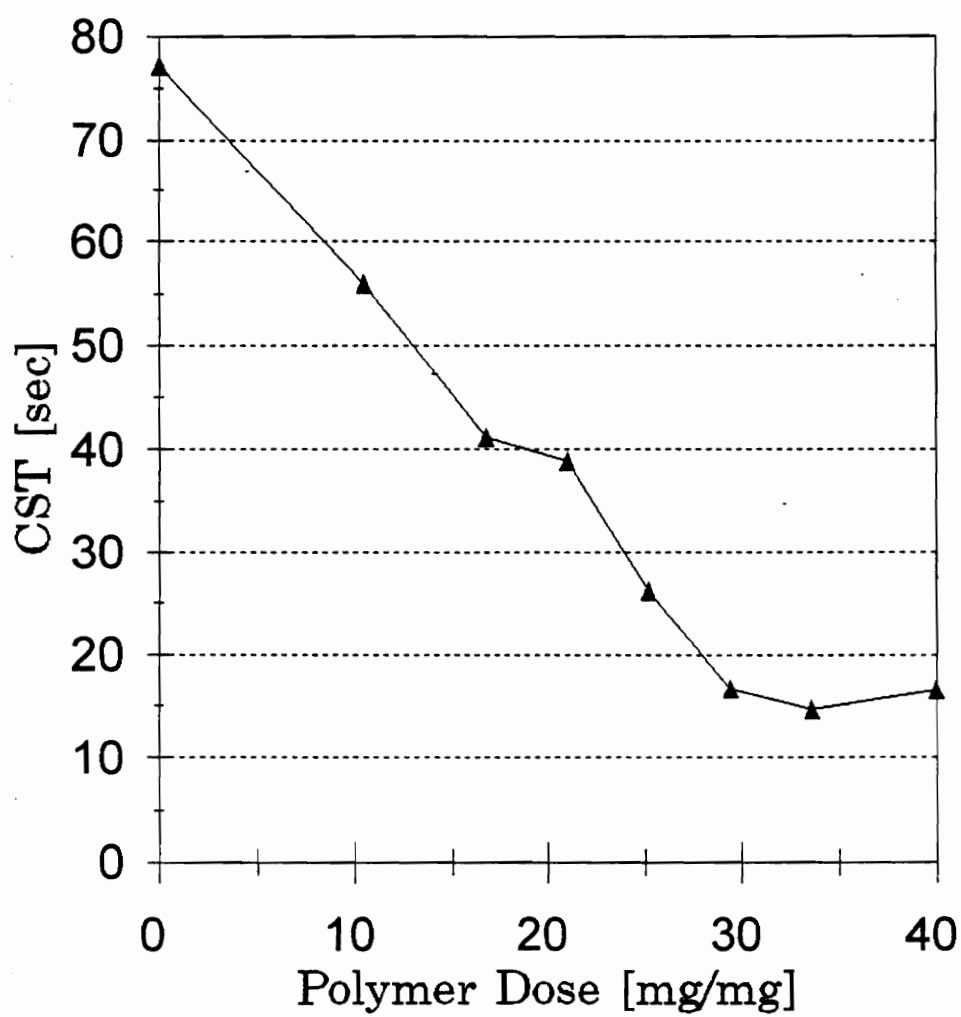
10. Snodgrass, W. J., Clark, M. M., and O'Melia, C. R., "Particle Formation and Growth in Dilute Aluminum (III) Solutions." *Journal Water Resources*, 18(4); pp 479-488, (1984)
11. Werle, C. P., "Effects of High-Stress Polymer Conditioning on the Filterability of Water and Wastewater Sludges." *Masters Thesis*, Virginia Polytechnic Institute and State University, (1984)
12. Bandak, "Effect of Mixing Intensity on Polymer Conditioning of Sludges." *Masters Thesis*, Virginia Polytechnic Institute and State University, (1986)
13. Argaman, Y., and Kaufman, W. J., "Turbulence and Flocculation." *Journal Environmental Engineering Division American Society of Civil Engineers*, 96(2); pp 223-224, (1970)
14. Novak, J. T., and Haugan, B. E., "Chemical Conditioning of Activated Sludge." *Journal Environmental Engineering Division American Society of Civil Engineers*, 105; pp 993-1008, (1978)
15. Clark, M. M, and Flora, J. V., "Floc-Restructuring in Varied Turbulent Mixing." *Journal Colloid and Interface Science*, 147(2); pp 407-421, (1991)
16. Bowen, P. T., and Keinath, T. M., "Effects of Polymer Molecular Weight and Charge Density on Sludge Conditioning." Presented to The Engineering Foundation, Hennicker, New Hampshire, (1985)
17. O'Brien, J. H., and Novak, J. T., "Effects of pH and Mixing on Polymer Conditioning of Chemical Sludges." *Journal American Water Works Association*, 69(11); pp 600-604, (1977)
18. Reitz, D. D., "Municipal Sludge Dewatering Using a Belt Filter Press." *Masters Thesis*, Virginia Polytechnic Institute and State University, (1988)
19. Burgos, W. D., "Laboratory Evaluation of Conditioning Requirements for Sludge Dewatering Using a Belt Filter Press.", *Master Thesis*, Virginia Polytechnic Institute and State University, (1990)

20. Vermeulen, A. C., Gues, J. W., Stol, R. J., and De Bruyn, P. L., "Hydrolysis-Precipitation Studies of Aluminum (III) Solutions; 1. Titration of Acidified Aluminum Nitrate Solutions." *Journal of Colloid and Interface Science*, 51(3); pp 449-458, (1975)
21. Clark, M. M., and Srivastava, R. M., "Mixing and Aluminum Precipitation." *Environmental Science and Technology*, 27(10); pp 2181-2189, (1993)
22. Smith, R. W., and Hem, J. D., U.S.G.S Water Supply Paper 1827-D., U.S. Government Printing Office: Washington D.C., (1972)
23. Knocke, W. R., and Kelley, R. T., "Improving Heavy Metal Sludge Dewatering Characteristics by Recycling Performed Sludge Solids." *Journal Water Pollution Control Federation*, 59(2); pp 86-91, (1987)
24. Stol, J. T., Van Helden, A. K., and De Bruyn, P. L., "Hydrolysis-Precipitation Studies of Aluminum (III) Solutions; 2. A Kinetic Study and Model." *Journal of Colloid and Interface Science*, 59(1); pp 115-131, (1976)
25. Greenburg, A. E., Clesceri, C. S., and Eaton, A. D., "Standard Methods for Examination of Water and Wastewater, 18th edition." pp 2/53-57, (1992)
26. Schecher, W., and McAvoy, D., "Mineql+: A Chemical Equilibrium Program for Personal Computers, version 2.1." The Procter and Gamble Company, Cincinnati, Ohio, (1991)
27. Allison, J. D., Brown, D. S., and Novo-Gradac, K, J., "Minteqa2/Prodefa2, A Geochemical Assessment Model For Environmental Systems: version 3.0." EPA Environmental Research Laboratory, Athens, Georgia, (1991)

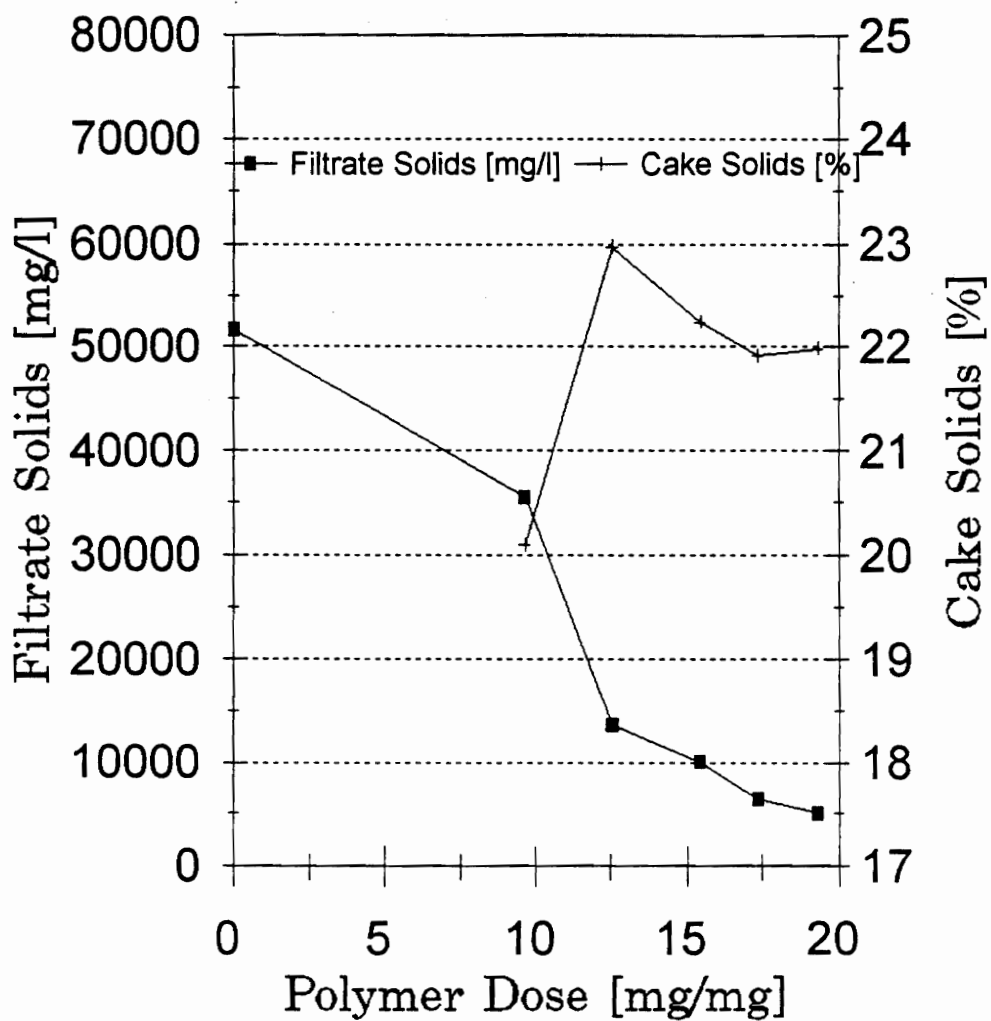
Appendix A - Wedge Zone Simulator Study Results



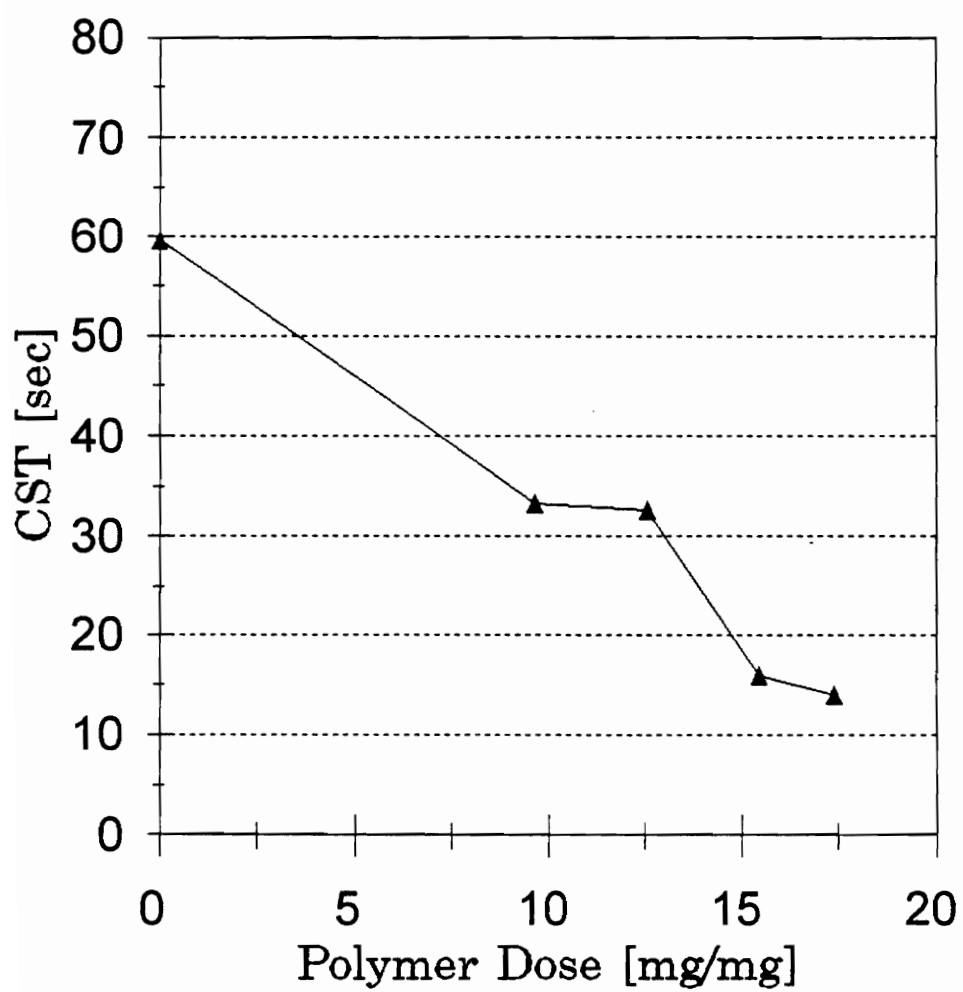
A1. Filtrate solids and cake solids versus A-L-7% polymer dose determined by WZS for 100 rpm mixing speed and 2 min mixing time



A2. Effect of A-L-7% polymer dose on CST for 100 rpm mixing speed and 2 min mixing time



A3. Filtrate solids and cake solids versus A-M-20% polymer dose determined by WZS for 100 rpm mixing speed and 2 min mixing time



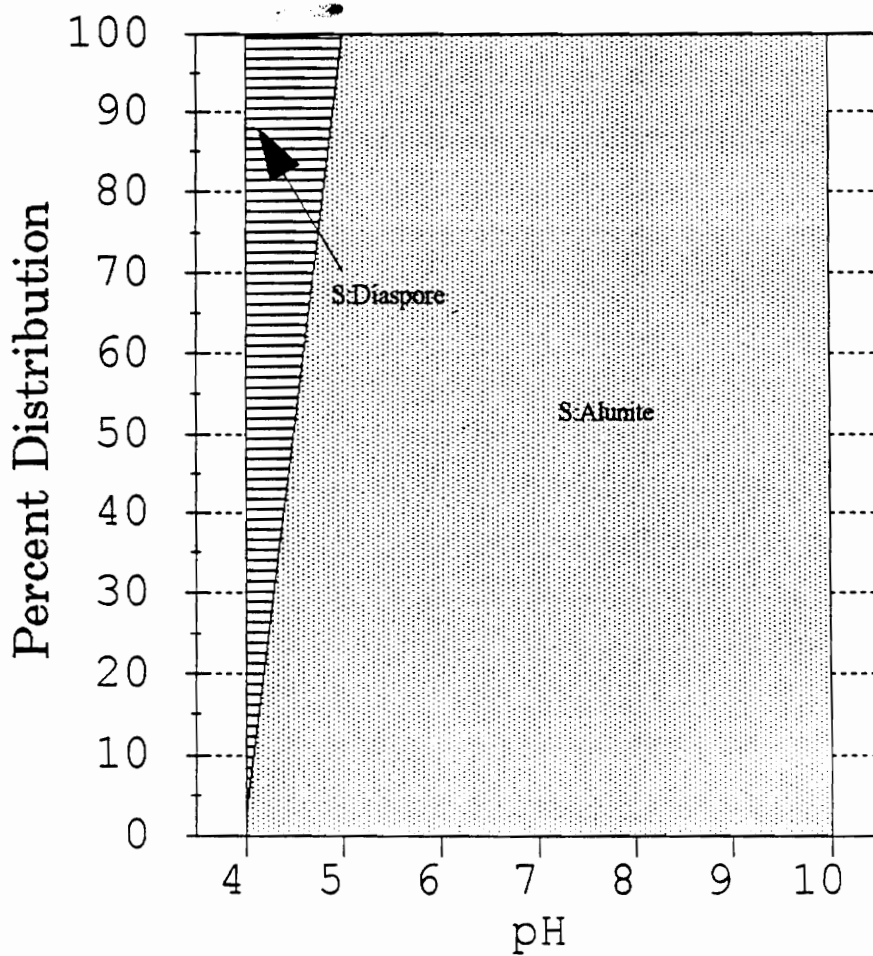
A4. Effect of A-M-20% polymer dose on CST for 100 rpm mixing speed and 2 min mixing time

Appendix B - Mineql+ and Minteqa2 Results

B1. Mineq1 molar distribution of components among aluminum species

pH	Al(3+)	Al(OH)2(+)	Al(OH)3 Aq	Al(OH)4 (-)	AlOH(+2)	AlSO4 +	Al(SO4)2 -	S:ALUNITE	S:AlPO4	S:DIASPORE
4	7.46E-06	5.93E-08	7.46E-10	7.46E-13	7.64E-07	2.14E-07	4.65E-10	0.00629	0.00187	0.635
5	7.46E-09	5.93E-09	7.46E-10	7.46E-12	7.64E-09	4.28E-09	1.86E-10	0.417	0.0136	0.656
6	7.47E-12	5.93E-10	7.46E-10	7.46E-11	7.64E-11	4.28E-12	1.86E-13	0.000417	0.000136	0.656
7	7.46E-15	5.93E-11	7.46E-10	7.46E-10	7.64E-13	4.69E-15	2.23E-16	4.99E-07	1.04E-06	0.656
8	7.46E-18	5.93E-12	7.46E-10	7.46E-09	7.64E-15	7.71E-18	6.04E-19	1.35E-09	1.1E-09	0.656
9	7.46E-21	5.93E-13	7.46E-10	7.46E-08	7.64E-17	7.71E-21	6.05E-22	1.35E-12	5.13E-13	0.656
10	7.46E-24	5.93E-14	7.46E-10	7.46E-07	7.64E-19	7.74E-24	6.08E-25	1.35E-15	2.39E-16	0.656

pH	S:Al2O3	S:Al4(OH)10SO4	S:AlOH5O4	S:AlOH3(A)	S:ALUM K	S:GIBBSITE (C)	S:BOEHMITE
4	5.83E-10	1.7E-08	0.00347	0.000311	1.2E-10	0.0127	0.0197
5	5.83E-10	3.39E-09	0.000695	0.000311	4.99E-11	0.0127	0.0197
6	5.83E-10	3.39E-11	6.95E-06	0.000311	4.98E-14	0.0127	0.0197
7	5.83E-10	3.72E-13	7.6E-08	0.000311	5.97E-17	0.0127	0.0197
8	5.83E-10	6.11E-15	1.25E-09	0.000311	1.61E-19	0.0127	0.0197
9	5.83E-10	6.11E-17	1.25E-11	0.000311	1.61E-22	0.0127	0.0197
10	5.83E-10	6.13E-19	1.25E-13	0.000311	1.62E-25	0.0127	0.0197



B2. pH versus percent distribution of aluminum species from Mineql+

B3. Mineq1 molar distribution of components among calcium species

pH	Ca(2+)	CaOH +	CaHPO4 AQ	CaSO4 AQ	S:LIME	S:PORTLANDITE	S:Ca5OH(PO4)3	S:GYPSUM
4	0.034	8.58E-11	1.75E-08	0.00019	5.43E-27	7.19E-17	5.48E-12	0.0656
5	0.0259	6.53E-10	1.33E-06	0.00289	4.13E-25	5.47E-15	0.014	0.00542
6	0.0144	3.62E-09	3.8E-07	0.00289	2.29E-23	3.04E-13	0.00306	0.00167
7	0.0144	3.62E-08	1.77E-08	0.00289	2.29E-21	3.04E-11	0.00306	0.00167
8	0.0144	3.62E-07	8.2E-10	0.00289	2.29E-19	3.03E-09	0.00306	0.00167
9	0.0144	3.62E-06	3.8E-11	0.00289	2.29E-17	3.03E-07	0.00306	0.00166
10	0.0143	3.62E-05	1.77E-12	0.00289	2.29E-15	3.03E-05	0.00306	0.00165

pH	S:CaHPO4	S:Ca4H(PO4)3	S:ANHYDRITE	Ca4(OH)2(PO4	Ca2OHPO4	CaH2PO4	Ca2ClPO4	Ca5Cl(PO4)3
4	0.000256	8.08E-16	0.0404	1120000000	1100000000	1.31E-06	0.000687	8.05E-18
5	0.0195	2.71E-08	0.615	3.77E+17	6360000000000	1E-05	0.398	2.06E-09
6	0.00556	3.49E-08	0.615	9.44E+19	1.01E+14	2.85E-07	0.629	1.47E-08
7	0.000258	3.49E-10	0.615	2.03E+21	4.67E+14	1.32E-09	0.292	1.47E-09
8	1.2E-05	3.49E-12	0.615	4.38E+22	2.17E+15	6.15E-12	0.136	1.47E-10
9	5.56E-07	3.49E-14	0.615	9.43E+23	1.01E+16	2.85E-14	0.0629	1.47E-11
10	2.58E-08	3.5E-16	0.615	2.03E+25	4.66E+16	1.33E-16	0.0292	1.47E-12

pH	CaPO4	Ca3(PO4)2
4	4.16E-13	5.87E-11
5	3.16E-10	2.59E-05
6	9.02E-10	0.000117
7	4.19E-10	2.52E-05
8	1.94E-10	5.42E-06
9	9.02E-11	1.17E-06
10	4.19E-11	2.52E-07

B4. Mineql molar distribution of components among chlorine species

pH	Cl ⁻	FeCl ₂ +	FeCl ₃ Aq	FeCl ⁺ +2	MnCl ⁺ +	MnCl ₃ -	MnCl ₂ Aq
4	0.0321	1.38E-15	4.42E-18	9.6E-15	1.22E-05	1.54E-09	1.06E-07
5	0.0321	1.38E-18	4.42E-21	9.6E-18	9E-06	1.14E-09	7.85E-08
6	0.0321	1.38E-21	4.42E-24	9.6E-21	9E-06	1.14E-09	7.85E-08
7	0.0321	1.38E-24	4.42E-27	9.6E-24	1.17E-05	1.48E-09	1.02E-07
8	0.0321	1.38E-27	4.41E-30	9.6E-27	2.46E-05	3.1E-09	2.15E-07
9	0.0321	1.38E-30	4.41E-33	9.6E-30	2.46E-05	3.1E-09	2.15E-07
10	0.0321	1.38E-33	4.42E-36	9.6E-33	1.59E-06	2.01E-10	1.39E-08

pH	S:FE(OH)2.7CL.3	S:MnCl ₂ , 4H ₂ O	S:HALITE	Ca ₂ ClPO ₄	Ca ₅ Cl(PO ₄) ₃
4	0.244	1.89E-10	0.00109	0.000686	8.04E-18
5	0.122	1.39E-10	0.00109	0.0054	5.13E-15
6	0.0614	1.39E-10	0.00109	0.054	5.13E-12
7	0.0308	1.82E-10	0.00109	0.345	1.47E-09
8	0.0154	3.81E-10	0.00109	0.136	1.47E-10
9	0.00772	3.81E-10	0.00109	0.0629	1.47E-11
10	0.00387	2.46E-11	0.00109	0.0292	1.47E-12

B5. Mineql molar distribution of components among iron species

pH	Fe(3+)	FeOH +2	FeOH2 +	Fe2(OH)2+4	FeOH3 AQ	FeOH4 -	Fe3(OH)4+5	FeHPO4 +
4	9.91E-15	6.4E-13	2.12E-12	1.1E-23	2.49E-16	2.49E-20	4.88E-33	2.53E-18
5	9.91E-18	6.4E-15	2.12E-13	1.1E-27	2.49E-16	2.49E-19	4.88E-38	3.43E-21
6	9.91E-21	6.4E-17	2.12E-14	1.1E-31	2.49E-16	2.49E-18	4.88E-43	3.43E-24
7	9.91E-24	6.4E-19	2.12E-15	1.1E-35	2.49E-16	2.49E-17	4.88E-48	2.63E-27
8	9.91E-27	6.4E-21	2.12E-16	1.1E-39	2.49E-16	2.49E-16	4.88E-53	2.79E-31
9	9.91E-30	6.4E-23	2.12E-17	1.1E-43	2.49E-16	2.49E-15	4.88E-58	1.3E-35
10	9.91E-33	6.4E-25	2.12E-18	1.1E-47	2.49E-16	2.49E-14	4.88E-63	6.05E-40

pH	FeCl2 +	FeCl3 AQ	FeCl +2	FeSO4 +	Fe(SO4)2 -	S:HEMATITE	S:FeOH)2.7CL.3	S:LEPIDOCROCIT
4	1.38E-15	4.42E-18	9.6E-15	2.26E-15	1.95E-18	0.0137	0.244	0.000422
5	1.38E-18	4.42E-21	9.6E-18	4.52E-17	7.82E-19	0.0137	0.122	0.000422
6	1.38E-21	4.42E-24	9.6E-21	4.52E-20	7.83E-22	0.0137	0.0614	0.000422
7	1.38E-24	4.42E-27	9.6E-24	4.94E-23	9.38E-25	0.0137	0.0308	0.000422
8	1.38E-27	4.41E-30	9.6E-27	8.13E-26	2.54E-27	0.0137	0.0154	0.000422
9	1.38E-30	4.41E-33	9.6E-30	8.13E-29	2.54E-30	0.0137	0.00772	0.000422
10	1.38E-33	4.42E-36	9.6E-33	8.16E-32	2.55E-33	0.0137	0.00387	0.000422

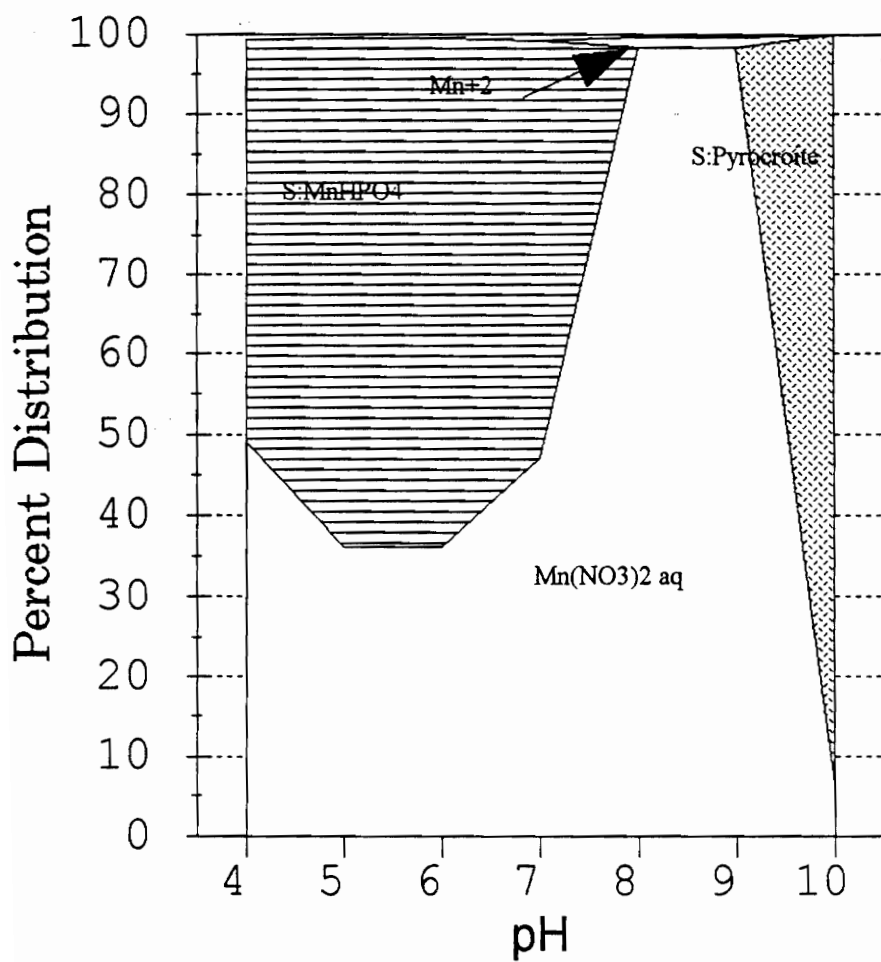
pH	S:GOETHITE	S:FERRHYDRITE	S:MAGHEMITE	S:JAROSITE K	S:JAROSITE NA	S:JAROSITE H	S:STRENGITE	S:FePO4
4	0.00313	1.27E-07	4.04E-11	6.65E-14	1.5E-16	9.17E-20	1.05E-05	2.65E-06
5	0.00313	1.27E-07	4.04E-11	2.77E-14	6E-17	3.68E-21	1.43E-07	3.59E-08
6	0.00313	1.27E-07	4.04E-11	2.77E-17	6E-20	3.68E-25	1.43E-09	3.59E-10
7	0.00313	1.27E-07	4.04E-11	3.32E-20	7.19E-23	4.41E-29	1.1E-11	2.75E-12
8	0.00313	1.27E-07	4.04E-11	8.96E-23	1.94E-25	1.19E-32	1.17E-14	2.93E-15
9	0.00313	1.27E-07	4.04E-11	8.96E-26	1.94E-28	1.19E-36	5.41E-18	1.36E-18
10	0.00313	1.27E-07	4.04E-11	9.01E-29	1.95E-31	1.2E-40	2.52E-21	6.34E-22

pH	S:FE2(SO4)3	FeH2PO4
4	5.29E-46	4.01E-15
5	4.25E-48	5.43E-19
6	4.25E-54	5.43E-23
7	5.57E-60	4.16E-27
8	2.48E-65	4.43E-32
9	2.48E-71	2.06E-37
10	1E-75	9.59E-43

B6. Mineql molar distribution of components among manganese species

pH	Mn(2+)	MnOH +	Mn(OH)3 -1	MnHPO4	MnCl +	MnCl3 -	MnCl2 Aq	Mn(NO3)2Aq	MnSO4 Aq
4	9.4E-05	2.42E-11	1.49E-27	6.31E-10	1.22E-05	1.54E-09	1.06E-07	0.0071	4.68E-07
5	6.93E-05	1.78E-10	1.1E-24	6.31E-10	9E-06	1.14E-09	7.85E-08	0.00525	6.91E-06
6	6.93E-05	1.78E-09	1.1E-21	6.31E-10	9E-06	1.14E-09	7.85E-08	0.00525	6.91E-06
7	9.05E-05	2.33E-08	1.43E-18	6.31E-10	1.17E-05	1.48E-09	1.02E-07	0.00684	9.88E-06
8	0.00019	4.88E-07	3.01E-15	1.41E-10	2.46E-05	3.1E-09	2.15E-07	0.0143	3.41E-05
9	0.00019	4.88E-06	3.01E-12	6.54E-12	2.46E-05	3.1E-09	2.15E-07	0.0142	3.41E-05
10	1.22E-05	3.15E-06	1.94E-10	1.97E-14	1.59E-06	2.01E-10	1.39E-08	0.00093	2.21E-06

pH	S:MnHPO4(C)	S:PYROCROITE	S:MnCl2, 4H2O	S:Mn3(PO4)2	S:MnSO4
4	0.0073	7.67E-12	1.89E-10	1E-23	5.51E-12
5	0.00917	5.66E-10	1.39E-10	7.38E-22	8.14E-11
6	0.00917	5.66E-08	1.39E-10	7.38E-20	8.14E-11
7	0.00755	7.39E-06	1.82E-10	9.63E-18	1.16E-10
8	0.223	0.00155	3.81E-10	1.01E-16	4.02E-10
9	0.0104	0.155	3.81E-10	2.17E-17	4.01E-10
10	3.12E-05	0.0136	2.46E-11	1.27E-21	2.6E-11



B7. pH versus percent distribution of manganese species from Mineql+

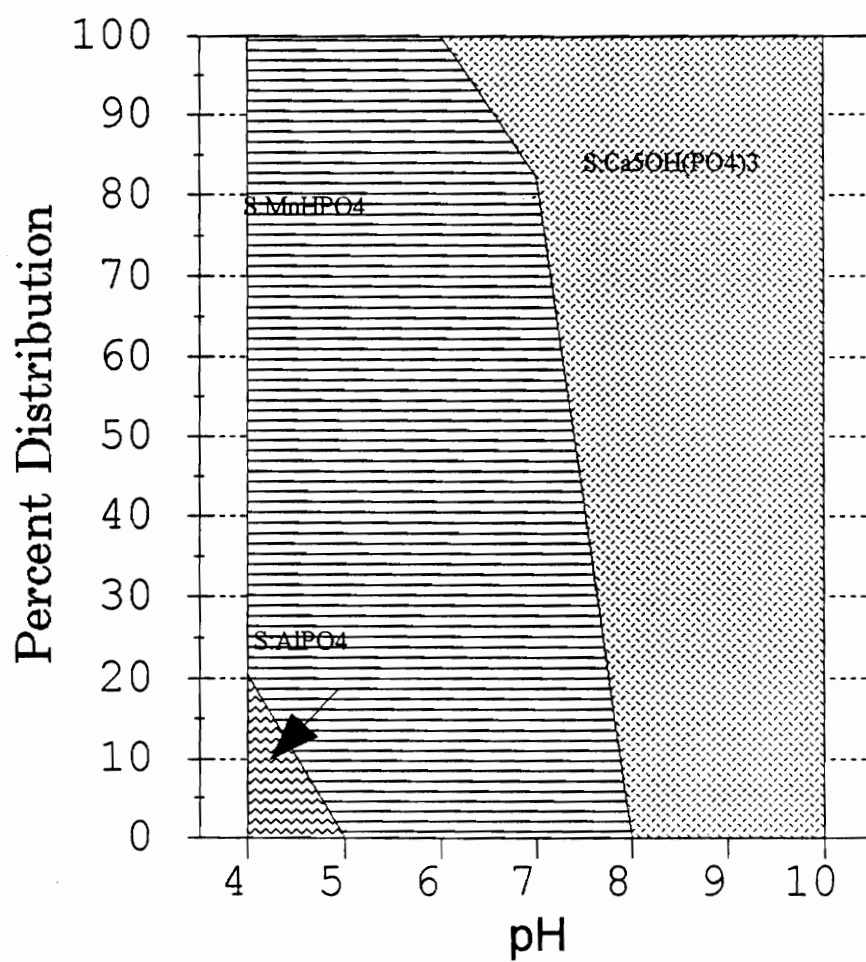
B8. Mined molar distribution of components among phosphorus species

ph	PO4(3-)	CaHPO4 AQ	FeHPO4 +	KHPO4 -	MnHPO4	H2PO4 -
4	4.24E-18	1.75E-08	2.53E-18	2.68E-10	6.31E-10	1.51E-06
5	5.74E-17	1.81E-08	3.43E-21	3.77E-10	6.31E-10	2.05E-07
6	5.74E-16	1.81E-08	3.43E-24	3.77E-10	6.31E-10	2.05E-08
7	4.40E-15	1.27E-08	2.63E-27	2.88E-10	6.31E-10	1.57E-09
8	4.88E-15	8.19E-10	2.79E-31	3.08E-11	1.41E-10	1.67E-11
9	2.17E-15	3.80E-11	1.30E-35	1.42E-12	6.54E-12	7.76E-14
10	1.01E-15	1.77E-12	6.05E-40	6.63E-14	1.97E-14	3.62E-16

ph	H3PO4	SAiPO4	SMNHPO4(O)	SCaSO4(PO4)3	SSTRENGITE	SCaHPO4
4	2.17E-08	1.87E-03	7.30E-03	5.48E-12	1.05E-05	2.58E-04
5	2.95E-10	1.36E-02	9.17E-03	3.50E-08	1.43E-07	2.64E-04
6	2.94E-12	1.36E-04	9.17E-03	3.50E-04	1.43E-08	2.64E-04
7	2.26E-14	1.04E-06	7.55E-03	5.39E-04	1.10E-11	1.85E-04
8	2.40E-17	1.10E-09	2.23E-01	3.08E-03	1.17E-14	1.20E-05
9	1.11E-20	5.13E-13	1.04E-02	3.08E-03	5.41E-18	5.56E-07
10	5.20E-24	2.39E-16	3.12E-05	3.08E-03	2.52E-21	2.58E-08

ph	SFePO4	SMN3(PO4)2	Ca4(OH)2(PO4	Ca2OHPO4	CaH2PO4	FeH2PO4
4	2.65E-06	1.00E-23	1.12E+10	1.10E+09	1.31E-06	4.01E-15
5	3.59E-08	7.38E-22	6.94E+13	8.62E+10	1.36E-07	5.43E-19
6	3.59E-10	7.38E-20	6.94E+17	8.62E+12	1.36E-08	5.43E-23
7	2.75E-12	9.63E-18	2.84E+21	5.51E+14	9.49E-10	4.19E-27
8	2.93E-15	1.01E-16	4.38E+22	2.17E+15	6.14E-12	4.43E-32
9	1.36E-18	2.17E-17	9.44E+23	1.01E+16	2.85E-14	2.06E-37
10	6.34E-22	1.27E-21	2.03E+25	4.66E+16	1.33E-16	9.59E-43

ph	Ca3(PO4)2	Ca2ClPO4	Ca5Cl(PO4)3	CaPO4
4	5.87E-11	6.86E-04	8.04E-18	4.16E-13
5	4.77E-09	5.40E-03	5.13E-15	4.29E-12
6	4.78E-07	5.40E-02	5.13E-12	4.29E-11
7	2.13E-05	3.45E-01	1.47E-09	3.00E-10
8	5.42E-06	1.36E-01	1.47E-10	1.94E-10
9	1.17E-06	6.29E-02	1.47E-11	9.01E-11
10	2.52E-07	2.92E-02	1.47E-12	4.19E-11



B9. pH versus distribution of phosphorous species from Mineql+

B10. Mineql molar distribution of components among potassium species

pH	K(+)	KHPO4 -	KSO4 -	S:ALUNITE	S:JAROSITE K	S:ALUM K
4	0.145	2.68E-10	2.8E-05	0.00629	6.65E-14	1.2E-10
5	0.15	3.77E-10	0.000583	0.417	2.77E-14	4.99E-11
6	0.15	3.77E-10	0.000584	0.000417	2.77E-17	4.98E-14
7	0.15	2.89E-10	0.000639	4.99E-07	3.32E-20	5.97E-17
8	0.15	3.06E-11	0.00105	1.35E-09	8.96E-23	1.61E-19
9	0.15	1.42E-12	0.00105	1.35E-12	8.96E-26	1.61E-22
10	0.15	6.63E-14	0.00105	1.35E-15	9.01E-29	1.62E-25

B11. Mineql molar distribution of components among sodium species

pH	Na(+)	NaSO4 -	JAROSITE NA	MIRABILITE	HALITE	THENARDITE	NaHPO4
4	1.3	0.000178	1.5E-16	0.000601	0.00109	6.98E-05	8.73E-09
5	1.3	0.00356	6E-17	0.012	0.00109	0.00139	8.7E-07
6	1.29	0.00641	1.95E-19	0.0215	0.00109	0.0025	4.46E-07
7	1.29	0.00641	1.95E-22	0.0215	0.00109	0.0025	2.07E-08
8	1.29	0.00641	1.95E-25	0.0215	0.00109	0.0025	9.62E-10
9	1.29	0.00641	1.95E-28	0.0215	0.00109	0.0025	4.47E-11
10	1.29	0.00642	1.95E-31	0.0215	0.00109	0.0025	2.08E-12

B12. Mineq1 molar distribution of components among sulfate species

pH	SO4(2-)	HSO4 -	AlSO4 +	Al(SO4)2 -	CaSO4 Aq	FeSO4 +	Fe(SO4)2 -	KSO4 -
4.0	2.74E-05	2.66E-07	2.14E-07	4.65E-10	0.00019	2.26E-15	1.95E-18	2.8E-05
5.0	0.000548	5.32E-07	4.28E-09	1.86E-10	0.00289	4.52E-17	7.82E-19	0.000583
6.0	0.000548	5.32E-08	4.28E-12	1.86E-13	0.00289	4.52E-20	7.83E-22	0.000584
7.0	0.0006	5.82E-09	4.69E-15	2.23E-16	0.00289	4.94E-23	9.38E-25	0.000639
8.0	0.000987	9.58E-10	7.71E-18	6.04E-19	0.00289	8.13E-26	2.54E-27	0.00105
9.0	0.000987	9.58E-11	7.71E-21	6.05E-22	0.00289	8.13E-29	2.54E-30	0.00105
10.0	0.00099	9.6E-12	7.74E-24	6.08E-25	0.00289	8.16E-32	2.55E-33	0.00105

pH	MnSO4 Aq	NaSO4 -	S:ALUNITE	S:AL4(OH)10SO4	S:ALOHSO4	S:JAROSITE K	S:JAROSITE NA	S:JAROSITE H
4.0	4.68E-07	0.000178	0.00629	1.7E-08	0.00347	6.65E-14	1.5E-16	9.17E-20
5.0	6.91E-06	0.00356	0.417	3.39E-09	0.000695	2.77E-14	6E-17	3.68E-21
6.0	6.91E-06	0.00356	0.000417	3.39E-11	6.95E-06	2.77E-17	6E-20	3.68E-25
7.0	9.88E-06	0.0039	4.99E-07	3.72E-13	7.6E-08	3.32E-20	7.19E-23	4.41E-29
8.0	3.41E-05	0.0064	1.35E-09	6.11E-15	1.25E-09	8.96E-23	1.94E-25	1.19E-32
9.0	3.41E-05	0.0064	1.35E-12	6.11E-17	1.25E-11	8.96E-26	1.94E-28	1.19E-36
10.0	2.21E-06	0.00642	1.35E-15	6.13E-19	1.25E-13	9.01E-29	1.95E-31	1.2E-40

pH	S:ALUM K	S:GYPSUM	S:MIRABILITE	S:ANHYDRITE	S:FE2(SO4)3	S:MNSO4	S:THENARDITE
4.0	1.2E-10	0.0656	0.000601	0.0404	5.29E-46	5.51E-12	6.98E-05
5.0	4.99E-11	0.00541	0.012	0.615	4.25E-48	8.14E-11	0.00139
6.0	4.98E-14	0.00541	0.012	0.615	4.25E-54	8.14E-11	0.00139
7.0	5.97E-17	0.00496	0.0131	0.615	5.57E-60	1.16E-10	0.00152
8.0	1.61E-19	0.00164	0.0215	0.615	2.48E-65	4.02E-10	0.00249
9.0	1.61E-22	0.00164	0.0215	0.615	2.48E-71	4.01E-10	0.00249
10.0	1.62E-25	0.00165	0.0215	0.615	1E-75	2.6E-11	0.0025

VITA

James Jason Stone was born in North Hollywood, CA, on May 11, 1970. The restaurant business allowed him to live in many different areas of the United States before settling down in Richmond, VA, and graduating high school in 1988. After five long years of pain and suffering, he graduated with a bachelors in Civil Engineering at VPI&SU in May, 1993. During this time, he CO-OP'ed with VDOT and interned with Danis Heavy Construction Company. Perturbed with the construction industry, he enrolled in the Environmental Engineering masters program at VPI&SU in August, 1993. In February, 1995, he finished his degree requirements for an M.S. in Environmental Engineering.

A handwritten signature in black ink, appearing to read "James Jason Stone". The signature is stylized with large, sweeping loops and a long horizontal line extending to the right.